LIÈGE université
Gembloux
Agro-Bio Tech

Impact of electrostatic field assisted controlled freezing point storage on pork quality attributes: Exploring the mechanism of water holding capacity improvement

Yuqian XU

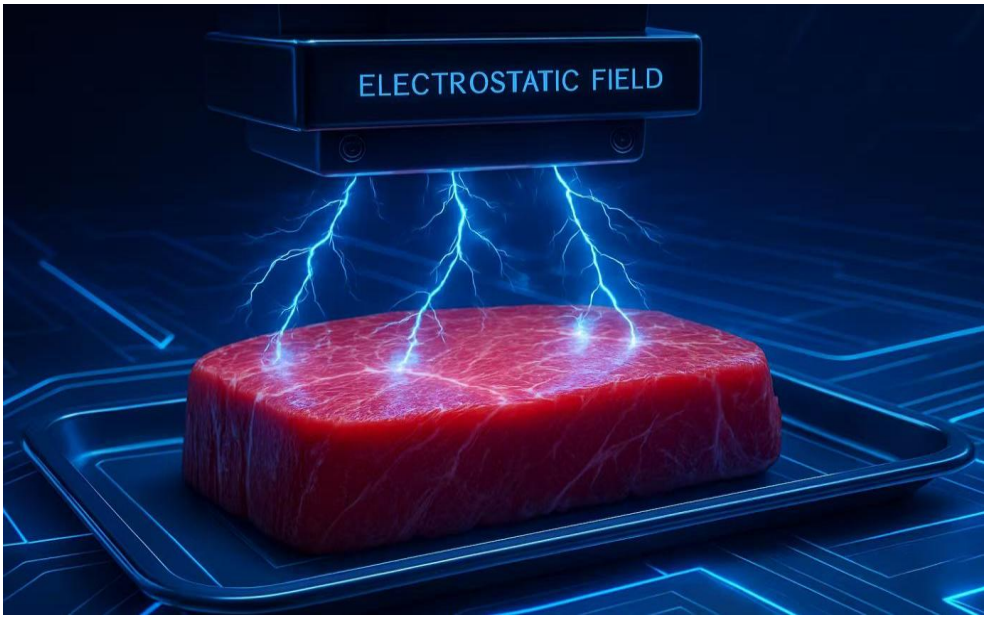

Promoteur(s) : Martine SCHROYEN
Co - promoteur: Dequan ZHANG
2025

COMMUNAUTÉ FRANÇAISE DE BELGIQUE
UNIVERSITÉ DE LIÈGE – GEMBLOUX AGRO-BIO TECH

Impact of electrostatic field assisted controlled freezing point storage on pork quality attributes: Exploring the mechanism of water holding capacity improvement

Yuqian XU

Dissertation originale présentée (ou essai présenté) en vue de l'obtention du grade de doctorat en sciences agronomiques et ingénierie biologique

Promoteur(s) : Martine SCHROYEN
Co - promoteur: Dequan ZHANG
Année civile (= année du dépôt) : 2025

Résumé

Yuqian XU. (2025). (Thèse de doctorat en anglais). « Impact du stockage à point de congélation contrôlé assisté par champ électrostatique sur les attributs qualité du porc : Exploration des mécanismes sous-jacents à l'amélioration de la capacité de rétention d'eau ». Gembloux, Belgique, Gembloux Agro-Bio Tech, Université de Liège, 166 pages, 4 tableaux, 37 figures.

Cette thèse explore systématiquement l'application du champ électrostatique (CE) dans la conservation de la viande, en se concentrant sur ses effets sur l'inhibition microbienne, la capacité de rétention d'eau (WHC) et les propriétés structurelles et fonctionnelles des protéines musculaires. Son objectif principal est d'élucider les mécanismes par lesquels le CE améliore la qualité de la viande pendant le stockage à point de congélation contrôlé (CFPS) et les phases post-mortem, afin de fournir des bases théoriques et pratiques pour l'optimisation des technologies de conservation alimentaire basées sur le CE.

Le chapitre 3 a évalué l'efficacité de différents modes d'application du champ électrostatique haute tension (CEHT) — continu, intermittent ou unique — sur la qualité du porc frais réfrigéré durant le CFPS. Les indicateurs de fraîcheur (pH, nombre total de colonies viables TVC, azote basique volatil total TVB-N), la dynamique des communautés bactériennes et la WHC (pertes d'humidité, perte centrifuge, relaxation T_2) ont été analysés. Les résultats montrent que les traitements intermittents (IHVEF) et continus (CHVEF) retardent significativement la baisse du pH, réduisent les valeurs de TVC et TVB-N, et suppriment les bactéries dominantes responsables de l'altération (telles que Pseudomonas, Latilactobacillus et Brochothrix), comparativement au groupe témoin. Le CHVEF a présenté l'effet antibactérien le plus marqué, en réduisant la diversité et l'abondance bactériennes, tout en préservant l'humidité et en limitant la migration de l'eau. Les améliorations de la WHC ont été attribuées à la stabilisation des couches d'hydratation et à la mobilité réduite de l'eau libre sous l'action du CE. Ces résultats soulignent que le CEHT, notamment en application continue, constitue une stratégie viable pour prolonger la durée de conservation du porc jusqu'à 16 jours, en limitant la croissance microbienne et les pertes en eau.

Le chapitre 4 a examiné l'influence de l'intensité du CE (faible LVEF : 4 kV ; élevée HVEF : 12 kV) sur la WHC et les propriétés de l'actomyosine en début de phase post-mortem pendant le CFPS. Les pertes à la cuisson, la relaxation T_2, l'indice de fragmentation des myofibrilles (MFI) et la dissociation de l'actomyosine ont été mesurés. Les échantillons traités par HVEF ont présenté des pertes à la cuisson plus faibles, des cristaux de glace de plus petite taille et un MFI réduit, indiquant une meilleure intégrité des myofibrilles. L'analyse granulométrique et la SDS-PAGE ont révélé que le HVEF retardait l'agrégation et la dissociation de l'actomyosine, maintenant ainsi la stabilité structurale du muscle. La spectroscopie FTIR et la MEB ont confirmé un renforcement des liaisons hydrogène et une réorganisation ordonnée de l'eau sous l'effet du CE, minimisant la conversion de l'eau immobilisée en eau libre. Ces observations suggèrent que le HVEF stabilise les interactions actomyosine, atténue les pertes d'eau liées à la rigidité cadavérique et améliore la WHC en modulant la dynamique protéine-eau au cours du stockage post-mortem.

Résumé

Le chapitre 5 a étudié les réponses structurelles et fonctionnelles de la myosine au traitement CE sous différentes conditions de pH (3,0 à 9,0). L'hydrophobicité de surface, la teneur en groupes sulfhydryles (-SH), le potentiel zêta, la structure secondaire et les propriétés des gels ont été analysés. La myosine traitée par CE a montré une hydrophobicité de surface plus faible et une rétention accrue des groupes -SH, traduisant une oxydation réduite et une stabilité structurale améliorée. Le CE a augmenté la répulsion électrostatique, supprimant l'agrégation protéique. La FTIR a indiqué une préservation du contenu en α-hélices et une limitation de la formation de feuillets β, en particulier aux pH extrêmes. Les gels traités par CE présentaient une WHC supérieure (relaxation T_2, perte centrifuge) et une texture renforcée, avec des réseaux protéiques plus denses, une dureté accrue et une meilleure rétention de l'eau immobilisée. Ces résultats soulignent le rôle du CE dans la stabilisation de la conformation de la myosine le long de gradients de pH, améliorant ainsi ses propriétés fonctionnelles déterminantes pour la qualité de la viande.

En synthèse, ces travaux positionnent le CE comme un outil de conservation polyvalent, prolongeant la durée de vie utile de la viande via l'inhibition des bactéries d'altération, l'optimisation de la WHC et le maintien de l'intégrité des protéines. Le CHVEF s'est révélé le mode le plus efficace pour le contrôle microbien et l'amélioration de la WHC dans le porc réfrigéré. Dans le muscle post-mortem, le HVEF a stabilisé les interactions actomyosine et réduit la migration de l'eau, tandis que la myosine traitée par CE a présenté une stabilité structurale indépendante du pH et une fonctionnalité gélifiante supérieure. Ces avancées éclairent la conception raisonnée de systèmes de conservation assistés par CE, ouvrant la voie à des solutions évolutives pour atténuer la détérioration qualitative, réduire le gaspillage et répondre à la demande des consommateurs en viande fraîche de haute qualité.

Abstract

Yuqian XU. (2025). (PhD Dissertation in English). “Impact of electrostatic field assisted controlled freezing point storage on pork quality attributes: Exploring the mechanism of water holding capacity improvement” Gembloux, Belgium, Gembloux Agro-Bio Tech, University of Liege, 166 pages, 4 tables, 37 figures.

Abstracts：

This series of studies systematically investigates the application of electrostatic field (EF) technology in meat preservation, focusing on its effects on microbial inhibition, water-holding capacity (WHC), and structural-functional properties of muscle proteins. The overarching objective is to elucidate the mechanisms by which EF treatments enhance meat quality during controlled freezing-point storage (CFPS) and postmortem periods, providing theoretical and practical insights for optimizing EF-based preservation technologies in the food industry.

The Chapter 3 evaluated the efficacy of different high-voltage EF (HVEF) modes (single, interval, and continuous application) on the storage quality of chilled fresh pork during CFPS. Key freshness indicators (pH, total viable count (TVC), total volatile basic nitrogen (TVB-N)), bacterial community dynamics, and WHC (moisture loss, centrifugal loss, T_2 relaxation) were analyzed. Results demonstrated that interval (IHVEF) and continuous HVEF (CHVEF) treatments significantly delayed pH decline, reduced TVC and TVB-N levels, and suppressed dominant spoilage bacteria (*Pseudomonas*, *Latilactobacillus*, *Brochothrix*) compared to controls. CHVEF exhibited the strongest antibacterial effect, reducing bacterial diversity and abundance while preserving moisture content and minimizing water migration. WHC improvements were linked to stabilized hydration layers and reduced free water mobility under EF. These findings highlight HVEF, particularly continuous application, as a viable strategy to extend pork shelf life to 16 days by mitigating microbial growth and water loss.

The Chapter 4 explored the impact of EF intensity (low: LVEF, 4 kV; high: HVEF, 12 kV) on WHC and actomyosin properties in early postmortem pork during CFPS. Cooking loss, T_2 relaxation, myofibril fragmentation index (MFI), and actomyosin dissociation were assessed. HVEF-treated samples exhibited lower cooking loss, smaller ice crystals, and reduced MFI, indicating preserved myofibril integrity. Particle size analysis and SDS-PAGE revealed that HVEF delayed actomyosin aggregation and dissociation, maintaining muscle structural stability. FTIR and SEM confirmed enhanced hydrogen bonding and ordered water alignment under EF, which minimized immobilized-to-free water migration. These results suggest that HVEF stabilizes actomyosin interactions, mitigates rigor mortis-related water loss, and improves WHC by modulating protein-water dynamics during early postmortem storage.

The Chapter 5 investigated the structural and functional responses of myosin to EF treatment under varying pH conditions (3.0~9.0). Surface hydrophobicity, sulfhydryl (-SH) content, zeta potential, secondary structure, and gel properties were analyzed. EF-treated myosin displayed lower surface hydrophobicity and higher -SH retention, indicating reduced oxidation and enhanced structural stability. Zeta potential and

particle size measurements revealed that EF increased electrostatic repulsion, suppressing protein aggregation. FTIR showed EF preserved α-helix content and minimized β-sheet formation, particularly at extreme pH values. Gel WHC (T_2 relaxation, centrifugal loss) and texture analysis demonstrated that EF strengthened protein-water interactions, forming denser gel networks with higher hardness and immobilized water retention. These findings underscore EF's role in stabilizing myosin conformation across pH gradients, thereby improving functional properties critical for meat quality.

In summary, these studies establish EF as a multifaceted preservation tool that extends shelf life by inhibiting spoilage bacteria, optimizing WHC, and maintaining protein integrity. Continuous HVEF emerged as the most effective mode for microbial control and WHC enhancement in chilled pork. In postmortem muscle, HVEF stabilized actomyosin interactions and reduced water migration, while EF treated myosin exhibited pH resistant structural stability and superior gel functionality. These insights advance the rational design of EF assisted preservation systems, offering scalable solutions to minimize quality deterioration, reduce waste, and meet consumer demand for high quality fresh meat.

Acknowledgements

As I bring this journey to a close and submit my thesis, I am filled with profound gratitude for the many individuals and institutions that have supported me throughout this challenging and rewarding experience. This work is not the result of my efforts alone—it is a testament to the encouragement, mentorship, and kindness I have received along the way.

First, I would like to express my deepest appreciation to Université de Liège (ULg) and Chinese Academy of Agricultural Sciences (CAAS). Being part of this academic community has been an hono. These two universities had provided me with not only the resources and facilities necessary for academic growth but also an environment that encourages critical thinking, intellectual curiosity, and a commitment to excellence. I am particularly grateful for the academic atmosphere that nurtured both my independent thought and collaborative learning. Every lecture, seminar, and discussion has played a vital role in shaping my research approach and academic identity.

I owe a special debt of gratitude to my supervisor, Prof. Martine Schroyen (ULg) and Prof. Dequan Zhang (CAAS), whose unwavering support, insightful guidance, and thoughtful feedback have been invaluable throughout this process. From the initial formation of my research topic to the final stages of revision, Prof. Martine Schroyen and Prof. Dequan Zhang have been a pillar of academic and moral support. Their ability to strike a perfect balance between challenging and encouraging me has pushed me to think more deeply and write more clearly. I have learned not only from their scholarly expertise but also from their integrity, patience, and humility—qualities I hope to carry with me in my own academic and professional pursuits.

I would also like to thank the members of my thesis committee, Prof. Hélène Soyeurt Prof. Nadia Everaert, Prof. Christophe Blecker, Prof. Ayadi Mohamed, and for their generous time, critical insights, and constructive comments. Their engagement with my work helped me see my project in new and important ways. Each of them offered valuable perspectives that enriched the depth and scope of my research. I am especially thankful for the respectful and thought-provoking discussions that challenged me to consider broader contexts and to refine my arguments with greater clarity and precision.

To my fellow students and friends—Sinmin Fan, Feifei Xie, Su Wang, Juan Chen, Xiaoyu Chai, Zhiyuan Xiao, and many others—thank you for being such a vital part of this journey. The long hours we spent in the library, the stimulating conversations over coffee, the collective stress during deadlines, and the shared moments of joy will remain among my most treasured memories. Your encouragement during times of doubt and your enthusiasm for my ideas gave me the motivation to continue. This thesis would not have been the same without your intellectual companionship and emotional support.

Finally, I would like to extend my heartfelt gratitude to my family. To my parents, Shulan Li, Dechun Xu, and Shurong Li, thank you for your unwavering belief in me and your unconditional love. Your sacrifices, encouragement, and constant presence have been the foundation of all my achievements. To my other family members who

stood by me through thick and thin, thank you for reminding me of my strength when I needed it most. Though miles apart at times, your support never failed to reach me.

In closing, while this thesis bears my name, it belongs equally to all those who have walked this path with me. I am deeply grateful to each of you for making this journey not only possible but meaningful. Thank you.

1. Table of Contents

Table of Contents

Table of Contents

Table of Contents

Table of Contents

Table of Contents

Table of Contents

Table of Contents

2. List of Figures

Table of Figures

3. List of Tables

4. List of Abbreviations

CFPS	Controlled freezing point storage
WHC	Water holding capacity
EF	Eletrostatic field
HVEF	High voltage electrostatic field
LVEF	Low voltage electrostatic field
SHVEF	Single-used high voltage electrostatic field
IHVEF	Interval-used high voltage electrostatic field
CHVEF	Continuous-used high voltage electrostatic field
AEF	Alternating electric field
PEF	Pulsed electric field
SEF	Static electric fields
HVPEF	High voltage prick electrostatic fields
CK	Control group samples
MYPs	myosin protein solution models
MYPp	Myosin protein solution powder
LTL	*M. Longissimus Thoracis Lumborum*
DC	Direct Current
PE	Polyethylene film
EDTA	Ethylene diamine tetraacetic acid
MAP	modified atmosphere packaging
TVC	Total viable count
TVB-N	Total volatile basic nitrogen
TBARS	Thiobarbituric acid reactive substances
MFI	Myofibril fragmentation index
-SH	Sulfhydryl group content
HB	Hydrogen bond
Aw	Water activity
PSE	Pale, soft, and exudative
pI	Isoelectric point

Table of Abbreviations

TD-NMR	Time domain nuclear magnetic resonance
SEM	Scanning electron microscopy
FTIR	Fourier transform infrared spectrometer
NMI	Nuclear magnetic resonance imaging
CPMG	Carr-purcell-meiboom-gill
TPA	Texture profile analysis
LC-MS/MS	Liquid chromatography-tandem mass spectrometry
LSD	Least significant differences
SE	Standard errors
PCA	principal component analysis
SRA	Sequence read archive
OTUs	Operational taxonomic units
LEfSe	Linear discriminant analysis effect size
KEGG	Kyoto encylopaedia of genes and genomes
GOC	Gene ontology consortium
MD	Molecular dynamics simulations
Cryo-SEM	Cryogenic scanning electron microscopy
PVDF	Polyvinylidene fluoride
IMP	Inosine monophosphate

Chapter 1

General Introduction

1. The importance of fresh meat preservation

1.1 The rising production and consumption of pork

China is one of the largest meat producers of the world. In recent years, driven by the modernization and expansion of animal husbandry as well as the continuous improvement of overall production capacity, the country has maintained a leading position in global meat production. In 2024, China was projected to produce 96.63 million tons of pork, beef, mutton, and poultry, with fresh meat consumption accounting for more than 70% of total consumption. Pork remains a cornerstone of animal protein production and consumption, making it the most consumed meat worldwide. Its dominance is particularly evident in China, which accounts for approximately 44% of global production and over 40% of consumption. Within China, pork is not merely a food but a dietary staple. The average per capita pork consumption in 2024 is estimated to be around 35 kg, accounting for over 55% of total meat consumption. This immense scale underscores its critical role in global food security, agricultural economies, and cultural dietary patterns, solidifying its unparalleled importance in the world's meat sector (Fig. 1).

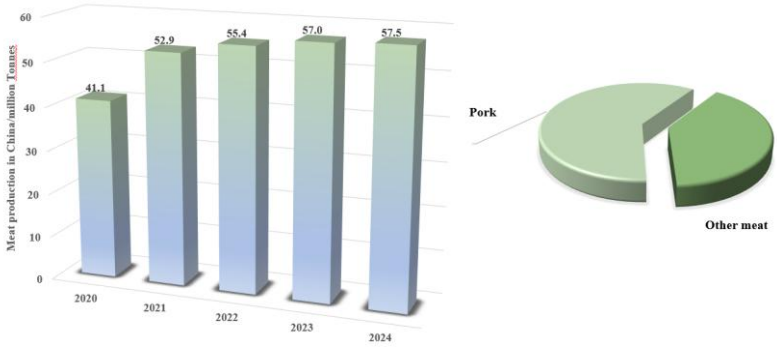

Figure 1. China‘s pork production in 2022-2024 and the proportion of pork and other meat products in 2024.

1.2 Changes in the consumption structure of pork

As production security improves and consumer preferences shift toward healthier and more diverse diets, the structure of meat production continues to be adjusted and optimized (Wang, 2022). There is a growing inclination towards hot-boned meat (fresh meat shortly after slaughter) and away from chilled meat. This preference is largely rooted in the perception that hot-boned meat is fresher, more authentic, and superior in flavor. However, this very preference presents a significant paradox, as the physiological and biochemical reactions that commence immediately post-mortem

become a primary obstacle to its quality, making the preservation of both hot-boned pork a critical challenge for the meat industry.

The transformation of muscle into meat is an intricate process governed by a series of post-mortem biochemical events. Upon exsanguination, oxygen supply ceases, forcing muscle cells to switch from aerobic respiration to anaerobic glycolysis. This leads to the rapid depletion of glycogen and the subsequent accumulation of lactic acid, causing a sharp decline in muscle pH from near neutrality (approximately pH 7.0) to an ultimate value around 5.4-5.8. The rate and extent of this pH drop are crucial determinants of meat quality. The most direct consequence of this is a severe reduction in water holding capacity (WHC).

Given this high demand, the preservation of fresh meat, especially hot-boned pork is of central importance, driving advancements in preservation technologies. These technologies not only serve as economic tools to reduce storage losses but also play a critical role in maintaining nutritional value, ensuring food safety, improving economic efficiency, and minimizing resource waste.

1.3 The Importance of retaining moisture in pork

The main goals of meat preservation are to prevent nutrient loss, maintain sensory attributes, and inhibit spoilage microorganisms. This process encompasses the evaluation of sensory attributes, physicochemical parameters, and technological properties (Zhou et al., 2010). Sensory attributes, such as color, flavor, tenderness, juiciness and other parameters, can affect the appearance of meat and directly determine consumption orientation of consumers. With respect to physicochemical parameters, key indicators such as pH value, fat content and distribution, protein composition, shear force, microbial counts, and WHC play a pivotal role in defining the fundamental quality attributes of meat. From the perspective of technological properties, for example, sausage with high emulsion stability has less fat precipitation, and ham with high curing permeability has higher yield. It is worth noting that whether it is sensory attributes, physicochemical parameters or technological properties, it is inseparable from the maintenance of moisture.

For instance, in terms of sensory attributes, the moisture content in muscle cells directly influences the perception of juiciness during chewing. It has been shown that sous vide (SV) cooking of hot-boned semimembranosus muscles significantly enhanced WHC and minimized muscle shortening compared to grilling or boiling (Xu et al., 2023). In terms of physicochemical parameters, sharp muscle contractions lead to moisture loss. A Study by Wang et al. (2024) has shown that the addition of composite coating for frozen chicken meatballs, forming a three-dimensional gel structure that protected the muscle fibers, reduced thawing, cooking, and drip losses to 0.23%, 1.56%, and 1.87%, respectively (Wang et al., 2024). Similarly, it is also stated with regard to technological properties that increasing the core temperature and prolonging low-temperature cooking durations (60 min) enhanced water content of the chicken breasts by 12% by elevating pH, protein solubility, and hydrophobicity (Li et al., 2024). Therefore, the maintenance of water has become a focal point in the

industry due to its critical influence on the taste of meat, economic efficiency, and processing performance.

2. Moisture changes of fresh meat during storage

The preservation of fresh meat fundamentally relies on a multidimensional approach that integrates biological, chemical, and physical control mechanisms. A critical challenge in this process is the loss of moisture, which constitutes approximately 65%~75% of fresh meat, making it the most abundant component (Warner, 2024). During storage, fresh meat is highly susceptible to significant drip loss, which not only deteriorates its sensory qualities but also leads to nutritional degradation, ultimately causing substantial economic losses. Consequently, minimizing drip loss in fresh meat during storage has become a focal point of research within the meat science community. Investigating WHC in fresh meat is essential for enhancing meat quality, improving industrial efficiency, and mitigating economic losses.

Water holding capacity (WHC) in meat refers to the ability of muscle tissue to retain its inherent moisture content, which is one of the most critical quality attributes of meat (Oswell et al., 2021). This property not only reflects changes in the moisture content of the meat but also significantly influences other essential quality characteristics, including nutritional value, tenderness, juiciness, and color. As such, WHC serves as a key indicator for assessing the overall value of meat. Typically, moisture in fresh meat exists in three distinct states: free water, which flows freely between muscle cells or myofibrillar fibers; bound water, which is tightly associated with protein molecules; and immobilized water, which resides within the myofilaments, the spaces between myofibrils, and the interfaces between myofibrils and membranes (Oswell et al., 2021). To evaluate the WHC of fresh meat, common indexes include drip loss, cooking loss, and centrifugal loss. It is generally believed that the higher levels of moisture loss are indicative of poorer WHC in meat. Of these types of moisture loss, the primary contributors in fresh meat are free water and immobilized water (Puolanne, 2022). Free water is susceptible to evaporation or loss (mechanical handling, such as cutting or compression), directly impacting the juiciness and freshness of the meat. Its loss often results in a dry, tough texture and reduced weight. Immobilized water is retained within the highly organized structures of muscle fibers, where it forms hydrogen bonds with proteins such as myofibrillar proteins and sarcoplasmic proteins. This type of water is resistant to evaporation or loss, playing a crucial role in maintaining muscle structure and stability. It significantly influences the WHC of meat, as well as its processing properties, including performance during salting and freezing (Puolanne, 2022).

2.1 External factors on WHC

External factors primarily influence the water content of fresh meat through physical evaporation, chemical oxidation, microbial interactions, and other mechanisms. Research has shown that temperature fluctuations significantly impact the WHC of fresh meat (Li et al., 2018). Variations in storage temperature accelerate moisture loss,

leading to surface drying of fresh meat, while also promoting microbial growth, protein and fat decomposition, and, consequently, an indirect reduction in the meat's WHC (Dimakopoulou-Papazoglou et al., 2022).

Refrigeration (0~4℃) and freezing (below -18℃), as common storage methods, differ significantly in their mechanisms of WHC. Under refrigeration, when humidity is low, surface water of fresh meat undergoes evaporation, forming a dry layer (weight loss), while internal moisture remains relatively stable. Additionally, low temperatures inhibit microbial and enzymatic activity, slow protein degradation, preserve the integrity of muscle cell membranes, and ultimately reduce moisture loss. Lee et al., (2023) suggested that supercooling, compared to conventional methods, preserved beef cuts with intermediate microbial counts between freezing and refrigeration, slowed discoloration, and minimized ice crystal formation, suggesting its potential to extend shelf life while balancing quality retention. Other studies support this conclusion, and they revealed that wooden breast broiler fillets exhibited altered water dynamics via time domain nuclear magnetic resonance (TD-NMR), with distinct water populations and interaction effects between storage temperature and the fillets' condition (Choi et al., 2024).

However, the freezing process and long-term frozen storage can irreversibly affect meat quality, as the volume of frozen meat increases by approximately 9%. During freezing process, large ice crystals initially form outside the cells, exerting pressure on the cell structure, leading to membrane rupture and the precipitation of some soluble proteins (Jia et al., 2022). Upon thawing, a significant amount of cellular fluid (water) is lost, with the exuded liquid accounting for approximately 7% of the original mass. This liquid is rich in nutrients such as proteins, resulting in substantial losses in both nutritional value and flavor (Qian et al., 2022). Prolonged freezing may also lead to ice recrystallization, where small ice crystals merge into larger ones, further promoting the migration of water molecules and damaging muscle fibers (Matsumoto et al., 2002). Furthermore, as the concentration of salts increases in the unfrozen phase, the resulting high ionic strength competes with existing electrostatic bonds, altering the structure of natural proteins. For instance, proteins such as myosin undergo structural changes at low temperatures, losing their water-binding capacity, which ultimately reduces the WHC of meat after thawing. Studies have demonstrated that frozen storage of cooked crayfish over 8 weeks induced pH and total volatile basic nitrogen (TVB-N) elevation, as well as microstructural damage caused by ice crystals. This results in the degradation of WHC, color, and texture, despite maintaining nutritional value, emphasizing the quality deterioration in ready-to-eat seafood as frozen storage duration increases (Abdelnaby et al., 2024). In addition, Li et al., (2024) suggested that fast sub-freezing significantly enhanced beef WHC and tenderness by minimizing muscle fiber damage, inhibiting protein oxidation, and facilitating cytoskeletal degradation during 42-week storage. These findings underscore its potential as an effective method for long-term beef preservation.

2.2 Internal factors on WHC

Relevant studies conducted both domestically and internationally have shown that the WHC of meat is influenced by various internal factors as well. These factors are primarily related to muscle structure, protein state, and postmortem anaerobic glycolysis of muscle glycogen (Melody et al., 2004). Research indicates that after slaughter, ATP is depleted in muscle cells, leading to the formation of cross-bridges between thick and thin filaments. This process induces the muscles to become rigid, reduces the space between myofilaments and myofibrils, and forces moisture out into the extracellular space, resulting in moisture loss (Zuo et al., 2022). Additionally, protein oxidation, denaturation, and cross-linking contribute to structural tightening, exposure of hydrophobic groups, and a decline in hydration capacity (Bowker & Zhuang, 2015). Ma & Kim, (2020) suggest that alterations in muscle protein structure affect the interaction between proteins and water, leading to changes in water distribution and migration, ultimately impacting the WHC of muscle. Furthermore, Ma et al., (2023) evaluated the early postmortem degradation of myofibrillar proteins (Desmin, troponin-T) in chicken through spectroscopic analysis. Their findings revealed a disruption of the ordered secondary structures, a reduced thermal stability, and a decreased WHC. Zhang et al., (2023) reached a similar conclusion. They revealed that sub-freezing aging reduced pork myofibrillar protein oxidation, preserved ordered secondary structures (α-helix/β-sheet), and enhanced WHC by minimizing conformational shifts to disordered states (β-turn/random coil), with optimal WHC achieved after 120 h. The degradation of cytoskeletal proteins can also lead to the relaxation of the myofibrillar network and the expansion of the space within the myotome, thereby influencing the WHC of meat (Kim et al., 2018). Studies have shown that the calpain-induced degradation of Desmin and nebulin may promote the formation of a spongy structure, which enhances the WHC of fresh meat (Qian et al., 2020). Some researchers have explored the relationship between differential calpain activity (autolysis, myofibril-bound μ-calpain) and proteolysis rates in porcine muscles and changes in tenderness and WHC. The results show that the psoas major exhibited an accelerated pH value decline, earlier μ-calpain autolysis, enhanced Desmin and Titin degradation, and a reduced drip loss, correlating with superior tenderness (Melody et al., 2004). Lawson, (2004) further observed that the degradation of connexins between actin-skeletal proteins and the cell membrane in postmortem muscle leads to the formation of a sarcoplasmic loss channel, through which moisture is lost. Additionally, the accumulation of lactic acid in livestock and poultry after slaughter causes a decrease in pH (typically ranging from 5.4~5.8). As the pH value approaches the isoelectric point of proteins, electrostatic repulsion is reduced, leading to a decrease in the net charge of myofibrillar proteins. Consequently, the proteins aggregate and release the water molecules that bind to it, reducing the WHC of muscle and increasing the likelihood of developing pale, soft, and exudative (PSE) meat (Zuo et al., 2016). At low pH value, excessive protein acidification and denaturation further disrupt the hydration layer, resulting in a significant decline in WHC.

3. Controlled freezing point storage

Currently, refrigeration and freezing are the most common traditional methods for meat storage and preservation. Refrigerated meat has a shorter shelf life, so frozen meat that can be stored for a longer period of time has become the first choice for most consumers (Li et al., 2019). However, freezing often results in significant nutrient loss and a deterioration in texture and flavor during thawing. Neither of these methods fully satisfies the dual requirements of quality preservation and shelf-life extension (Estévez et al., 2011). To address these limitations, researchers have explored alternative storage technologies that combine the advantages of both methods while minimizing their drawbacks (Lee et al., 2022). As a result, controlled freezing point storage (CFPS) has emerged as a promising approach for maintaining meat quality and has become a focal point of research in meat storage and preservation.

3.1 Definition of CFPS

CFPS refers to storing meat within a temperature range below 0°C but above its freezing point, positioning it between refrigeration and freezing (Fig. 2) (Wang et al., 2018). At this temperature, the meat remains unfrozen, preventing the formation of ice crystals and thereby minimizing damage to cell structures. Studies have shown that within this temperature range, the rate of physicochemical changes in meat is significantly reduced (Moriya et al., 2019). Cellular physiological activity is largely preserved, while microbial growth and enzymatic activity are effectively inhibited. As a result, the original quality of the meat is maintained without the substantial moisture loss and tissue damage typically associated with the thawing of frozen meat.

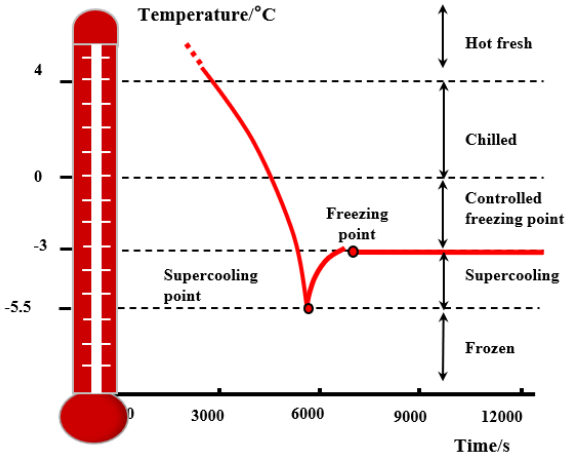

Figure 2. The temperature range of CFPS.

Research has shown that CFPS synergistically inhibits microbial growth, lipid oxidation, protein degradation, and textural deterioration (Zhu et al., 2015). Wang et al., (2014) used vacuum packaging combined with CFPS to investigate the colony

changes and shelf life of shrimp meat. The results showed that vacuum modified atmosphere packaging (MAP) extended shrimp shelf-life by suppressing spoilage bacteria via CO_2 bacteriostasis, inhibiting proteolysis, and maintaining low pH value. CFPS was able to effectively maintain the storage quality of fresh meat by precise control and avoiding freezing, and the preservation ability was significantly better than that of traditional refrigeration and freezing (Zhang et al., 2021). Li et al., (2017) compared the characteristic changes of sheep *Longissimus Thoracis Lumborum* (LTL) stored at 4℃ with CFPS, and found that CFPS enhanced color stability, maintaining high levels of a* and b*, chroma, oxymyoglobin, and NADH within 10 days, while suppressing metmyoglobin formation. The improvement of redox homeostasis was evidenced by elevated metmyoglobin reductase activity, underpinned delayed myoglobin oxidation and superior color retention. A study by Sun et al. (2020) demonstrated that CFPS significantly attenuated biochemical deterioration in yak meat by delaying TVB-N accumulation, pH value elevation, and lipid oxidation compared to 0℃ storage, suggesting oxidative and proteolytic inhibition mechanisms under CFPS (Sun et al., 2020). Wang et al., (2018) elucidated the interdependent oxidative dynamics of myoglobin, lipids, and proteins in rabbit meat under refrigerated storage and CFPS. Progressive increases in thiobarbituric acid reactive substances (TBARS), metmyoglobin formation, protein carbonyls, and non-heme iron were observed alongside sulfhydryl group depletion. CFPS attenuated oxidation rates more compared to refrigeration. Principal component analysis demonstrated strong correlations between lipid peroxidation, protein carbonylation, and metmyoglobin accumulation, suggesting mutually catalytic oxidation pathways during storage.

3.2 Optimizing WHC with CFPS

Studies have demonstrated that CFPS offers significant advantages in maintaining the WHC of fresh meat. At CFPS temperature conditions, water in the muscle remains in a critical unfrozen state, preventing the formation of ice crystals that could puncture cell membranes during freezing (Chan et al., 2020). In turn, it reduces moisture loss during thawing. In addition, the appropriate low temperature delays protein denaturation, slows lipid oxidation, and inhibits the activity of spoilage bacteria and autolytic enzymes in meat. As a result, CFPS effectively slows down the softening of meat and reduces the increase in exudate, thereby preserving muscle WHC and reducing cooking losses in practical applications. You et al., (2020) evaluated quality factors, including drip loss, in beef samples stored under CFPS and compared them with those of refrigerated, frozen (-10 °C, SF; -20 °C, RF), and fresh samples. After 14 days of storage, cellular damage was assessed using optical microscopy. Although intracellular freezing in frozen beef led to drip loss and tenderization, these physical changes were not observed during CFPS storage. Spatiotemporal analysis of Atlantic salmon preserved under CFPS revealed comparable liquid loss between surface and center regions during 1~14 days, despite prior ice crystal size variations (Kaale et al., 2014). Park et al., (2022) implemented a stepwise cooling algorithm to stabilize CFPS of pork belly and chicken breast, achieving phase transition-free preservation for 12 days. CFPS effectively reduced drip loss and inhibited microbial growth.

3.3 Application limitations and challenges of CFPS in fresh meat preservation

As an emerging food preservation technology, CFPS effectively inhibits microbial proliferation and enzymatic reactions through precise temperature regulation at sub-zero levels, thereby extending the shelf life of fresh meat products (Mi et al., 2013). However, CFPS operates within a limited operational temperature range compared to conventional low temperature methods (-0.5℃~-2.0℃), typically maintaining samples within a narrow 1.5℃ thermal window. Therefore, the widespread application of this technology in commercial meat preservation systems still faces multiple technical bottlenecks and substantial implementation costs (Sun et al., 2013).

First, the freezing point difference of meat presents a critical constraint in low temperature storage system design. Fresh meat exhibits variable freezing points determined by its biochemical composition (moisture content, lipid distribution, protein content) and postmortem metabolic status (Chen et al., 2022). Significant inter- and intra-species variations exist, with differential freezing points observed not only between meat types but also across muscle regions within the same carcass (Fig. 3 & 4). When the meat with different freezing points co-exists in the same storage space, temperature management protocols require temperature calibration to the specimen with the lowest freezing point threshold. Consequently, muscles possessing higher freezing points (such as pork muscle) remain in metastable supercooled states rather than achieving complete frozen. Under these conditions, meat muscles are prone to localized ice crystal formation, inducing structural damage to cellular membranes and subsequent exudate release. Furthermore, temperature instability in storage environments stimulates metabolic acceleration in psychrotrophic microbiota, particularly Pseudomonas spp., thereby reducing the shelf life of meat (Sun et al., 2013).

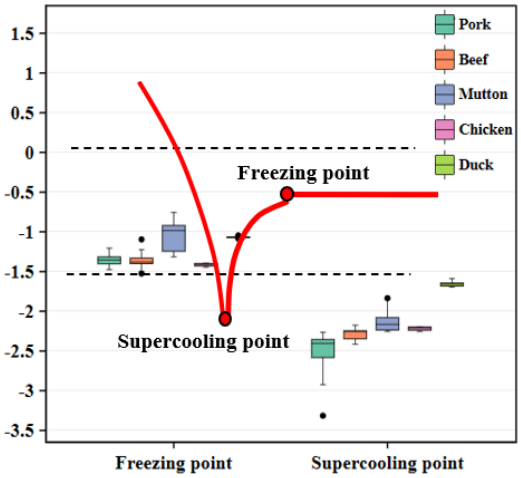

Figure 3. The freezing points and supercooling point of different meat.

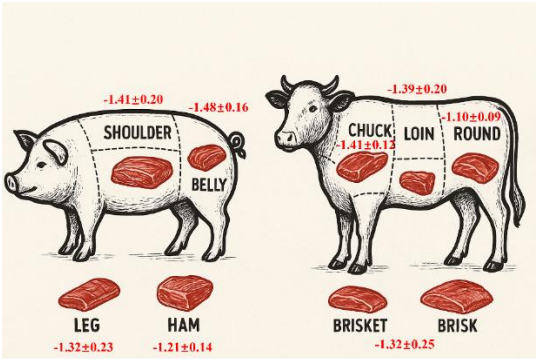

Figure 4. The freezing points of different parts of pork and beef meat.

Second, CFPS implementation necessitates temperature regulation (±0.3℃ stability), demanding advanced refrigeration architectures, which puts extremely high requirements on equipment performance (Lan et al., 2016). Current industrial cold chain infrastructures and domestic preservation devices exhibit critical deficiencies: suboptimal refrigerant selection compromising phase-change efficiency; inadequate heat transfer rates during load variations, and insufficient feedback control precision (±1.2℃). These technological limitations fundamentally undermine the efficacy of CFPS.

Third, the cost of storage and transportation equipment, along with the economic barriers of supporting facilities, poses significant challenges. Implementation requires precision refrigeration systems and advanced monitoring infrastructure with real-time feedback loops, coupled with significant auxiliary facility investments for humidity and temperature regulation. These costs pose significant barriers to widespread application in commercial meat supply chains.

While CFPS demonstrates theoretical advantage in the preservation of fresh meat, its industrial deployment remains challenged by the meat freezing point difference, insufficient equipment accuracy and economic defects. Addressing these constraints necessitates system-level innovations, ultimately requiring cross-disciplinary collaboration to achieve scalable technological translation.

4. Electrostatic field

The electric field can be classified into the following types based on its action form, frequency, and generation mode: electrostatic field (EF), alternating electric field (AEF) (Wu et al., 2023), pulsed electric field (PEF) (Kantono et al., 2019), cold plasma (Mol et al., 2023)， and ohmic Heating (Guo et al., 2024).

EF is defined by a constant electric field formed by Direct Current (DC) voltage. It is a unique form of matter that exists in the space surrounding a charge, characterized by its strong influence on any static charge placed within it (Dalvi-Isfahan et al., 2023). By the late 20th century, advancements in molecular biology and cytogenetics enabled

scientists to uncover the electromagnetic properties of biological cells and their interactions (Kekez et al., 1996). This discovery sparked a series of studies on EF (Kudra & Martynenko, 2015; Zheng et al., 2011). In recent years, EF has been widely applied in food processing and preservation, gaining significant recognition from both academia and industry (Chen et al., 2022; Wang et al., 2018). Over the past five years, the number of relevant research publications has shown a steady annual increase. Institutions such as Cornell University, Jiangnan University, and Horizon 2020 of the European Union (FULLRECOMM: FULL Recovery of Food Waste through Circular Economy and Multi-Stakeholder Engagement: 101023456) have actively engaged in research and development projects exploring the applications of EF across various industries (Han et al., 2022). In the commercial sector, China and the United States have integrated EF modules into refrigerators, leading to a 25% increase in market penetration. Meanwhile, Toshiba in Japan has introduced commercial EF refrigerators and EF device is actively promoting their industrialization (Fig. 5).

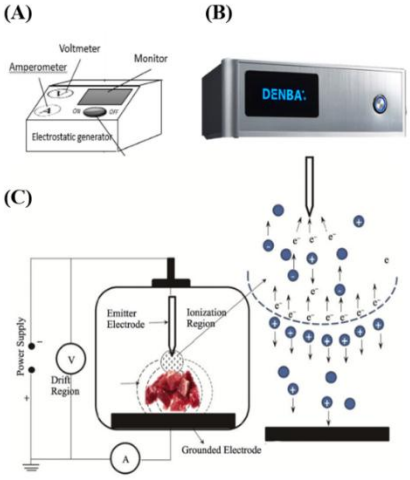

Figure 5. The device of EF.

(A): Practice figure of EF device; (B): Figure of device (Denba_Janpan); (C) Electrode emission of EF deviced.

4.1 The difference between high-voltage EF and low-voltage EF

In practical applications, EF can be classified into low voltage EF (LVEF) and high voltage EF (HVEF). By adjusting the voltage supplied by the power source, either low frequency or high-frequency vibrations can be applied, enabling a broad range of EF outputs (Liu et al., 2025).

High-Voltage Electrostatic Field (HVEF) technology offers the significant advantage of a potent bactericidal effect, capable of disrupting microbial cell

membranes to markedly extend the shelf-life of fresh meat. However, this comes with considerable drawbacks, including high system complexity, substantial energy consumption, and the critical issue of potential ozone generation, which can promote oxidative rancidity and degrade meat quality. Consequently, due to these cost and safety challenges, HVEF remains primarily confined to research and pilot-scale applications rather than widespread industrial use.

In contrast, Low-Voltage Electrostatic Field (LVEF) technology is characterized by its energy efficiency, operational safety, and lower cost (Lin et al., 2024). It functions by subtly influencing the meat's metabolism and the surrounding air ions to inhibit spoilage. Its practical and economic advantages have facilitated more tangible commercial uptake, particularly in specialized display cabinets in markets like Japan, though it is still far from being a mainstream technology globally. The primary trade-off is its weaker, indirect preservative effect, making it less effective than HVEF for direct sterilization. Meanwhile, LVEF is less frequently used than HVEF in the preservation of agricultural products. This is primarily because a higher output voltage of HVEF can more effectively enhance the preservation effect within a certain temperature range (Ko et al., 2016).

Table 1: A comparison of high-voltage EF and low-voltage EF in meat preservation

Type	Subject	Voltage / Field Strength Conditions	Research Findings
HVEF	Beef	4 kV/cm	Effectively inhibited microbial growth (specifically Pseudomonas spp.) and significantly retarded the oxidation of myoglobin, thereby better preserving the bright red color of the beef.
	Chicken	5 kV	Significantly reduced total aerobic bacterial count compared to the control group and better maintained the pH value and sensory attributes of the chicken during storage.
	Atlantic Salmon Fillets	1, 2.5, 4 kV/cm	Markedly attenuated lipid oxidation (as measured by TBARS value) and suppressed the accumulation of total volatile basic nitrogen (TVB-N), effectively extending the shelf life, with higher field strengths yielding more pronounced effects.
LVEF	Pork	100, 200, 300 V	Effectively delayed the increase in pH and inhibited the production of TVB-N in pork during storage. The treatment at 200 V demonstrated the optimal preservation efficacy.

Beef	150 V/m, 250 V/m	By modifying water distribution and protein conformation, the treatment reduced cooking loss and improved the tenderness of the beef.
Tilapia Fillets	500 V	Suppressed the growth of specific spoilage microorganisms and delayed the degradation of adenosine triphosphate (ATP) and its related compounds, thereby better maintaining the freshness of the fish fillets.

4.2 Advantages of EF

As a non-thermal technology, EF has many advantages. First, the equipment of EF is notably simple and cost-effective. Its key advantages include low energy consumption, highly efficient electrostatic generation with minimal power draw, and a low initial setup cost. This combination of high efficiency and affordability makes it highly suitable for both commercial and household applications. Second, EF does not generate heat during use and has a non-thermal effect. Therefore, it can effectively avoid the destruction of protein and vitamins at high temperature, and retain the original flavor and nutrition of food (Hülsheger et al., 1983; Luo et al., 2005). Third, EF does not produce chemical residues during the process, which is in line with the Clean Label trend. In addition, EF can affect the existence of microorganisms and enzymes by affecting the migration and distribution of charged particles, which is beneficial for maintaining the original flavor and nutrition of food (Golberg et al., 2016; Léonard et al., 2021). Finally, EF operates synergistically with other technologies. For instance, when integrated with low temperature treatments, air-conditioned packaging, and other advanced approaches, EF demonstrates the superior capacity to enhanced the preservation of fresh meat (Leong et al., 2016; Wang et al., 2018).

4.3 Application of EF assisted low temperature storage in meat

Compared with the traditional heat treatment technology, the EF technology, dominated by the relevant theories of electromagnetic biology, has gradually emerged in the field of meat application research because of its advantages of less damage to meat nutrients, simple equipment and low energy consumption (Hu et al., 2022; Jia et al., 2017). Currently, researchers have integrated and advanced various applications of EF technology in meat processing, leading to its rapid development and increasing adoption. This technology holds great potential for future applications, particularly in the following aspects.

First, the main effects of EF on microorganisms entail growth inhibition, structure destruction and death induction. The core mechanism involves electrophysical action and biochemical stress reaction. It has the advantages of non-heat and no chemical residue, offering a potent antimicrobial strategy for meat preservation (Huang et al., 2021). A study of He et al., (2013) demonstrated that HVEF thawing reduced

microbial counts, while suppressing volatile basic nitrogen increase. Ko et al., (2016) combined a HVEF with refrigeration, demonstrating the efficiency of HVEF in meat preservation. The research showed that HVEF preserve tilapia freshness by inhibiting microbial growth, slowing ATP degradation, protein denaturation, and lipid oxidation, thereby reducing TVB-N and K-values (degradation products of inosine monophosphate, IMP) to extend shelf-life beyond untreated samples. In a study by Huang et al., (2020), the HVEF extends catfish fillet shelf-life by electrostatically inhibiting spoilage bacteria, delaying protein and lipid oxidation, preserving texture and WHC, and suppressing microbial growth, thereby prolonging freshness by 2 days compared to untreated controls. Similarly, studies have shown that high voltage prick electrostatic fields (HVPEF) extends ready-to-eat salmon shelf life by electrostatically inhibiting microbial growth while preserving nutrients and texture. It slows protein degradation and modulates lipid oxidation, proving a non-damaging antimicrobial method (Qi et al., 2022).

Second, the EF accurately regulates enzyme activity through multi-scale mechanisms such as electrostatic preorganization and conformational regulation, which provides a physical intervention strategy for rational design of efficient artificial enzymes and development of new biocatalytic technologies (Ohshima et al., 2021). Based on Warshel's electrostatic preorganization theory, the EF induces substrate orientation by optimizing the charge distribution of the active site of the enzyme and reduces the activation energy of the reaction. Hennefarth & Alexandrova, (2022) proposed an idea by which they emphasized the role of electrostatic preorganization in enzymatic catalysis, advocating for optimized long-range electrostatics in computational enzyme design to bridge efficacy gaps between artificial and natural enzymes, offering new strategies for bioengineering high-performance biocatalysts through EF modulation. EF changes the stability of the secondary structure and reduces the activity of lipase, polyphenol oxidase and other enzyme substances by polarizing the charged groups within the enzyme molecules (Bradshaw et al., 2020). The application of an external EF increases the active site of the enzyme, and the electrostatic complementarity between the substrate and the enzyme is improved, so the catalytic specificity is also increased. Zoi et al., (2017) used vibrational Stark spectroscopy and simulations to demonstrate that fast motions amplify EF near bond-breaking regions, thereby creating electrostatically favorable configurations for catalysis. Observed in ketosteroid isomerase and other enzymes, these dynamics-driven fields synergize with chemical steps, suggesting a universal mechanism where conformational flexibility optimizes electrostatic catalysis. The study of Peng et al., (2022) revealed that EF acts as a ‘smart reagent’, highlighting the role of electrostatic catalysis in modulating metalloenzyme reactivity. Li et al., (2022) demonstrated the role of PEF in modulating enzyme dynamics for improved catalytic function. They revealed that PEF enhanced alcalase activity by inducing partial unfolding of secondary structures and altering tertiary conformations, which optimize substrate binding through structural flexibility.

Third, research shows that EF affects protein stability through charge redistribution in two ways. To begin with, the EF induces the charged groups (such as amino and

carboxyl groups) on the protein surface to migrate or polarize, and the hydrogen bond, ionic bond or hydrophobic interaction are strengthened, protein aggregation caused by loose or even partially unfolded structures. Next, the charge released by EF can affect the electrostatic interactions within proteins, thereby enhancing their thermodynamic stability, and contribute to the stabilization of protein structures (Rodrigues et al., 2020).

Jia et al., (2018) revealed that -10 kV HVEF thawing inhibited free radical-mediated myofibrillar protein oxidation and preserved protein structure, enhancing gel texture/rheological properties compared to air thawing. Similarly, Amiri et al., (2019) suggested that higher electrodes boost surface charge and sulfhydryl reactivity, alter protein aggregation, and improve rheological properties, suggesting that optimized EF distribution enhances structural stability and functional attributes. Jia et al., (2020) demonstrated that HVEF thawing induces comparable sarcoplasmic protein denaturation in pork tenderloin to air and water methods. Fourier transform infrared spectrometer (FTIR) and principal component analysis (PCA) revealed structural shifted in Amide I regions, suggesting altered secondary configurations, yet no significant denaturation differences were observed via solubility or thermal analyses. Xie, et al., (2021) demonstrated the potential of LVEF for minimizing freezing-induced quality degradation. LVEF mitigated beef microstructure damage by enhancing muscle fiber compactness, reducing sarcomere Z-line fractures, and suppressing protein oxidation, while preserving secondary structures, demonstrating the efficacy of LVEF in maintaining beef quality during low temperature processing. This result was also confirmed in another study by Huang et al., (2023). The latter revealed that HVEF alters channel catfish myofibrillar protein properties voltage-dependently: lower voltages enhance solubility, zeta potential, and gelation by structural unfolding and charge stabilization, while higher voltages induced aggregation and denaturation, degrading functionality. Optimal 30 kV balanced structural preservation and improved physicochemical traits, guiding HVEF applications in aquatic protein processing.

4.4 Application of EF assisted low temperature storage in meat related to WHC

With the increasing application of EF in meat preservation, EF assisted low temperature storage has been continuously developed and optimized, demonstrating unique potential and advantages in enhancing the WHC of fresh meat. By inducing molecular polarization, regulating ice crystal formation, and applying torque, the EF enables multi-level interventions in the behavior of water molecules, providing a solid physical foundation for advancing low temperature preservation technologies in the meat industry (Suwandy et al., 2015).

First, the EF regulates the diffusion pathways of water molecules, thereby controlling the growth direction of ice crystals. The application of EF promotes the uniform nucleation of ice crystals and inhibits the formation of large ice crystals. This mechanism effectively minimizes the mechanical damage caused by ice crystals to cellular structures, reducing muscle fiber destruction during meat freezing, decreasing

drip loss, and significantly enhancing WHC after freezing and thawing (Wu et al., 2017). Xanthakis et al., (2013) were pioneers in applying HVEF to the freezing of pork tenderloin, revealing that the use of static electric fields (SEF) controls nucleation, reduces microstructural damage, and refines ice crystals. Field intensity critically modulated ice crystals size and supercooling, with negligible energy demand compared to conventional freezing. In a similar study, they concluded that EF freezing effectively reduced ice crystal size in pork and the degree of supercooling. This finding highlights its potential to mitigate freeze-induced microstructural damage through controlled ice crystallization (Xanthakis et al., 2013). In addition, Dalvi-Isfahan et al., (2016) revealed that EF freezing in lamb meat reduced ice crystal size by 60% and drip loss while preserving color and hardness, demonstrating energy efficient industrial potential for minimizing freezing damage and maintaining meat quality. A study of Xie, et al., (2021) demonstrated that LVEF mitigates texture and juiciness loss in beef steaks by accelerating freezing-thawing rates and enhancing WHC. It was revealed that synergistic LVEF and antifreeze treatment mitigated freeze-induced quality loss in steaks by modulating ice crystallization. The combination accelerated nucleation, reduced ice crystal size, and stabilized water distribution, minimizing thawing loss (Xie, et al., 2023).

Second, it is well known that water is a polar molecule. The presence of an EF induces the alignment of dipole moments in polar molecules, leading to the formation of an ordered structure (You et al., 2020). By reducing the random thermal motion of water molecules, the EF alters the phase transition dynamics of water, thereby enhancing the efficiency of freezing and thawing. Rahbari et al., (2018) used HVEF to thaw frozen chicken breasts. Compared to conventional static air thawing, HVEF thawing optimized chicken breast quality by reducing thawing time and enhancing myofibrillar WHC, despite drip loss fluctuations. Hu et al., (2021) demonstrated that LVEF combined with high humidity thawing optimized pork quality by reducing thawing time and centrifugation losses, enhancing WHC, and improving texture via microstructural preservation, offering a synergistic strategy for premium thawed meat production.

It is also worth noting that the interaction of water molecules with other macromolecular substances is also affected by EF. At the solid-liquid interface, such as the protein surface, the EF strengthens the interaction between water molecules and charged groups, facilitating the formation of an oriented adsorption layer. The study by Hartvig et al., (2011) confirmed this viewpoint. They revealed that a phenomenological adsorption model, which incorporates interfacial ion distribution, charge regulation, and mass balance, successfully predicted pH value and surface charge-dependent protein adsorption. By leveraging bulk-derived parameters, this model provides a universal framework for optimizing charged surfaces in biotechnological applications. Furthermore, EF could protect the conformation of protein and other biological macromolecules, reduce freezing degeneration and reduce the damage of myofibrillar structure. Qian et al., (2019) proved LVEF thawing's potential for minimizing quality deterioration in frozen beef processing. LVEF could efficiently reduce thawing time while preserving microstructure,

lowering thawing loss and promoting myofibrillar protein renaturation via enhanced ionic and hydrogen bonds. Similarly, the research of Amiri et al., (2019) showed that HVEF had an effect on the physicochemical properties of meat myofibrillar protein. During the thawing process, the integrity and functionality of myofibrillar protein were maintained and the shelf life of meat was extended. Xie, et al., (2023) pointed out that LVEF enhanced frozen beef WHC by suppressing myosin filament aggregation induced myofilament disarray. LVEF reduced myofibril density via regulated electrostatic/hydrophobic interactions and inhibited immobilized-to-free water migration, elevating myofibrillar WHC by 36%, providing mechanistic strategies for mitigating freeze induced meat quality deterioration.

5. Research question need to be answered

It is found that the external EF can influence various conductors, semiconductors, dielectrics, and charged particles within biological systems. By mediating the movement of these particles, EF can achieve the purpose of affecting the physiological and biochemical reactions of an organism (Fei et al., 2021). When applied as a preservation technology, EF primarily leverages the electrical properties of biological materials to release charges on charged particles in food, thereby stimulating their activity and inducing a series of physiological and biochemical reactions, collectively referred to as biological effects (Qi et al., 2022). Therefore, EF has been proven to be highly adaptable to diverse working environments and exhibits significant potential in enhancing WHC during low temperature storage of meat (Levkov et al., 2019). Studies have shown that the charges released by EF disrupt the equilibrium state of molecular clusters, thereby inhibiting water nucleation during cooling (Fei et al., 2021). Owing to this unique advantage, most of the research on EF preservation has focused on its applications in freezing, thawing, and refrigeration processes. It has demonstrated that HVEF thawing enhanced frozen rabbit meat quality by reducing thawing time, suppressing microbial growth, preserving WHC/texture, and minimizing myofibrillar protein denaturation, proving its industrial viability for premium meat processing (Jia et al., 2017). Mousakhani-Ganjeh et al., (2015) revealed that HVEF thawing accelerated thawing rates and enhanced total volatile binding nitrogen in tuna. Similarly, Li et al., (2017) used EF to thaw salted carp cubes, and they found that -12 kV HVEF thawing minimized time, microbial counts, and water loss in salted carp cubes while preserving inosine monophosphate (IMP) and modulating enzyme activities versus air/water methods.

Although the integration of EF with low temperature storage (CFPS) has demonstrated promising results in preserving meat moisture under freezing and refrigeration conditions, the mechanisms by which EF might support CFPS and enhance its preservation capabilities remain inadequately understood. Currently, this field is still in the early stages of theoretical exploration. Determining whether EF can overcome the inherent limitations of CFPS preservation and effectively address the critical challenge balancing ‘temperature-WHC-quality’ within CFPS has emerged as a significant area of interest for further research.

Reference

Abdelnaby, T., Feng, T., Tiantian, Z., Jiang, X., Yuming, W., Li, Z., & Xue, C. (2024). Impact of frozen storage on physicochemical parameters and quality changes in cooked crayfish. Heliyon, 10(11), e31649. https://doi.org/10.1016/j.heliyon.2024.e31649

Amiri, A., Mousakhani-Ganjeh, A., Shafiekhani, S., Mandal, R., Singh, A. P., & Kenari, R. E. (2019). Effect of high voltage electrostatic field thawing on the functional and physicochemical properties of myofibrillar proteins. Innovative Food Science & Emerging Technologies, 56, 102191. https://doi.org/10.1016/j.ifset.2019.102191

Bowker, B., & Zhuang, H. (2015). Relationship between water-holding capacity and protein denaturation in broiler breast meat1. Poultry Science, 94(7), 1657–1664. https://doi.org/10.3382/ps/pev120

Bradshaw, R. T., Dziedzic, J., Skylaris, C.-K., & Essex, J. W. (2020). The role of electrostatics in enzymes: Do biomolecular force fields reflect protein electric fields? Journal of Chemical Information and Modeling, 60(6), 3131–3144. https://doi.org/10.1021/acs.jcim.0c00217

Chan, S. S., Roth, B., Skare, M., Hernar, M., Jessen, F., Løvdal, T., Jakobsen, A. N., & Lerfall, J. (2020). Effect of chilling technologies on water holding properties and other quality parameters throughout the whole value chain: From whole fish to cold-smoked fillets of Atlantic salmon (Salmo salar). Aquaculture, 526, 735381. https://doi.org/10.1016/j.aquaculture.2020.735381

Chen, X., Dong, P., Li, K., Zhu, L., Yang, X., Mao, Y., Niu, L., Hopkins, D. L., Luo, X., Liang, R., & Zhang, Y. (2022). Effect of the combination of superchilling and super-chilled storage on shelf-life and bacterial community dynamics of beef during long-term storage. Meat Science, 192, 108910. https://doi.org/10.1016/j.meatsci.2022.108910

Chen, Y., Bassey, A. P., Bai, Y., Teng, S., Zhou, G., & Ye, K. (2022). Synergistic effect of static magnetic field and modified atmosphere packaging in controlling blown pack spoilage in meatballs. Foods, 11(10), Article 10. https://doi.org/10.3390/foods11101374

Choi, J., Shakeri, M., Kim, W. K., Kong, B., Bowker, B., & Zhuang, H. (2024). Water properties in intact wooden breast fillets during refrigerated storage. Poultry Science, 103(3), 103464. https://doi.org/10.1016/j.psj.2024.103464

Dalvi-Isfahan, M., Hamdami, N., & Le-Bail, A. (2016). Effect of freezing under electrostatic field on the quality of lamb meat. Innovative Food Science & Emerging Technologies, 37, 68–73. https://doi.org/10.1016/j.ifset.2016.07.028

Dalvi-Isfahan, M., Havet, M., Hamdami, N., & Le-Bail, A. (2023). Recent advances of high voltage electric field technology and its application in food processing: A review with a focus on corona discharge and static electric field. Journal of Food Engineering, 353, 111551. https://doi.org/10.1016/j.jfoodeng.2023.111551

Dimakopoulou-Papazoglou, D., Lazaridou, A., Biliaderis, C. G., & Katsanidis, E. (2022). Effect of process temperature on the physical state of beef meat constituents – implications on diffusion kinetics during osmotic dehydration. Food and Bioprocess Technology, 15(3), 706–716. https://doi.org/10.1007/s11947-022-02778-4

Estévez, M., Ventanas, S., Heinonen, M., & Puolanne, E. (2011). Protein carbonylation and water-holding capacity of pork subjected to frozen storage: Effect of muscle type, premincing, and packaging. Journal of Agricultural and Food Chemistry, 59(10), 5435–5443. https://doi.org/10.1634/stemcells.2004-0024

Fei, J., Ding, B., Koh, S. W., Ge, J., Wang, X., Lee, L., Sun, Z., Yao, M., Chen, Y., Gao, H., & Li, H. (2021). Mechanistic investigation of electrostatic field-enhanced water evaporation. Advanced Science, 8(18), 2100875. https://doi.org/10.1002/advs.202100875

Golberg, A., Sack, M., Teissie, J., Pataro, G., Pliquett, U., Saulis, G., Stefan, T., Miklavcic, D., Vorobiev, E., & Frey, W. (2016). Energy-efficient biomass processing with pulsed electric fields for bioeconomy and sustainable development. Biotechnology for Biofuels, 9(1), 94. https://doi.org/10.1186/s13068-016-0508-z

Guo, Y., Han, M., Chen, L., Zeng, X., Wang, P., Xu, X., Feng, X., & Lu, X. (2024). Pulsed electric field: A novel processing technology for meat quality enhancing. Food Bioscience, 58, 103645. https://doi.org/10.1016/j.fbio.2024.103645

Han, Y., Zhang, T., Guo, X., & Jiao, T. (2022). Insights into the mechanism of electrostatic field promoting ozone mass transfer in water: A molecular dynamics perspective. Science of The Total Environment, 848, 157710.

Hartvig, R. A., van de Weert, M., Østergaard, J., Jorgensen, L., & Jensen, H. (2011). Protein adsorption at charged surfaces: The role of electrostatic interactions and interfacial charge regulation. Langmuir, 27(6), 2634–2643. https://doi.org/10.1021/la104720n

He, X., Liu, R., Nirasawa, S., Zheng, D., & Liu, H. (2013). Effect of high voltage electrostatic field treatment on thawing characteristics and post-thawing quality of frozen pork tenderloin meat. Journal of Food Engineering, 115(2), 245–250. https://doi.org/10.1016/j.jfoodeng.2012.10.023

Hennefarth, M. R., & Alexandrova, A. N. (2022). Advances in optimizing enzyme electrostatic preorganization. Current Opinion in Structural Biology, 72, 1–8. https://doi.org/10.1016/j.sbi.2021.06.006

Hu, F., Qian, S., Huang, F., Han, D., Li, X., & Zhang, C. (2021). Combined impacts of low voltage electrostatic field and high humidity assisted-thawing on quality of pork steaks. LWT- Food Science and Technology, 150, 111987. https://doi.org/10.1016/j.lwt.2021.111987

Hu, R., Zhang, M., & Mujumdar, A. S. (2022). Novel assistive technologies for efficient freezing of pork based on high voltage electric field and static magnetic field: A comparative study. Innovative Food Science & Emerging Technologies, 80, 103087. https://doi.org/10.1016/j.ifset.2022.103087

Huang, H., Sun, W., Xiong, G., Shi, L., Jiao, C., Wu, W., Li, X., Qiao, Y., Liao, L., Ding, A., & others. (2020). Effects of HVEF treatment on microbial communities and physicochemical properties of catfish fillets during chilled storage. LWT - Food Science and Technology, 131, 109667. https://doi.org/10.1016/j.lwt.2020.109667

Huang, H., Xiong, G., Shi, L., Wu, W., Li, X., Qiao, Y., Liao, L., Ding, A., & Wang, L. (2021). Application of HVEF treatment in bacteriostasis against Acinetobacter radioresistens. Food Control, 124, 107914. https://doi.org/10.1016/j.foodcont.2021.107914

Huang, J., Que, F., Xiong, G., Qiao, Y., Wu, W., Wang, J., Ding, A., Liao, L., Shi, L., &

Wang, L. (2023). Physicochemical and functional properties changes in myofibrillar protein extracted from channel catfish by a high-voltage electrostatic field. Food and Bioprocess Technology, 16(2), 395–403. https://doi.org/10.1007/s11947-022-02937-7

Hülsheger, H., Potel, J., & Niemann, E.-G. (1983). Electric field effects on bacteria and yeast cells. Radiation and Environmental Biophysics, 22(2), 149–162. https://doi: 10.1007/BF01338893

Jia, G., Chen, Y., Sun, A., & Orlien, V. (2022). Control of ice crystal nucleation and growth during the food freezing process. Comprehensive Reviews in Food Science and Food Safety, 21(3), 2433–2454.

Jia, G., Liu, H., Nirasawa, S., & Liu, H. (2017). Effects of high-voltage electrostatic field treatment on the thawing rate and post-thawing quality of frozen rabbit meat. Innovative Food Science & Emerging Technologies, 41, 348–356. https://doi.org/10.1016/j.ifset.2017.04.011

Jia, G., Nirasawa, S., Ji, X., Luo, Y., & Liu, H. (2018). Physicochemical changes in myofibrillar proteins extracted from pork tenderloin thawed by a high-voltage electrostatic field. Food Chemistry, 240, 910–916. https://doi.org/10.1016/j.foodchem.2017.07.138

Jia, G., van den Berg, F., Hao, H., & Liu, H. (2020). Estimating the structure of sarcoplasmic proteins extracted from pork tenderloin thawed by a high-voltage electrostatic field. Journal of Food Science and Technology, 57(4), 1574–1578.

Kaale, L. D., Eikevik, T. M., Rustad, T., & Nordtvedt, T. S. (2014). Changes in water holding capacity and drip loss of Atlantic salmon (Salmo salar) muscle during superchilled storage. LWT - Food Science and Technology, 55(2), 528–535. https://doi.org/10.1016/j.lwt.2013.10.021

Kantono, K., Hamid, N., Oey, I., Wang, S., Xu, Y., Ma, Q., Faridnia, F., & Farouk, M. (2019). Physicochemical and sensory properties of beef muscles after pulsed electric field processing. Food Research International, 121, 1–11. https://doi.org/10.1016/j.foodres.2019.03.020

Kekez, M. M., Savic, P., & Johnson, B. F. (1996). Contribution to the biophysics of the lethal effects of electric field on microorganisms. Biochimica et Biophysica Acta (BBA) - Biomembranes, 1278(1), 79–88.

Kim, Y. H. B., Ma, D., Setyabrata, D., Farouk, M. M., Lonergan, S. M., Huff-Lonergan, E., & Hunt, M. C. (2018). Understanding postmortem biochemical processes and post-harvest aging factors to develop novel smart-aging strategies. Meat Science, 144, 74–90. https://doi.org/10.1016/j.meatsci.2018.04.031

Ko, W. C., Yang, S. Y., Chang, C. K., & Hsieh, C. W. (2016). Effects of adjustable parallel high voltage electrostatic field on the freshness of tilapia (Orechromis niloticus) during refrigeration. LWT - Food Science and Technology, 66, 151–157. https://doi.org/10.1016/j.lwt.2015.10.019

Kudra, T., & Martynenko, A. (2015). Energy aspects in electrohydrodynamic drying. Drying Technology, 33(13), 1534–1540.

Lan, Y., Shang, Y., Song, Y., & Dong, Q. (2016). Changes in the quality of superchilled rabbit meat stored at different temperatures. Meat Science, 117, 173–181.

Lawson, M. A. (2004). The role of integrin degradation in post-mortem drip loss in pork. Meat Science, 68(4), 559–566. https://doi.org/10.1016/j.meatsci.2004.05.019

Lee, H. J., Kwon, J. A., Kim, M., Lee, Y. E., Ryu, M., & Jo, C. (2023). Effect of supercooling on storage ability of different beef cuts in comparison to traditional storage methods. Meat Science, 199, 109137. https://doi.org/10.1016/j.meatsci.2023.109137

Lee, S., Park, D. H., Kim, E. J., Kim, H., Lee, Y., & Choi, M.-J. (2022). Development of temperature control algorithm for supercooling storage of pork loin and its feasibility for improving freshness and extending shelf life. Food Science of Animal Resources, 42(3), 467.

Léonard, N. G., Dhaoui, R., Chantarojsiri, T., & Yang, J. Y. (2021). Electric fields in catalysis: From enzymes to molecular catalysts. ACS Catalysis, 11(17), 10923–10932. https://doi.org/10.1021/acscatal.1c02084

Leong, S. Y., Burritt, D. J., & Oey, I. (2016). Effect of combining pulsed electric fields with maceration time on merlot grapes in protecting CACO-2 cells from oxidative stress. Food and Bioprocess Technology, 9(1), 147–160. https://doi.org/10.1007/s11947-015-1604-y

Levkov, K., Vitkin, E., González, C. A., & Golberg, A. (2019). A laboratory IGBT-based high-voltage pulsed electric field generator for effective water diffusivity enhancement in chicken meat. Food and Bioprocess Technology, 12(12), 1993–2003. https://doi.org/10.1007/s11947-019-02360-5

Li, D., Jia, S., Zhang, L., Wang, Z., Pan, J., Zhu, B., & Luo, Y. (2017). Effect of using a high voltage electrostatic field on microbial communities, degradation of adenosine triphosphate, and water loss when thawing lightly-salted, frozen common carp (Cyprinus carpio). Journal of Food Engineering, 212, 226–233. https://doi.org/10.1016/j.jfoodeng.2017.06.003

Li, J., Wang, Q., Liang, R., Mao, Y., Hopkins, D. L., Li, K., Yang, X., Luo, X., Zhu, L., & Zhang, Y. (2024). Effects and mechanism of sub-freezing storage on water holding capacity and tenderness of beef. Meat Science, 215, 109540. https://doi.org/10.1016/j.meatsci.2024.109540

Li, N., Zhang, Y., Wu, Q., Gu, Q., Chen, M., Zhang, Y., Sun, X., & Zhang, J. (2019). High-throughput sequencing analysis of bacterial community composition and quality characteristics in refrigerated pork during storage. Food Microbiology, 83, 86–94. https://doi.org/10.1016/j.fm.2019.04.013

Li, X., Wang, H., Mehmood, W., Qian, S., Sun, Z., Zhang, C., & Blecker, C. (2018). Effect of storage temperatures on the moisture migration and microstructure of beef. Journal of Food Quality, 2018, e3873179. https://doi.org/10.1155/2018/3873179

Li, X., Zhang, Y., Li, Z., Li, M., Liu, Y., & Zhang, D. (2017). The effect of temperature in the range of −0.8 to 4°C on lamb meat color stability. Meat Science, 134, 28–33. https://doi.org/10.1016/j.meatsci.2017.07.010

Li, Y., Zhang, S., Bao, Z., Sun, N., & Lin, S. (2022). Exploring the activation mechanism of alcalase activity with pulsed electric field treatment: Effects on enzyme activity, spatial conformation, molecular dynamics simulation and molecular docking parameters. Innovative Food Science & Emerging Technologies, 76, 102918. https://doi.org/10.1016/j.ifset.2022.102918

Li, Z., He, Q., Lai, J., Lin, J., Wu, S., Guo, Z., & Zheng, H. (2024). Effect of stepwise cooking on the water-retention capacity and protein denaturation degree of chicken breast. International Journal of Gastronomy and Food Science, 38,

101012. https://doi.org/10.1016/j.ijgfs.2024.101012

Lin, H., Wu, G., Hu, X., Chisoro, P., Yang, C., Li, Q., Blecker, C., Li, X., & Zhang, C. (2024). Electric fields as effective strategies for enhancing quality attributes of meat in cold chain logistics: A review. Food Research International, 193, 114839. https://doi.org/10.1016/j.foodres.2024.114839

Liu, F., Zhang, Y., Zeng, M., Duan, F., & Wang, J. (2025). Quantified low voltage electrostatic field: The effects of intensity on cherry tomato preservation and mechanism. Food Chemistry, 463, 141100. https://doi.org/10.1016/j.foodchem.2024.141100

Luo, Q., Wang, H., Zhang, X., & Qian, Y. (2005). Effect of direct electric current on the cell surface properties of phenol-degrading bacteria. Applied and Environmental Microbiology, 71(1), 423–427.

Ma, D., & Kim, Y. H. B. (2020). Proteolytic changes of myofibrillar and small heat shock proteins in different bovine muscles during aging: Their relevance to tenderness and water-holding capacity. Meat Science, 163, 108090. https://doi.org/10.1016/j.meatsci.2020.108090

Ma, Y., Wang, Y., Wang, Z., Chen, B., Xie, Y., Kong, L., Zhou, H., & Xu, B. (2023). Mechanisms of chicken processing quality changes during the early postmortem time: The role of the changes in myofibrillar protein. International Journal of Food Science & Technology, 58(4), 1775–1786. https://doi.org/10.1111/ijfs.16286

Matsumoto, M., Saito, S., & Ohmine, I. (2002). Molecular dynamics simulation of the ice nucleation and growth process leading to water freezing. Nature, 416(6879), Article 6879. https://doi.org/10.1038/416409a

Melody, J. L., Lonergan, S. M., Rowe, L. J., Huiatt, T. W., Mayes, M. S., & Huff-Lonergan, E. (2004). Early postmortem biochemical factors influence tenderness and water-holding capacity of three porcine muscles. Journal of Animal Science, 82(4), 1195–1205. https://doi.org/10.2527/2004.8241195x

Mi, H., Qian, C., Zhao, Y., Liu, C., & Mao, L. (2013). Comparison of superchilling and freezing on the microstructure, muscle quality and protein denaturation of grass carp (ctenopharyngodon Idellus). Journal of Food Processing and Preservation, 37(5), 546–554. https://doi.org/10.1111/j.1745-4549.2012.00678.x

Mol, S., Akan, T., Kartal, S., Coşansu, S., Tosun, Ş. Y., Alakavuk, D. Ü., Ulusoy, Ş., Doğruyol, H., & Bostan, K. (2023). Effects of air and helium cold plasma on sensory acceptability and quality of fresh sea bass (Dicentrarchus labrax). Food and Bioprocess Technology, 16(3), 537–548. https://doi.org/10.1007/s11947-022-02950-w

Moriya, K., Nakazawa, N., Osako, K., & Okazaki, E. (2019). Effect of subzero temperature treatment at −2 °C before thawing on prevention of thaw rigor, biochemical changes and rate of ATP consumption in frozen chub mackerel (Scomber japonicus). LWT, 114, 108396. https://doi.org/10.1016/j.lwt.2019.108396

Mousakhani-Ganjeh, A., Hamdami, N., & Soltanizadeh, N. (2015). Impact of high voltage electric field thawing on the quality of frozen tuna fish (Thunnus albacares). Journal of Food Engineering, 156, 39–44.

Ohshima, T., Tanino, T., Guionet, A., Takahashi, K., & Takaki, K. (2021). Mechanism of

pulsed electric field enzyme activity change and pulsed discharge permeabilization of agricultural products. Japanese Journal of Applied Physics, 60(6), 060501. https://doi.org/10.35848/1347-4065/abf479

Oswell, N. J., Gilstrap, O. P., & Pegg, R. B. (2021). Variation in the terminology and methodologies applied to the analysis of water holding capacity in meat research. Meat Science, 178, 108510. https://doi.org/10.1016/j.meatsci.2021.108510

Park, D. H., Lee, S., Kim, E. J., Jo, Y.-J., & Choi, M.-J. (2022). Development of a stepwise algorithm for supercooling storage of pork belly and chicken breast and its effect on freshness. Foods, 11(3), Article 3. https://doi.org/10.3390/foods11030380

Peng, W., Yan, S., Zhang, X., Liao, L., Zhang, J., Shaik, S., & Wang, B. (2022). How do preorganized electric fields function in catalytic cycles? The case of the enzyme tyrosine hydroxylase. Journal of the American Chemical Society, 144(44), 20484–20494. https://doi.org/10.1021/jacs.2c09263

Puolanne, E. (2022). Chapter 10—Developments in our understanding of water holding in meat. In P. Purslow (Ed.), New Aspects of Meat Quality (Second Edition) (pp. 237–263). Woodhead Publishing. https://doi.org/10.1016/B978-0-323-85879-3.00018-0

Qi, M., Yan, H., Zhang, Y., & Yuan, Y. (2022). Impact of high voltage prick electrostatic field (HVPEF) processing on the quality of ready-to-eat fresh salmon (Salmo salar) fillets during storage. Food Control, 137, 108918. https://doi.org/10.1016/j.foodcont.2022.108918

Qian, S., Hu, F., Mehmood, W., Li, X., Zhang, C., & Blecker, C. (2022). The rise of thawing drip: Freezing rate effects on ice crystallization and myowater dynamics changes. Food Chemistry, 373, 131461. https://doi.org/10.1016/j.foodchem.2021.131461

Qian, S., Li, X., Wang, H., Mehmood, W., Zhong, M., Zhang, C., & Blecker, C. (2019). Effects of low voltage electrostatic field thawing on the changes in physicochemical properties of myofibrillar proteins of bovine Longissimus dorsi muscle. Journal of Food Engineering, 261, 140–149. https://doi.org/10.1016/j.jfoodeng.2019.06.013

Qian, S., Li, X., Wang, H., Wei, X., Mehmood, W., Zhang, C., & Blecker, C. (2020). Contribution of calpain to protein degradation, variation in myowater properties and the water-holding capacity of pork during postmortem ageing. Food Chemistry, 324, 126892. https://doi.org/10.1016/j.foodchem.2020.126892

Rahbari, M., Hamdami, N., Mirzaei, H., Jafari, S. M., Kashaninejad, M., & Khomeiri, M. (2018). Effects of high voltage electric field thawing on the characteristics of chicken breast protein. Journal of Food Engineering, 216, 98–106. https://doi.org/10.1016/j.jfoodeng.2017.08.006

Rodrigues, R. M., Avelar, Z., Machado, L., Pereira, R. N., & Vicente, A. A. (2020). Electric field effects on proteins – Novel perspectives on food and potential health implications. Food Research International, 137, 109709. https://doi.org/10.1016/j.foodres.2020.109709

Sun, S., Zhao, J., Luo, Z., Lin, Q., Luo, F., & Yang, T. (2020). Systematic evaluation of the physicochemical properties and the volatile flavors of yak meat during chilled and controlled freezing-point storage. Journal of Food Science and Technology, 57(4), 1351–1361. https://doi.org/10.1007/s13197-019-04169-8

Sun, T. L., Zhang, P., Ren, Z. H., Zhang, P., & Yue, X. Q. (2013). Optimization of the combination of three natural preservatives in beef storage with controlled freezing point technique. Advanced Materials Research, 781–784, 1700–1707. https://doi.org/10.4028/www.scientific.net/AMR.781-784.1700

Suwandy, V., Carne, A., van de Ven, R., Bekhit, A. E.-D. A., & Hopkins, D. L. (2015). Effect of repeated pulsed electric field treatment on the quality of cold-boned beef loins and topsides. Food and Bioprocess Technology, 8(6), 1218–1228. https://doi.org/10.1007/s11947-015-1485-0

Wang, C., Chu, J., Fu, L., Wang, Y., Zhao, F., & Zhou, D. (2018). iTRAQ-based quantitative proteomics reveals the biochemical mechanism of cold stress adaption of razor clam during controlled freezing-point storage. Food Chemistry, 247, 73–80. https://doi.org/10.1016/j.foodchem.2017.12.004

Wang, H. H. (2022). The perspective of meat and meat-alternative consumption in China. Meat Science, 194, 108982. https://doi.org/10.1016/j.meatsci.2022.108982

Wang, L., Liu, Z., Dong, S., Zhao, Y., & Zeng, M. (2014). Effects of vacuum and modified atmosphere packaging on microbial flora and shelf-life of pacific white shrimp (Litopenaeus vannamei) during controlled freezing-point storage at −0.8°C. Food Science and Technology Research, 20(6), 1141–1152. https://doi.org/10.3136/fstr.20.1141

Wang, Q., Li, Y., Sun, D.-W., & Zhu, Z. (2018). Enhancing food processing by pulsed and high voltage electric fields: Principles and applications. Critical Reviews in Food Science and Nutrition, 58(13), 2285–2298. https://doi.org/10.1080/10408398.2018.1434609

Wang, Y., Chang, J., Wang, M., Zhang, Y., Han, L., & Ren, G. (2024). Effect of the composition of coating water retaining agent on the quality of conditioned chicken meatballs after frozen storage. Food Control, 166, 110752. https://doi.org/10.1016/j.foodcont.2024.110752

Wang, Z., He, Z., Gan, X., & Li, H. (2018). Interrelationship among ferrous myoglobin, lipid and protein oxidations in rabbit meat during refrigerated and superchilled storage. Meat Science, 146, 131–139. https://doi.org/10.1016/j.meatsci.2018.08.006

Warner, R. D. (2024). Chemical and physical characteristics of meat—Water-holding capacity. In M. Dikeman (Ed.), Encyclopedia of Meat Sciences (Third Edition) (pp. 405–418). Elsevier. https://doi.org/10.1016/B978-0-323-85125-1.00164-2

Wu, G., Yang, C., Bruce, H. L., Roy, B. C., Li, X., & Zhang, C. (2023). Effects of alternating electric field assisted freezing-thawing-aging sequence on longissimus dorsi muscle microstructure and protein characteristics. Food Chemistry, 409, 135266. https://doi.org/10.1016/j.foodchem.2022.135266

Wu, X.-F., Zhang, M., Adhikari, B., & Sun, J. (2017). Recent developments in novel freezing and thawing technologies applied to foods. Critical Reviews in Food Science and Nutrition, 57(17), 3620–3631. Scopus. https://doi.org/10.1080/10408398.2015.1132670

Xanthakis, E., Havet, M., Chevallier, S., Abadie, J., & Le-Bail, A. (2013). Effect of static electric field on ice crystal size reduction during freezing of pork meat. Innovative Food Science & Emerging Technologies, 20, 115–120. https://doi.org/10.1016/j.ifset.2013.06.011

Xie, Y., Chen, B., Guo, J., Nie, W., Zhou, H., Li, P., Zhou, K., & Xu, B. (2021). Effects of low voltage electrostatic field on the microstructural damage and protein structural changes in prepared beef steak during the freezing process. Meat Science, 179, 108527. https://doi.org/10.1016/j.meatsci.2021.108527

Xie, Y., Zhou, K., Chen, B., Al-Dalali, S., Li, C., Wang, Y., Wang, Z., Zhou, H., Li, P., & Xu, B. (2023). Synergism effect of low voltage electrostatic field and antifreeze agents on enhancing the qualities of frozen beef steak: Perspectives on water migration and protein aggregation. Innovative Food Science & Emerging Technologies, 84, 103263. https://doi.org/10.1016/j.ifset.2022.103263

Xie, Y., Zhou, K., Chen, B., Ma, Y., Tang, C., Li, P., Wang, Z., Xu, F., Li, C., Zhou, H., & Xu, B. (2023). Mechanism of low-voltage electrostatic fields on the water-holding capacity in frozen beef steak: Insights from myofilament lattice arrays. Food Chemistry, 428, 136786. https://doi.org/10.1016/j.foodchem.2023.136786

Xie, Y., Zhou, K., Chen, B., Wang, Y., Nie, W., Wu, S., Wang, W., Li, P., & Xu, B. (2021). Applying low voltage electrostatic field in the freezing process of beef steak reduced the loss of juiciness and textural properties. Innovative Food Science & Emerging Technologies, 68, 102600. https://doi.org/10.1016/j.ifset.2021.102600

Xu, B., Zhang, Q., Zhang, Y., Yang, X., Mao, Y., Luo, X., Hopkins, D. L., Niu, L., & Liang, R. (2023). Sous vide cooking improved the physicochemical parameters of hot-boned bovine semimembranosus muscles. Meat Science, 206, 109326. https://doi.org/10.1016/j.meatsci.2023.109326

You, Y., Her, J.-Y., Shafel, T., Kang, T., & Jun, S. (2020). Supercooling preservation on quality of beef steak. Journal of Food Engineering, 274, 109840. https://doi.org/10.1016/j.jfoodeng.2019.109840

Zhang, H., Cao, Y., Dong, X., Li, X., & Zhang, C. (2023). Effect of different postmortem ageing conditions on physicochemical properties, structure and water-holding capacity of pork. International Journal of Food Science & Technology, 58(3), 1662–1672. https://doi.org/10.1111/ijfs.16182

Zhang, Y., Magro, A., Puolanne, E., Zotte, A. D., & Ertbjerg, P. (2021). Myofibrillar protein characteristics of fast or slow frozen pork during subsequent storage at −3 °C. Meat Science, 176, 108468. https://doi.org/10.1016/j.meatsci.2021.108468

Zheng, D.-J., Liu, H.-J., Cheng, Y.-Q., & Li, L.-T. (2011). Electrode configuration and polarity effects on water evaporation enhancement by electric field. International Journal of Food Engineering, 7(2).

Zhou, G. H., Xu, X. L., & Liu, Y. (2010). Preservation technologies for fresh meat – A review. Meat Science, 86(1), 119–128. https://doi.org/10.1016/j.meatsci.2010.04.033

Zhu, Y., Zhang, K., Ma, L., Huo, N., Yang, H., & Hao, J. (2015). Sensory, physicochemical, and microbiological changes in vacuum packed channel catfish (Clarias lazera) patties during controlled freezing-point storage. Food Science and Biotechnology, 24(4), 1249–1256. https://doi.org/10.1007/s10068-015-0160-6

Zoi, I., Antoniou, D., & Schwartz, S. D. (2017). Electric fields and fast protein dynamics in enzymes. The Journal of Physical Chemistry Letters, 8(24), 6165–6170. https://doi.org/10.1021/acs.jpclett.7b02989

Zuo, H., Han, L., Yu, Q., Niu, K., Zhao, S., & Shi, H. (2016). Proteome changes on water-

holding capacity of yak longissimus lumborum during postmortem aging. Meat Science, 121, 409–419. https://doi.org/10.1016/j.meatsci.2016.07.010

Zuo, H., Wang, P., Guo, Z., Luo, X., Zhang, Y., & Mao, Y. (2022). Metabolites analysis on water-holding capacity in beef longissimus lumborum muscle during postmortem aging. Metabolites, 12(3), Article 3. https://doi.org/10.3390/metabo12030242

Chapter 2

Objectives, Research overview and Thesis outline

1. Objectives

The present thesis aimed to (1) determine whether electrostatic field (EF) could improve the water holding capacity (WHC) of fresh meat during controlled freezing point storage (CFPS), (2) investigate the optimal conditions under which EF can assist CFPS to improve the WHC of muscle, (3) analyze whether EF has positive effects on the retention of water molecules in muscle tissue, (4) explore whether EF could enhance electrostatic interactions between proteins, thereby improving the structural and functional characteristics of proteins and strengthening the connection between proteins and water molecules.

2. Research overview

An overview of this thesis is shown in Fig. 6. Several experiments were performed to investigate the effect of EF assisted CFPS on the WHC of chilled fresh meat. The EF generation equipment was built by ourselves in the laboratory, and the voltage range used was between 0 and 16 kV, effectively covering both, a high voltage EF (HVEF) and a low voltage EF (LVEF).

In the first two chapters, we established different EF conditions to explore whether different modes of EF action would help to extend the shelf life of chilled fresh meat. Additionally, we examined the behavior of water molecules within muscle tissue under EF. After clarifying the effect of EF on water molecules, we further analyzed whether the interaction between protein and water molecules would be affected by EF, and explored the mechanism of EF on water molecules from another perspective.

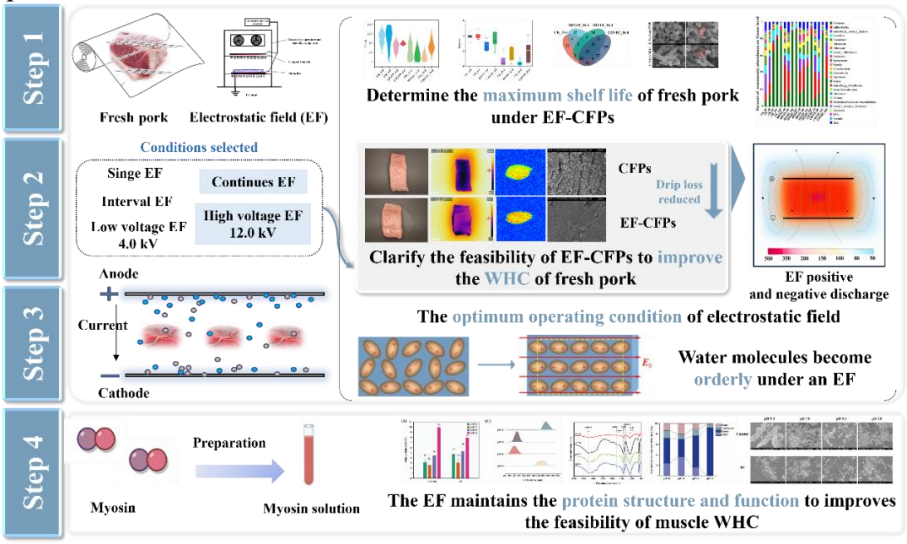

Figure 6. The outline figure of the thesis.

More specifically, in steps 1 and 2, four distinct EF treatment protocols were implemented: no EF, single-used HVEF, interval-used HVEF, and continuous-used

HVEF. These treatments were applied to fresh pork samples stored under CFPS conditions (−1.0 ± 0.5 °C). The study quantitatively assessed the pH value, total viable count (TVC), total volatile basic nitrogen (TVB-N), thiobarbituric acid reactive substances (TBARS), and microbial community dynamics. Additionally, WHC was systematically monitored throughout the storage period. The study aimed to evaluate the potential of EF assisted CFPS technology in enhancing moisture retention and extending pork shelf life, while simultaneously identifying optimal EF application modalities through comparative assessment. Additionally, the investigation sought to elucidate the interdependent relationship between microbial proliferation dynamics and moisture content evolution during storage.

In step 3, the optimal EF modality (continuous-used HVEF) identified through steps 1 and 2, was applied to early postmortem pork samples. The transition from stored pork to postmortem pork was driven by the critical observation that rapid moisture variation during the initial postmortem period significantly influences WHC during subsequent storage. The investigation in step 3 focused on elucidating the effects of high and low voltage EF on the patterns of moisture retention, with particular emphasis on moisture distribution within muscle, microstructural modifications of muscle fibers, and the interaction between actomyosin dissociation and combination, which is an essential factor in maintaining muscle fiber integrity.

In step 4, the effects of EF on myosin structure and function at different pH values were investigated. Myosin was selected as target protein to establish myosin protein solution models (MYPs) at 4 different pH conditions (9.0, 7.0, 5.0, 3.0). The EF parameters were optimized, selecting continuous EF from step 1 and 2 and high voltage EF from step 3 based on superior performance. The MYPs treated with and without the application of 12.0 kV HVEF for 6 h. The changes of secondary structure, microstructure, oxidation properties, texture properties and thermal processing properties of MYPs were comprehensively analyzed. The purpose of this step is to further reveal the internal mechanism of EF maintaining WHC in fresh meat, which may be related to maintaining the structural and functional activities of the protein.

3. Thesis outline

Chapter 1 is a general introduction.

Chapter 2 includes the objectives, research overview and thesis outline.

In **Chapter 3** the *longissimus dorsi* muscle of pork was selected as the research subject. Various modes of EF action (no EF, single-used HVEF, interval-used HVEF, continuous-used HVEF) were employed to assist the CFPS process. The variations in freshness of the chilled fresh meat were studied. In addition, the changes in pH value, total viable content (TVC), total volatile basic nitrogen (TVB-N), and bacterial

community composition of the muscle were detected for the different treatments. We also determined whether the shelf life of the chilled fresh meat could be extended by EF assisted CFPS. Additionally, the changes of the WHC of chilled fresh meat were assessed. Changes of storage loss, centrifugal loss, cooking loss, and water migration of muscle were examined for the different treatments. The results showed that HVEF could effectively prolong the shelf-life of pork to 16 days by inhibiting the growth of bacteria during storage and maintaining the stability of water molecules of chilled fresh meat, indicating that HVEF had the potential to be used in meat preservation.

Publication of Chapter 3

Xu, Y., Wen, X., Zhang, D., Schroyen M., Wang D., Li X., Hou C. Changes in the freshness and bacterial community of fresh pork in controlled freezing point storage assisted by different electrostatic field usage frequencies. *Food Bioprocess and Technology* 17, 939–954 (2024).

https://doi.org/10.1007/s11947-023-03180-4

Xu, Y., Zhang, D., Xie, F., Li X., Schroyen M., Chen L., Hou C. Changes in water holding capacity of chilled fresh pork in controlled freezing-point storage assisted by different modes of electrostatic field action. *Meat Science* 204, 109269 (2024).

https://doi.org/10.1016/j.meatsci.2023.109269

Chapter 4 investigated the different intensities of EF assisted CFPS after slaughter for 5 days. The applied EFs were 4.0 kV (low voltage EF) and 12.0 kV (high voltage EF). In this chapter, the WHC of muscle was examined by comparing the change in properties such as cooking loss, moisture distribution, myofibril fragmentation index (MFI), muscle microstructure, protein particle size, and secondary structure of actomyosin. Furthermore, actomyosin degradation and dissociation were evaluated using SDS-PAGE and Western-Blot. The overall objective of this study was to investigate the impact of different EF intensities assisting CFPS on the WHC of fresh meat during the early postmortem period. This chapter attempted to evaluate the mechanism by which the EF influences WHC of fresh meat, focusing on the interaction between actin and myosin, including their combination and dissociation. The results showed that the HVEF treatment had an impact on the distribution and fluidity of intermuscular water molecules during the early postmortem period. Additionally, it is suggested that the EF may facilitate the dissociation of actomyosin in the post-mortem period, thereby contributing to an increase in muscle WHC.

Publication of Chapter 4

Xu, Y., Leng, D., Li, X., Wang D., Chai X., Schroyen M., Zhang, D., Hou C. Effects of different electrostatic field intensities assisted controlled freezing point storage on water holding capacity of fresh meat during the early postmortem period. *Food Chemistry* 439, 138096 (2024).

https://doi.org/10.1016/j.foodchem.2023.138096

In **Chapter 5** we selected myosin as the target protein to establish myosin models at 4 different pH value conditions (9.0, 7.0, 5.0, 3.0). The changes of secondary structure, microstructure, oxidation properties, texture properties and thermal processing properties of myosin with and without the application of HVEF were comprehensively analyzed. This chapter attempts to explain how the HVEF maintains the integrity of myosin at different pH values from the perspective of maintaining the structure and function of protein, thereby enhancing the WHC of meat. The results showed that the HVEF could enhance the electrostatic interaction between proteins by releasing electric charges, thereby improving the structural and functional characteristics of proteins damaged at all pH values. This may be beneficial to the future elucidation of the mechanism by which HVEF enhances the WHC in muscle.

Publication of Chapter 5

Xu, Y., Leng, D., Schroyen M., Li, X., Wang D., Zhang, D., Hou C. Structure and functional properties of myosin induced by electrostatic fields at different pH values. *Innovative Food Science & Emerging Technologies*, 102, 104004 (2025).

https://doi.org/10.1016/j.ifset.2025.104004

Chapter 6 is the general discussion, conclusion and perspectives.

Chapter 3

Changes in the storage quality of chilled fresh pork in CFPs assisted by different modes of EF action

In this chapter the *longissimus dorsi* muscle of pork was selected as research subject. Various modes of EF action (no EF, single-used HVEF, interval-used HVEF, continuous-used HVEF) were employed to assist the CFPS process. The variations in freshness of the chilled fresh pork were studied. In addition, the changes in pH value, total viable content (TVC), total volatile basic nitrogen (TVB-N), and bacterial community composition of the muscle were detected for the different treatments. We also determined whether the shelf life of the chilled fresh pork could be extended by EF assisted CFPS. Additionally, the changes of the WHC of chilled fresh pork were assessed. Changes of storage loss, centrifugal loss, cooking loss, and water migration of muscle were examined for the different treatments. The results showed that HVEF could effectively prolong the shelf-life of pork to 16 days by inhibiting the growth of bacteria during storage and maintaining the stability of water molecules of chilled fresh pork, indicating that HVEF had the potential to be used in meat preservation.

This chapter is adapted from:

Xu, Y., Wen, X., Zhang, D., Schroyen M., Wang D., Li X., Hou C. Changes in the freshness and bacterial community of fresh pork in controlled freezing point storage assisted by different electrostatic field usage frequencies. Food Bioprocess and Technology 17, 939–954 (2024).

https://doi.org/10.1007/s11947-023-03180-4

Xu, Y., Zhang, D., Xie, F., Li X., Schroyen M., Chen L., Hou C. Changes in water holding capacity of chilled fresh pork in controlled freezing-point storage assisted by different modes of electrostatic field action. Meat Science 204, 109269 (2024).

https://doi.org/10.1016/j.meatsci.2023.109269

1. Abstract

CFPS assisted by the EF has been proven to maintain the quality of fresh pork effectively. In this study, we evaluated the freshness and WHC variation of pork under CFPS assisted by different high voltage EF (HVEF) action, including single used HVEF (SHVEF), interval used HVEF (IHVEF) and continuous used HVEF (CHVEF). The pH value, total volatile basic nitrogen (TVB-N), total viable count (TVC), bacterial community composition and water holding capacity (WHC) were determined. The results showed that the pH value in the three groups gradually decreased, while the TVB-N and TVC increased along with the growth of bacteria. The IHVEF and CHVEF treatment effectively delayed the decrease in pH value and significantly reduced the overall level of TVC and TVB-N in chilled fresh pork at a later storage period ($P < 0.05$). Bacterial community composition analysis showed that the dominant bacteria in all three treatments were *Pseudomonas*, *Latilactobacillus*, and *Brochothrix*, and HVEF treatment can significantly decrease their diversity and abundance ($P < 0.05$). The functional analysis showed that HVEF treatment has influenced the pathways of amino acid metabolism, carbohydrate metabolism, and energy metabolism during CFPS. In addition, it was determined that the moisture loss of the CHVEF treatment lower than other groups ($P < 0.05$). This difference was proven by analyzing the moisture content, storage loss, centrifugal loss, cooking loss, and nuclear magnetic resonance imaging. It suggests that CFPS assisted by EF could promote the WHC of chilled fresh pork during long-term storage. In conclusion, the HVEF treatment has significant ($P < 0.05$) inhibitory effect against dominant bacteria, improved the WHC of chilled fresh pork. These results could provide theoretical guidance for the possible application of HVEF technology in CFPS preservation of meat.

Keywords

EF, CFPS, Total viable count, Total volatile basic nitrogen, Bacteria community composition change, WHC, Chilled fresh pork

2. Introduction

Fresh meat is popular with consumers due to its better color, flavor, and nutritional value (Li et al., 2017; Sun et al., 2020). However, fresh meat was prone to a series of complicated physicochemical reactions during controlled freezing point storage (CFPS), such as the growth and multiplication of bacteria and the inevitable moisture loss (Chen et al., 2022; Sun et al., 2013; Wang et al., 2018). At this time, the reasonable approach to tackle this issue could be using specific assisted technologies to achieve good preservation quality of fresh meat (Sun et al., 2013; Zhu et al., 2015).

In the last decade, electric field has been proposed as a preservation technology applied in research and industry to mitigate the deterioration of meat and enhance the WHC of meat (Alahakoon et al., 2019; Ding et al., 2016; Huang et al., 2021; Huang et al., 2023; Qi et al., 2022). Different from the pulsed electric field, the EF interventions features a simpler system, lower equipment cost and energy consumption, also provides a stationary field that could effectively reduce the growth and reproduction of bacteria during chilled storage (Huang et al., 2020; Hussain et al., 2021; Pavlin et al., 2007; Wang et al., 2018; Yan et al., 2017). Huang et al. (2020) found that HVEF could inhibit the growth of *Acinetobacter* and *Streptococcus* and effectively extend the shelf life of catfish fillets at 4°C. Qi et al. (2021) reported a similar finding that HVEF treatment could damage cell membrane integrity, morphology, and esterase activity of *Staphylococcus aureus* when the voltage was higher than 10 kV, which effectively enhanced the antibacterial rate of HVEF at 4°C. Moreover, Li et al. (2017) showed that HVEF treatment could significantly reduce the total viable count and the abundance of *Pseudomonas* and *Lactic acid* bacteria after 8 days of refrigeration storage. In addition, lots of research has proven that the EF could assist low temperature storage to reduced drip loss (Dalvi-Isfahan et al., 2016). Li et al., (2017) found that the use of EF assisted frozen fish for 8 consecutive days could reduce drip loss. Xu et al., (2020) investigated dry-cured beef stored for 14 days under a high voltage EF and still maintain a positive WHC. Rahbari et al., (2018) emphasized that using the high voltage EF for a short time (40 min) could improve the thawing rate and the WHC of the meat. Similarly, Dalvi-Isfahan et al., (2016) applied short-term EF to freezing meat and found that drip loss of meat was reduced. However, whether it is for the evaluation of meat freshness or WHC, the current research on EF was mainly focused on freezing, thawing and part of refrigerating. The optimum conditions for EF assisted CFPS are not yet determine. In this study, whether the combination of HVEF and CFPS could contribute to further improving the antibacterial and WHC performance of chilled fresh pork become the focus of this study.

Therefore, this study evaluated the effect of different HVEF action (single HVEF, interval HVEF, and continuous HVEF) on the freshness and WHC of pork during CFPS. The changes of freshness index (pH value; total viable count, TVC; total volatile basic nitrogen, TVB-N, bacterial community diversity) and WHC index (moisture content, cooking loss, storage loss, centrifugal loss, T_2 transverse relaxation, H-proton density imaging spectra) during storage were determined. This work will provide information for maintaining the storage quality of chilled fresh pork.

3. Materials and methods

3.1 Materials

The *M. Longissimus thoracis et lumborum* (LTL) muscles were procured from 5 carcasses (Landrace × Yorkshire × Duroc pig, six-month-old, 75 kg live weight). The pigs were collected in the Beijing Shunxin Agricultural Co., Ltd. Pengcheng Food Branch by standard procedure. The visible fat, ligaments, and tendons of LTL muscles were taken out. The muscles were packaged in sterile bags and transported to the laboratory in a portable chilled box (0~4°C) within 2 hours. Each pig's LTL muscle (size, length × width: 22~24 cm × 10~12 cm; weight: 1.2 kg) was cut into 17 pieces, wrapped with polyethylene film (PE; thickness: 150 μm, oxygen permeance ratio: 4.0 m^3/m^2/24 hr, water vapor permeability: 4.5 cm^3/m^2/24 hr). PE film was selected for three primary reasons. Firstly, our previous research confirmed it does not impede the penetration of the electrostatic field (EF), unlike other materials. Secondly, as a common, low-cost cling film with moderate oxygen permeability, PE is widely used in supermarket meat packaging, ensuring practical relevance. Finally, in our pilot tests, unwrapped meat in the air-cooled chamber developed severe surface desiccation, forming a hard "crust" that compromised sample integrity. The PE wrap effectively prevented this moisture loss.

Sixteen pieces from each pig's LTL muscle were randomly allocated to four treatment groups for respective storage times. The four treatment groups were as follows: the control group samples (CK) were stored with no HVEF; the single-used HVEF (SHVEF) group samples were treated with 12.0 kV HVEF for 48 h and then stopped using HVEF until the end of storage; the interval-used HVEF (IHVEF) group samples treated with 12.0 kV HVEF every 24 h interval until the end of storage; the continuous-used HVEF (CHVEF) group samples were continuously treated with 12.0 kV HVEF until the end of storage. The last piece was selected as the sample for day 0.

All the sample were constantly stored at -1.0 ± 0.5°C in a constant temperature and humidity equipment (JYH-103, HENGWELL Co. Ltd., Shanghai, China, volume: 256 L). During the storage period, the weather meter (Kestrel 5500, NIELSEN-KELLERMAN Co. Ltd., Minneapolis, USA) were used to test temperature change in the constant temperature and humidity equipment. The temperature range was maintained at about −1 ± 0.2°C, ensuring that the LTL of the pig were constantly stored at CFPS.

The storage temperature of -1.0 ± 0.5°C was selected for the experiments based on the previously determined thermal properties of the LTL muscle used in this study, Preliminary investigations, specifically a study measuring the freezing points of different porcine carcass sections, established that the mean freezing point for the LTL muscle is -1.41 ± 0.20°C, with a mean supercooling point of -2.67 ± 0.12°C. Consequently, the temperature of -1.0 ± 0.5°C was chosen to maintain the meat in a

stable superchilled state, precisely within the crucial temperature window between its supercooling and freezing points to achieve the desired CFPS effects.

Two constant temperature and humidity equipment (A and B) of the same brand and model were used to allocate four treatment groups. Equipment A was connected to the EF, and equipment B was not. CK group was put into equipment B. SHVEF group was put into equipment B after a stay in equipment A for 48 h. IHVEF group was put into equipment A for 24 hours, transferred to equipment B for 24 hours regarding as a cycle, and cycle 8 times until the end of the storage period. CHVEF group constantly stayed in equipment A.

Samples were obtained in each treatment group at 4-day intervals. The pH value, moisture content, cooking loss, storage loss, centrifugal loss, T_2 transverse relaxation and H-proton density imaging spectra was measured immediately after sample splitting. Twenty-five grams of samples were cryopreserved in liquid nitrogen and used to measure the TVC, TVB-N, and bacteria community.

3.2 High voltage EF treatment system

A new facility was constructed for this experiment (Fig. 7). It comprises a direct current DC electrostatic field generator (TCM6000i, TAISIMAN Co. Ltd., Dalian, China, output voltage: 0~30.0 kV, output power: 30.0 W, input frequency: 60.0 Hz, rated current:1.0 mA, with an accuracy of ± 0.01%), a constant temperature and humidity equipment, a treatment platform.

The constant temperature and humidity equipment was wrapped in acrylic insulating tape to prevent the machine from being damaged. The HVEF generator output port connects to two copper boards. The samples were set between those two boards, and the distance between the two boards was 10.0 cm. The HVEF experimental system was set up in a laboratory with a fixed temperature (-1.0 ± 0.5℃) and humidity (85.0 ± 0.5%).

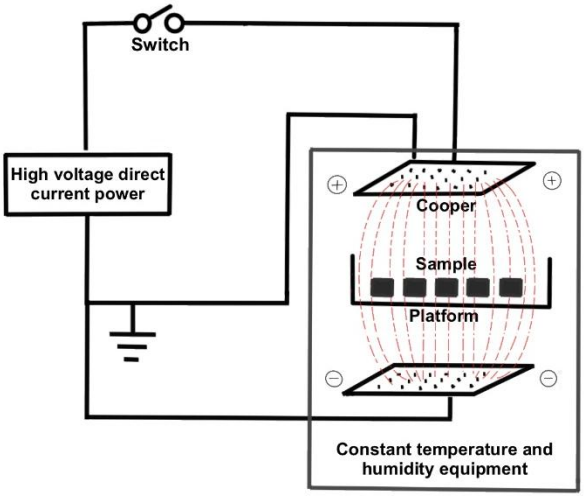

Figure 7. Equipment for EF radiation and temperature control.

3.3 pH value determination

A portable pH meter (Testo 205, SE & KGaA Co. Ltd., Testo, Schwarzwald, German) was used for the pH value measurements of samples. After calibration with pH standard buffers, the meter was directly inserted into the samples about 1.5 cm deeply and measured at different locations 4 times.

3.4 Total viable count (TVC) determination

The TVC analysis were analyzed according to the method described with some modifications (Qi et al., 2022). Ten grams of samples were homogenized with 90 mL sterilized water using a tap homogenizer (HX-4, HUXISHIYE Co. Ltd., Shanghai, China) for 2 min. One mL of the aliquot was mixed with 9 mL of sterile saline to prepare the dilution. Select the appropriate concentration (100 μL) of dilutions, put onto Plate Count Agar (PCA agar; LUQIAO Co. Ltd., Beijing, China) in duplicate and incubated at 37°C for 48 h.

3.5 Total volatile basic nitrogen (TVB-N) determination

The TVB-N was investigated according to the Chinese standard GB 5009.228-2016, 2016. Ten grams of sample was mixed completely with 50 mL distilled water, filtered after vibration for 30 min and then stored at 4°C. Adding 5 mL of 10 g/L magnesium oxide suspension fluid into 5 mL filtrate, then distilled using the Auto Kjeldahl Analysis Equipment (KJELTEC 8200, Foss Co., Hilleroed, Denmark). The distillate was put into a conical flask with indicator (1:5, methyl red ethanol solution, and bromocresol green ethanol solution). The TVB-N was calculated as follows (1):

$$\text{TVB-N (unit mg/100 g)} = (V1-V2)\times C\times 14/m\times 5/100\times 100 \quad (1)$$

The sample solution titration volume is denoted as V1, while V2 represents the control group titration volume. The concentration of the standard HCl solution titrant is noted as C, and m denotes the mass of sample.

3.6 The 16S rRNA sequencing determination

Bacterial DNA was extracted from each sample using the E.Z.N.A. soil DNA Kit (Omega Bio-tek, Norcross Co., Georgia, United States). PCR amplification was performed with primers 338F and 806R to target the V3-V4 region of the 16S rRNA gene. The PCR procedure was performed according to Wen et al. (2022) described. All the sequencing was conducted on the Illumina MiSeq PE300 platform/NovaSeq PE250 platform (Illumina, San Diego, California, United States). All the raw data have been saved in NCBI Sequence Read Archive (SRA) under BioProject ID (SUB13202242). The paired-end sequencing reads underwent demultiplexing and

quality filtering. Next, UPARSE (version 7.1) was used to cluster operational taxonomic units (OTUs) at a 97% similarity threshold. The resulting OTU representative sequences were subjected to taxonomic classification using the RDP naive Bayesian Classifier (version 2.2) with a confidence threshold of 0.7. The taxonomic information was obtained by querying the Silva database.

3.7 Bacterial community composition analysis

The effective sequences were obtained after merging and screening of the raw sequencing data through QIIME (version 1.8.0) and FLASH (version 1.2.7). The UCLUST algorithm was used to cluster the remaining sequences into operational taxonomic units (OTUs) with a similarity threshold of 97%. Taxonomic classification was performed using the SILVA database. The Chao1 and Shannon value were calculated using QIIME and R packages (version 3.2.0), while QIIME and R software were used to examine OTU distributions at the phylum and genus levels. Hierarchical clustering analysis using the weighted UniFrac distance was carried out by QIIME and R software. Additionally, to further investigate the bacterial community differences among different treatments, the linear discriminant analysis effect size (LEfSe) and PICRUSt2 were applied, which were used to estimate the magnitude of the impact of each component (species) abundance on the differential effect and obtain the level of metabolic pathway information and abundance tables based on the Kyoto Encylopaedia of Genes and Genomes (KEGG) database for each level.

3.8 Moisture content determination

The sample weight of all samples was about 4.0 ± 0.2 g and recorded as M1. Samples were precisely weighed and dried at 105°C for 6 h until constant weight. After that, the samples were removed from the drying oven, and the weight then measured was reported as M2. The moisture content is calculated by Eq. (2):

$$\text{Moisture content (\%)} = (M1-M2)/M1 \times 100 \quad (2)$$

3.9 Cooking loss determination

The cooking loss determination was measured as reported by Hopkins et al., (2010) with some modifications. Samples have taken from different treatment groups at the storage time of 4, 8, 12, and 16 days, and simultaneous determination of samples from different treatment groups at the same time point. The sample weight was about 20.00 ± 0.05 g and recorded as M3, placed in sterile bags, and the air was extracted from the bag. Then, the sample in the bag was cooked in a constant temperature water bath at 71°C. Subsequently, bags were kept under running water and cooled down to room temperature. The sample surface moisture was dried with filter paper. This weight was recorded as M4. The cooking loss was calculated by Eq. (3):

$$\text{Cooking loss (\%)} = (M3-M4)/M3 \times 100 \quad (3)$$

3.10 Storage loss determination

Storage loss was accurately calculated as the difference between the initial weight of the sample mass (M5) and the final weight of the sample after storage M6. The storage loss was calculated by Eq. (4):

Storage loss (%) = = (M5-M6)/M5 × 100 (4)

3.11 Centrifugal loss determination

The samples used for the centrifugal loss determination were weighed 1.00 ± 0.02 g (M7) and placed in a 1.5 mL centrifuge tube, centrifuged at 8000 × g at 4°C for 30 min. The water was absorbed by filter paper and weighed (M8). The centrifugal loss was calculated by Eq. (5):

Centrifugal loss (%) = (M7-M8)/M7 × 100 (5)

3.12 T_2 transverse relaxation measurement

The T_2 transverse relaxation measurement was measured using a hydrogen proton Nuclear Magnetic Resonance Imaging (NMI) (NMI20-040H-I, NIUMAG, Suzhou, China). The sample was cut into cuboids of 2 cm × 2 cm × 1 cm and placed in the sample tube. The test parameters were as follows: Magnetic field strength 0.5 T; Proton resonance frequency 23 MHz; SF=23 MHz; P90=9 μs; P180=18 μs; TD=59990; TR=3000 ms; NS=16; Echo Count=2000. The CPMG (Carr-Purcell-Meiboom-Gill) pulse sequence exponential decay curve was inversed by the Multi-Exp Inv Analysis software to obtain the T_2 value. P_{21}: immobilized water, P_{22}: free water, P_{2b}: bound water.

3.13 H-proton density imaging spectra measurement

H-proton density imaging spectra were performed on the imaging system of NMI, putting the experimental sample into the center of the magnetic field for imaging experiments. The main parameters were as follows: repetition time 2 000 MS, performing 4 repetition times, longitudinal relaxation time 20 MS, spin echo time 20 MS.

3.14 Statistical analysis

Statistical analysis was conducted using IBM SPSS (version 26, USA). The effect of the different treatments on the pH value, TVC, TVB-N, moisture content, cooking loss, storage loss, centrifugal loss, and T_2 transverse relaxation were analyzed using the general linear model program. The different treatments, storage time, and their interaction were used as fixed effects, and the carcass (n=5) was regarded as a random term. The least significant differences (LSD) test was used to identify the significance

of the analysis of the differences ($P < 0.05$). The data were reported as the mean ± standard errors (SE).

4. Results and discussion

4.1 Changes in pH value

The effect of different EF action on the pH value of chilled fresh pork during CFPS is shown in Fig. 8. The pH value of samples from the CK group increased continuously and reached the highest value on day 16. In general, three different HVEF treatments exhibited a downward trend, and then gradually rised during storage. The pH value in the IHVEF and CHVEF groups was relatively stable and significantly lower than those of the CK and SHVEF groups ($P < 0.05$). The pH value of muscle exhibited an increased trend during CFPS. The possible reason for this phenomenon is that the protein was decomposed, and the basic nitrogen compounds, such as amine, were released at the same time, thus resulting in a constant increase in pH value (Chen et al., 2022; Scheier et al., 2014). In addition, as shown previously in other studies, the enzyme activities at the later storage period have also induced the change in pH value (Chauhan & England, 2018; Chen et al., 2022; Hu et al., 2022; Suwandy et al., 2015; Zhao et al., 2017). However, the EF technology offered a possibility to mitigate this phenomenon (Suwandy et al., 2015). Previous research showed that the EF could inactivate most undesirable enzymes and induce the conformational changes of protein, mainly by affecting their secondary, tertiary, and quaternary structures of them (Chen et al., 2022; Hennefarth & Alexandrova, 2022; Ohshima et al., 2021; Poojary et al., 2016; Vanga et al., 2021). It was speculated that the EF has inhibited the growth and reproduction of bacteria in the meat during the late part of the storage period, slowed down the formation rate of amines, and delayed the rise of pH during the storage (Ko et al., 2016). In another study of our research, it was found that the emergence of an EF effectively alleviated the process of glycolysis. After slaughtering, due to the existence of physiological and biochemical reactions, the pH value of the muscle shows a downward trend, and the meat becomes more relaxed from being stiff. Throughout this process, glycolytic enzymes are always involved. The EF itself has the function of inhibiting enzyme activity, thus the glycolysis process was slowed down, the consumption of glycogen was reduced, and the degree of pH decline was decreased. This also explains from another perspective the reason why the pH value of the muscle treated by the EF decreases slowly.

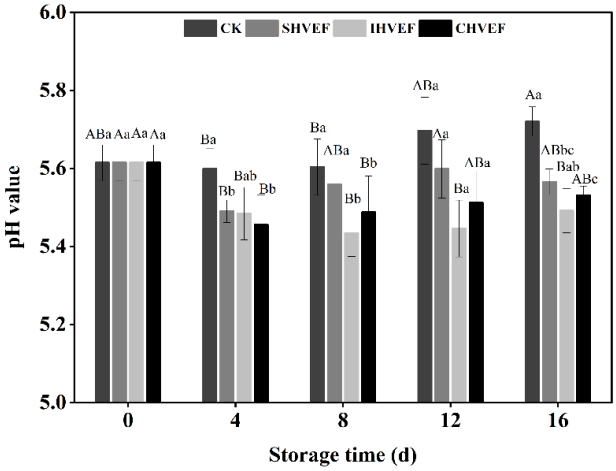

Figure 8. Effect of different EF action on the pH value of chilled fresh pork.

Values represent means ± SE (n=5). A-D: Different letters represent the significance of pH value in the same treatment group at different storage days ($P < 0.05$). a-d: Different letters represent the significance of pH value in different treatment groups on the same storage day ($P < 0.05$). Abbreviations: EF: electrostatic field; CK: stored at -1.0 ± 0.5℃ with no high voltage EF; SHVEF: stored at -1.0 ± 0.5℃ and treated with 12.0 kV high voltage EF for 48 h and then stopped using HVEF until the end of storage; IHVEF: stored at -1.0 ± 0.5℃ and treated with 12.0 kV high voltage EF every 24 h interval until the end of storage; CHVEF: stored at -1.0 ± 0.5℃ and continuously treated by 12.0 kV HVEF until the end of storage.

4.2 Changes in TVC

The effect of different EF action on the TVC of chilled fresh pork during CFPS is shown in Fig. 9. The TVC in each treatment group increased at a prolonged storage time. SHVEF, IHVEF, and CHVEF groups performed lower TVC than the CK group ($P < 0.05$). On the last day of storage, the TVC content of samples from the CK group exceeded 6.0 CFU/g, while the other groups were still significantly lower than the threshold ($P < 0.05$). As described in the Chinese national standard GB 20799-2016, when the TVC content on the surface of the meat reaches an unacceptable level (10^6 CFU/g). At this point, the meat usually begins to show obvious signs of spoilage (such as off-flavors and mucus), and is no longer visually acceptable. Huang et al. (2020) have concluded that, to some extent, the EF inhibits the growth and reproduction of bacteria, and the TVC could effectively be reduced by a logarithm, which was in agreement with the result of this study. This might be caused by releasing electrons to disrupt the electrical potential inside and outside the cell membrane of the bacteria (Huang et al., 2021). Research shows that the organism's cells are a multi-phase,

anisotropic dielectric material with highly resistive yet capacitive properties (Ross, 2017; Yusupov et al., 2017). Under normal conditions, the difference in microbial cell potential is minor. The state of the cell membrane usually depends on the stability of the biological environment (Dimakopoulou-Papazoglou et al., 2022). When exposed to an external EF, the membrane potential of the cell membrane changes to form a transmembrane potential, resulting in the electrical disintegration of the membrane (Dimakopoulou-Papazoglou et al., 2022; Zhu et al., 2018). In addition, a large number of trace ozone, negative ions, and other strong oxidizing substances were produced by the external EF and destructed the cell membrane structure, resulting in a lower TVC in meat, which is consistent with another study by Qian et al. (2019).

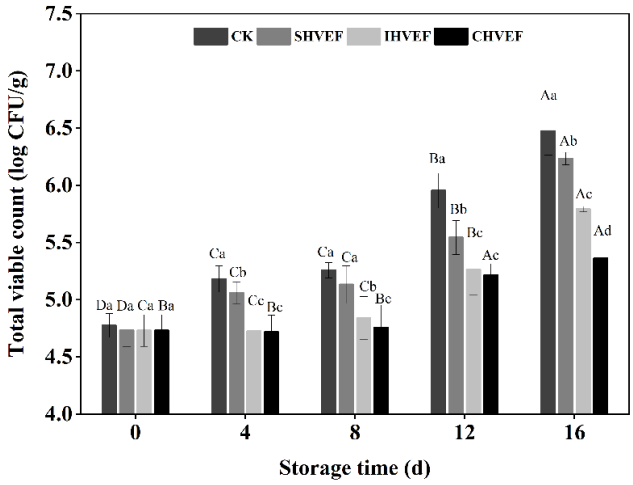

Figure 9. Effect of different EF action on the TVC of chilled fresh pork.

Values represent means ± SE (n=5). A-D: Different letters represent the significance of TVC in the same treatment group at different storage days ($P < 0.05$). a-d: Different letters represent the significance of TVC in different treatment groups on the same storage day ($P < 0.05$).

In the fresh meat, the specific spoilage microorganisms, particularly *Pseudomonas* and *Shewanella* species, proliferate as TVC increases (Li et al., 2019). During their metabolic activities, these bacteria utilize sulfur-containing amino acids in the meat, leading to the direct production of volatile sulfides like hydrogen sulfide (H_2S) and methyl mercaptan (Holman et al., 2021; Song et al., 2020). These compounds are responsible for characteristic off-odors. In another study of ours, an electronic nose was employed to determine whether the flavor of fresh meat changed under EF conditions. Some of the results are displayed here to verify the validity of the TVC results (Fig. 10). The results of electronic nose were showed that as storage time

increased, the response intensities of sensors W1W, W5S, and W1S gradually rose, indicating a gradual increase in substances such as sulfides, nitrogen oxides, and methyl compounds, along with a decline in freshness. On the 7 day of storage, the response intensity of the CK group pork to the W1W sensor was higher than that of all other EF groups, while the CHVEF group exhibited the lowest sensor response intensity. This suggests that EF-assisted CFPS could reduce the production of sulfides in pork during storage.

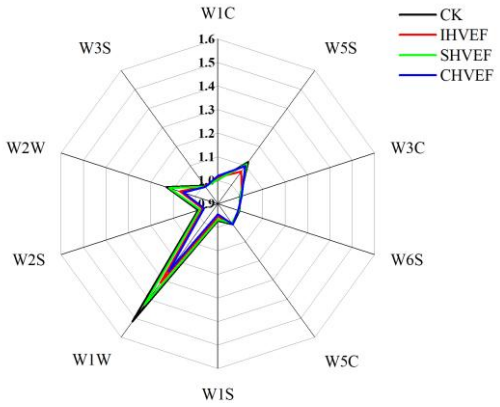

Figure 10. Effect of different EF action on the falvour of chilled fresh pork.

Values represent means ± SE (n=5). W1C is sensitive to aromatic components of benzene, W5S to nitrogen oxides, W3C to ammonia and aromatic components, W6S to hydrides, W5C to aromatic components of short-chain alkanes, W1S to methyl groups, W1W to sulfides, and W2S to alcohols, aldehydes and ketones. W2W is sensitive to organic sulfides and aromatic components, while W3S is sensitive to long-chain alkanes.

4.3 Changes of TVB-N

The effect of different EF action on the TVB-N of chilled fresh pork during CFPS is shown in Fig. 11. The TVB-N value of the CK group was increased along with storage time extension ($P < 0.05$). Similar trends were observed for the other groups. On days 4 and 8, the TVB-N value of SHVEF showed no significant differences in the CK group ($P > 0.05$). After that, the TVB-N value of SHVEF was constantly lower than the CK group. IHVEF and CHVEF groups exhibited a perceptible difference between CK and SHVEF groups. Previous studies demonstrated that both the TVB-N and TVC could reflect the degree of meat shelf life (Cai et al., 2015; Holman et al., 2021; Li et al., 2019; Song et al., 2020). As the results shown above, the value of

TVB-N observed a similar trend during the extension of storage time, which was similar to the previous research reported by Chen et al. (2020). The structure and permeability of cell membranes were changed in the presence of HVEF, and the function of some membrane proteases became dysfunctional or disabled. (Gonzalez & Barrett, 2010; Gumbart et al., 2012; Valdivia-Nájar et al., 2017; Wang et al., 2016). In this study, the sample treated by IHVEF and CHVEF showed a decreased trend in enzyme activity, generally attributed to the inhibition effect caused by the EF (Dalvi-Isfahan et al., 2016). The metabolic function of various bacteria was irreversibly destroyed by HVEF. The volume expansion leads to the rupture of the membrane, eventually leading to death, which was consistent with other research (Leong et al., 2016; Qi et al., 2022).

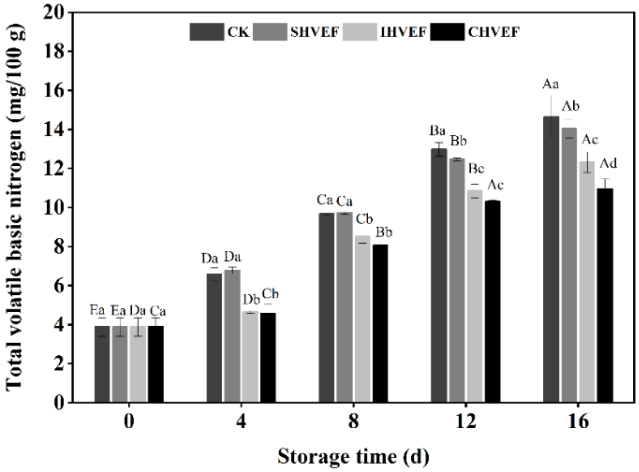

Figure 11. Effect of different EF action on the TVB-N of chilled fresh pork.

Values represent means ± SE (n=5). A-D: Different letters represent the significance of TVB-N in the same treatment group at different storage days ($P < 0.05$). a-d: Different letters represent the significance of TVB-N in different treatment groups on the same storage day ($P < 0.05$).

During the progress of this experiment, I took photos of the meat in the CKgroup and the CHVEF group during the storage period. The difference in color can be clearly seen through comparison (Fig. 11). Under CFPS storage at -1°C, muscle tissue exhibits a darker color, whereas with EF-assisted CFPS, the meat retains a brighter red appearance. This difference can be attributed to the antioxidant effect enabled by EF technology. Specifically, EF inhibits microbial growth and releases electrons into the air, generating trace amounts of ozone-like substances that exert antioxidative activity (Hautanen et al., 1986; Seyfi et al., 2020). As a result, the oxidation of myoglobin, the oxygen-binding protein in muscle, is slowed. In the absence of EF,

myoglobin oxidizes more readily into metmyoglobin, which gives the meat a darker, less fresh appearance. Thus, EF helps preserve myoglobin in its reduced state, maintaining the desirable red color of the meat.

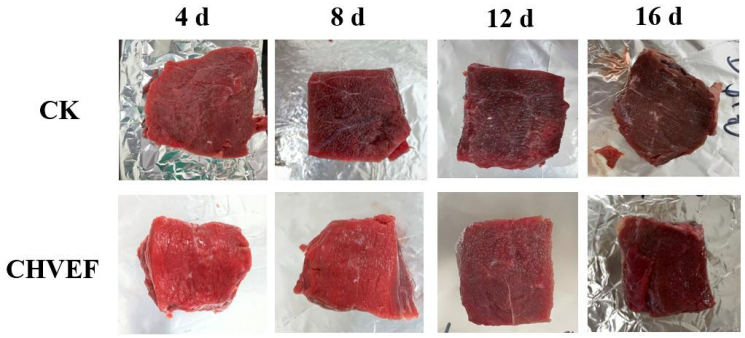

Figure 12. Effect of different EF action on the falvour of chilled fresh pork.

4.4 The variation of bacterial community composition

The value of Chao1 value and Shannon value in the different EF action on chilled fresh pork is shown in Fig. 13A and 13B. They are regarded as the calculation of the richness and diversity of the bacterial community composition, respectively. The results inhibited the higher richness and diversity of bacterial species at day 0, which was consistent with the previous study (Chaillou et al., 2015; Xu et al., 2023). In the last storage period, the Chao1 value and Shannon value of all samples of different groups were lower than the original samples. This might be due to the increase of main dominant spoilage bacteria inhibiting the growth of other bacteria (Xiao et al., 2020). On the final day, both the SHVEF and CK groups exhibited decreased Chao1 and Shannon values, whereas the CHVEF group demonstrated the highest Chao1 and Shannon values.

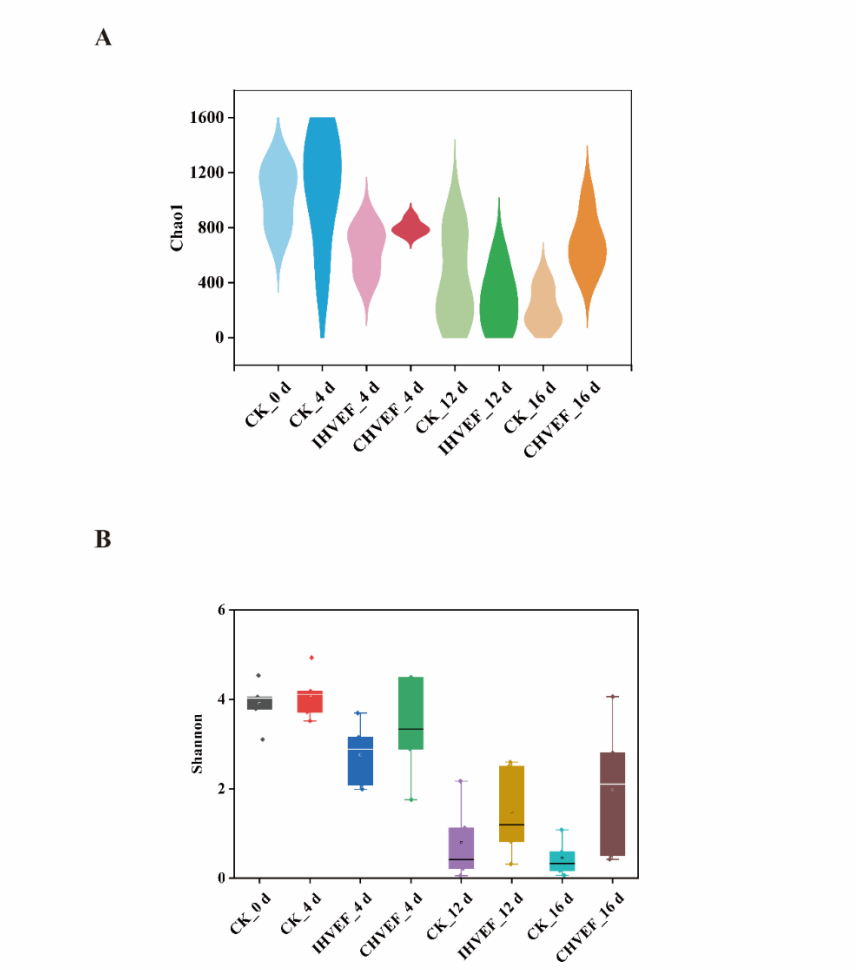

Figure 13. Effect of different EF action on alpha diversity indices of the bacterial community during storage. (A): chao1; (B): Shannon.

Values represent means ± SE (n=5).

As shown in Fig. 14, the unique and shared genera of different treatments were changed noticeably during storage. The shared genera gradually decreased in different groups with the extension of storage. Especially on the last day of storage, compared with the CK group, the shared genera between the other three groups and the CK group decreased. The shared genera of all groups decreased from 24.85% to 12.81%.

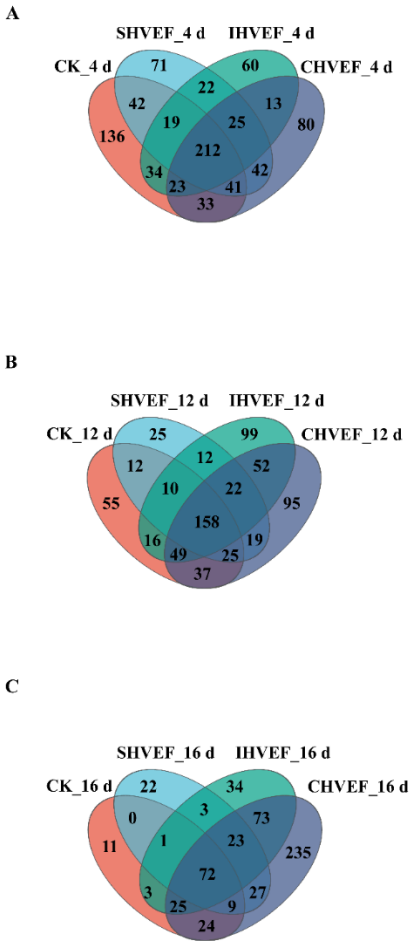

Figure 14. Venn diagram showing unique and shared genera among different EF action on chilled fresh pork during storage. (A): 4 d; (B): 12 d; (C): 16 d.

Values represent means ± SE (n=5).

4.5 The abundances of major phyla and genera

The phylum and genus level dynamic changes of bacterial community were shown in Fig. 15A and Fig. 15B. Proteobacteria was the main phylum in the chilled fresh pork, followed by Firmicutes. In the early storage time, the contents of that two phyla were relatively uniform. With the extension of storage time, the proportion of

Proteobacteria gradually increased, it had exceeded 91.6% by the last day, and Firmicutes was 7.24%. After being treated with three different HVEF groups, the proportion of *Proteobacteria* decreased significantly after days 8, 12, and 16 of storage. At the genus level, *Pseudomonas*, *Latilactobacillus*, Unclassified bacteria, and *Proteobacteria* were more abundant in the samples. These bacterial compositions in the HVEF treatment groups were quite different from the CK group.

The initial bacteria community in the chilled fresh pork (CK_ 0 d) was a collection of diverse bacterial groups with relatively uniform distribution. On the contrary, *Pseudomonas*, which occupied the main advantage during the storage period, showed less initial abundance in chilled fresh pork. *Pseudomonas* gradually increased with the extension of storage time and reached the highest value at the final storage, increasing from 35.40% to 91.60% throughout the storage period. As a typical gram-negative psychrophilic bacterium, *Pseudomonas* easily proliferated during CFPS (de la Cruz Quiroz et al., 2020; Mai et al., 2022; Robazza et al., 2017). After HVEF treatment, in the SHVEF group, EFs showed good inhibited effects on days 8 and 12. However, the content of *Pseudomonas* increased after day 16 of storage, which may be due to the short time of single-used EF treatment. The better oxygen supply in the later stages of storage, with oxygen passing through the PE film, briefly promoted the growth and reproduction of *Pseudomonas.* After treatment with IHVEF and CHVEF, the excellent performance of the EF on days 4, 8, and 16 reduced the total content of *Pseudomonas*. In the CHVEF group, 32.56% and 44.26% decreased on days 8 and 16, respectively. In an applied EF, bacterial cells can be regarded as cylindrical capacitors. This analogy stems from their structural and electrical properties: the cell membrane acts as a dielectric layer separating the conductive internal and external environments, allowing the cell to store and accumulate charge in a capacitor-like manner (Pavlin et al., 2007). When the accumulated charges at the two ends of the cell generate a transmembrane potential that reaches a critical threshold, the membrane experiences electrical breakdown. If the external EF strength continuously exceeds the inherent transmembrane voltage the cell can sustain, the membrane becomes highly susceptible to irreversible breakdown (Pavlin et al., 2007). This process, known as electroporation, initially leads to the formation of small, transient pores. However, if these pores expand beyond a critical size and fail to reseal, the damage becomes irreversible. Consequently, the loss of membrane integrity results in the uncontrolled leakage of intracellular components, disruption of cellular homeostasis, and ultimately, cell death (Tsong, 1990; Ross, 2017). *Pseudomonas* has produced a variety of metabolic substances that led to meat spoilage, the formation of slime, and an unpleasant smell (de la Cruz Quiroz et al., 2020; Xu et al., 2023). Generally, meat rich in *Pseudomonas* show softened tissue, adhesion, and strange smells (Gu et al., 2021; Wickramasinghe et al., 2019; Xu et al., 2023). The CFPS treated by an EF had a good appearance and was without discoloration, which was consistent with the previous results (Wang et al., 2014).

Latilactobacillus was the second dominant bacteria in the result. The abundance of *Latilactobacillus* in the CK group decreased during storage, suggesting that *Latilactobacillus* had poor competitiveness at the later stage. The abundance of *Latilactobacillus* in each HVEF treatment group increased at the initial storage time

(4 and 8 days) and then decreased at the later stage of storage (12 and 16 days). Notably, the growth of the SHVEF treatment groups was significantly lower than the CK group on days 4 and 8 and the CHVEF treatment group was significantly lower on day 12. During storage, each EF treatment group produced large quantities of substances, such as ozone, by ionizing the outside air (Hautanen et al., 1986; Seyfi et al., 2020). The oxygen concentration in the external environment decreased contributing to less oxygen transmittance in the PE film. The decrease of oxygen supply at this time has provided an anaerobic environment for the reproduction of *Latilactobacillus* (Fidan et al., 2022; Vasconcelos et al., 2014; Wang et al., 2013). Furthermore, the characteristic of *Latilactobacillus* led to the development of a sour smell and carbon dioxide by using carbohydrates in the meat, thus tending to fill the packaging and reducing meat exposure to oxygen (Borch & Agerhem, 1992; Wang et al., 2013). On days 12 and 16, the abundance of *Latilactobacillus* decreased in SHVEF and CHVEF groups, and this may also be attributed to the effect of the EF, which holds the same view as previous studies (Xanthakis et al., 2013; Mason et al., 2005). Under the EF, the biological cells and tissues suffered an increased membrance permebility which could be called a phenomenon as electroporation (Levkov et al., 2019). The lipid molecular layer of the cell membrane underwent chaos and formed holes, which enhanced the permeability of the cell membrane and destroyed the viability of the bacteria (Gómez et al., 2019). *Latilactobacillus* is more common during the storage of chilled fresh meat and is the dominant spoilage bacteria under anaerobic conditions (Ivanovic et al., 2015; Xu et al., 2023). Thus, the decreased abundance of *Latilactobacillus* is essential for improving the storage quality of chilled fresh meat.

Furthermore, *Brochothrix* also accounted for a large proportion of the total bacterial population (Alexandrakis et al., 2012; Papadopoulou et al., 2012). In this study, the proportion of *Bromothrix* first increased and then decreased with the extension of storage in the CK group. When comparing the different treatment groups, the abundance of *Brochothrix* in SHVEF and IHVEF was significantly lower than that in the CK group on days 8 and 12. The abundance of *Brochothrix* in CHVEF was significantly lower than in the other groups on days 8 and 12. Both *Bromothrix* and *Latilactobacillus* are facultatively anaerobic and commonly appear in chilled storage, leading to meat decay during storage (Nowak et al., 2012; Papadopoulou et al., 2012; Vasconcelos et al., 2014). Ding et al. (2016) demonstrated that the EF could destroy the biofilm of bacteria and block the important channel of material exchange between bacterial cells and the external environment. In the SHVEF group, the relative content of *Brochothrix* was higher than that of *Latilactobacillus* at the final storage. The study showed competition between the different genera, which means that they competed for nutrients, oxygen, and carbon sources and produced different metabolic substances such as organic acids, bacteriocins, and volatile substances (Andreevskaya et al., 2018). The same situation occurred in the other groups at all time points. In addition, looking at the results of *Pseudomonas*, it could be seen that the level of *Pseudomonas* decreased and *Latilactobacillus* increased at CHVEF_16 d.

Also, we found that Unclassified bacteria accounted for a large proportion of chilled fresh pork (CK_0 d) and gradually became lower in proportion as the storage time extended. After three kinds of EF treatment, the overall trend was downward. Although the specific genera are not clear at present, it could also be explained from another aspect that the EF also has a destructive effect on them.

The heatmap and cluster analysis of samples were generated to assess the dynamic changes of bacteria in different treatment groups during storage (Fig. 15C). The response modes of different strains to the HVEF were quite different, indicating that the effect of HVEF on the growth of bacteria was species dependent (García et al., 2007). Several spoilage-related bacteria, including *Pseudomonas*, *Latilactobacillus*, *Brochothrix*, *Psychrobacter*, and *Acinetobacter* also suffered an inhibition in the HVEF treatment groups in this study, which was similar to what was reported by Xiao et al. (2020). This might be attributed to the bacterial biofilm penetration effect in the HVEF treatment. Gram-negative bacteria were more sensitive to the stimulation of HVEF than gram-positive bacteria (Fernando et al., 2019; Hülsheger et al., 1983). This may be due to the different membrane structure between the gram-negative bacteria and gram-positive bacteria, the lack of an outer phospholipid membrane made bacteria more sensitive to EF (Youssef et al., 2023). The thermographic results showed that *Latilactobacillus* and *Brochothrix* reacted more strongly to the EF, resulting in a lower survival rate in meat.

The histogram of LDA score distribution of significantly different genera analyzed by LEfSe (the default value is 4.0) is shown in Fig. 15D. It can be seen from the figure that there was a significant difference among each group in the number of *Psychrobacter*, *Acinetobacter*, *Arthroactor* and *Rhododocus* of day 0. In addition to the unclassified bacteria, *Psychrobacter* was significantly enriched on day 0 (red), which means that the abundance of *Psychrobacter* on day 0 was significantly higher than that of other groups. At the same time, the LDA score of *Psychrobacter* is higher than that of another group, indicating that it has a greater impact on the differences between groups on that day. Similarly, on day 4, day 8, and day 12, the highest LDA scores were *Latilactobacillus*, *Brochothrix*, and *Pseudomonas*, respectively, indicating that they were significantly enriched in their respective groups, and the abundance was higher than that of other genera.

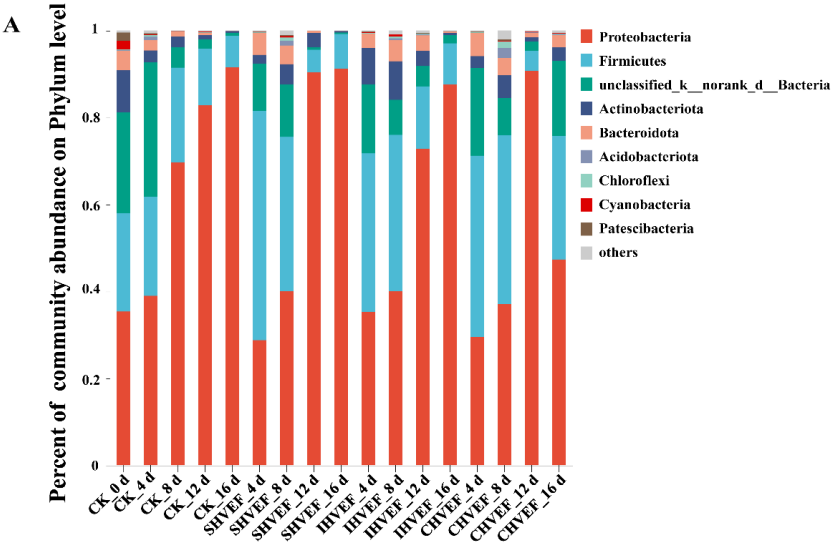
A
Percent of community abundance on Phylum level
1
0.8
0.6
0.4
0.2
0
CK_0 d
CK_4 d
CK_8 d
CK_12 d
CK_16 d
SHVEF_4 d
SHVEF_8 d
SHVEF_12 d
SHVEF_16 d
IHVEF_4 d
IHVEF_8 d
IHVEF_12 d
IHVEF_16 d
CHVEF_4 d
CHVEF_8 d
CHVEF_12 d
CHVEF_16 d
Proteobacteria
Firmicutes
unclassified_k__norank_d__Bacteria
Actinobacteriota
Bacteroidota
Acidobacteriota
Chloroflexi
Cyanobacteria
Patescibacteria
others

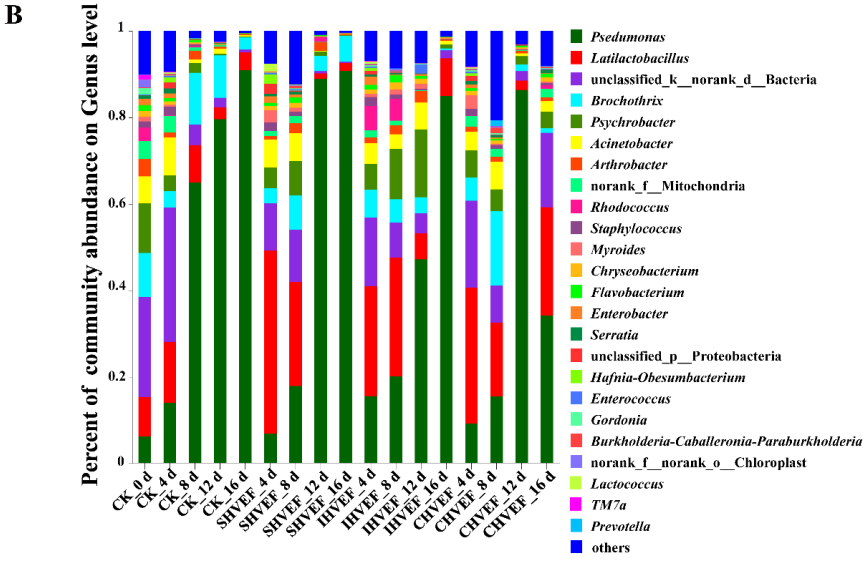
B
Percent of community abundance on Genus level
1
0.8
0.6
0.4
0.2
0
CK_0 d
CK_4 d
CK_8 d
CK_12 d
CK_16 d
SHVEF_4 d
SHVEF_8 d
SHVEF_12 d
SHVEF_16 d
IHVEF_4 d
IHVEF_8 d
IHVEF_12 d
IHVEF_16 d
CHVEF_4 d
CHVEF_8 d
CHVEF_12 d
CHVEF_16 d
Psedumonas
Latilactobacillus
unclassified_k__norank_d__Bacteria
Brochothrix
Psychrobacter
Acinetobacter
Arthrobacter
norank_f__Mitochondria
Rhodococcus
Staphylococcus
Myroides
Chryseobacterium
Flavobacterium
Enterobacter
Serratia
unclassified_p__Proteobacteria
Hafnia-Obesumbacterium
Enterococcus
Gordonia
Burkholderia-Caballeronia-Paraburkholderia
norank_f__norank_o__Chloroplast
Lactococcus
TM7a
Prevotella
others

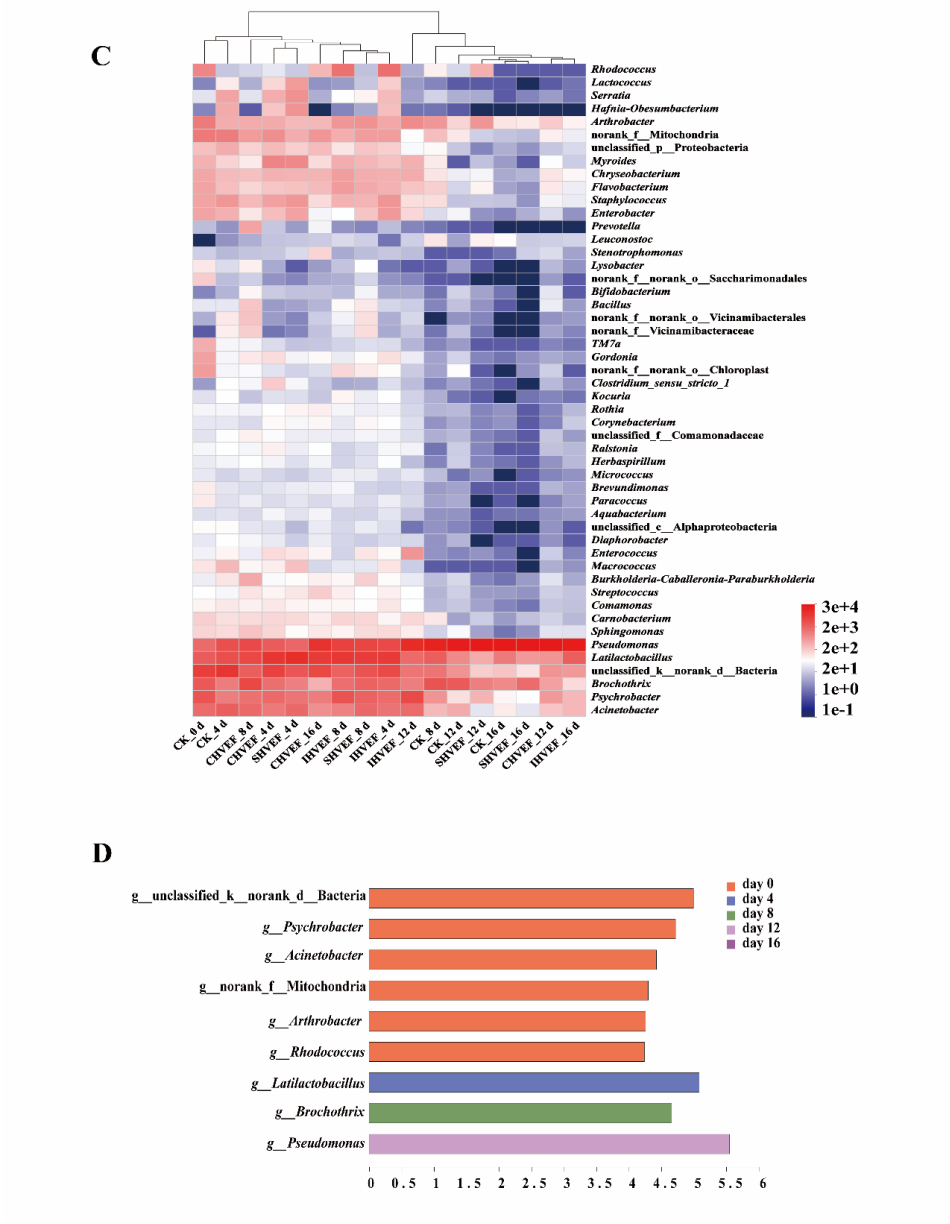

Figure 15. The bacterial composition changes in different EF action on chilled fresh pork during storage. (A): Phylum level; (B): Genus level; (C): The heatmap of the top 50 abundant genera; (D): LDA score distribution of significantly different genera.

Values represent means ± SE (n=5).

4.6 The microbial metabolic function pathway functional genes analysis

The statistical analysis of the KEGG pathway showed that the samples obtained five level 1 microbial metabolic function pathway functional genes (Fig. 16), including metabolism, environmental information processing, genetic information processing, cellular processes, and metaboli. It mainly focuses on metabolism, environmental information processing, and genetic information processing. Using the Gene Ontology Consortium (GOC) database for comparison, the top 30 functional gene groups with significant activity were selected (Fig. 16), and the dominant ones were metabolism of cofactors and vitamins, amino acid metabolism, carbohydrate metabolism, energy metabolism, cellular community-products, nucleotide metabolism, translation, membrane transport, energy production and conversion, signal transmission, and Global and overview maps (Pathway level 2) can be summarized as energy and material transport metabolism.

When stored for 4 days, compared with CK_4 d, IHVEF_4 d showed more obvious expression in pathway level 2. The genes were ko01120, ko01110, and ko01100, which respectively represented microbiological metabolism in diverse environments, metabolic paths, and biosynthesis of secondary metabolites. When stored for 8 days, compared with CK_8 d, the other three groups showed lower expression levels in ko00190, ko02025, ko02024, ko00230, ko03070, ko02010, ko02020, ko01200, ko01230, ko01120, and ko01110, which respectively represented the oxidative physiology, biofilm formation in *Pseudomonas aeruginosa*, quorum sensing, purine metabolism, bacterial secret system, ABC transporters, two-component system, carbon metabolism sm microbial metabolism in diverse environments, metabolic pathways. The expression of HVEF in the biosynthesis of amino acids is higher than that in CK_8 d, which indicates that HVEF influences the above metabolic pathways. Similarly, by 12 days, the gene expression of IHVEF was generally lower than that of the CK group, while CHVEF and SHVEF were close to the CK group. On day 16, the overall gene abundance of CHVEF was lower than that of the other treatment groups, especially in ko02010, ko02020, ko01200, ko01230, ko01120, and ko01110. IHVEF group was associated with the bacterial secret system, ABC transporters, two-component system, carbon metabolism, microbial metabolism in diverse environments, and metabolic pathways.

Bacteria could use carbon from many different sources as energy to convert complex organic compounds into simple compounds while providing substrates for other bacteria, which has a great impact on the off-flavors and rancidity of meat. By comparing the expression abundance of gene metabolism pathways in different treatment groups, it could be seen that HVEF has a certain influence on the amino acid metabolism, carbohydrate-metabolism, and energy metabolism of chilled fresh pork during storage, which may explain the reason why EF assisted chilled storage preservation.

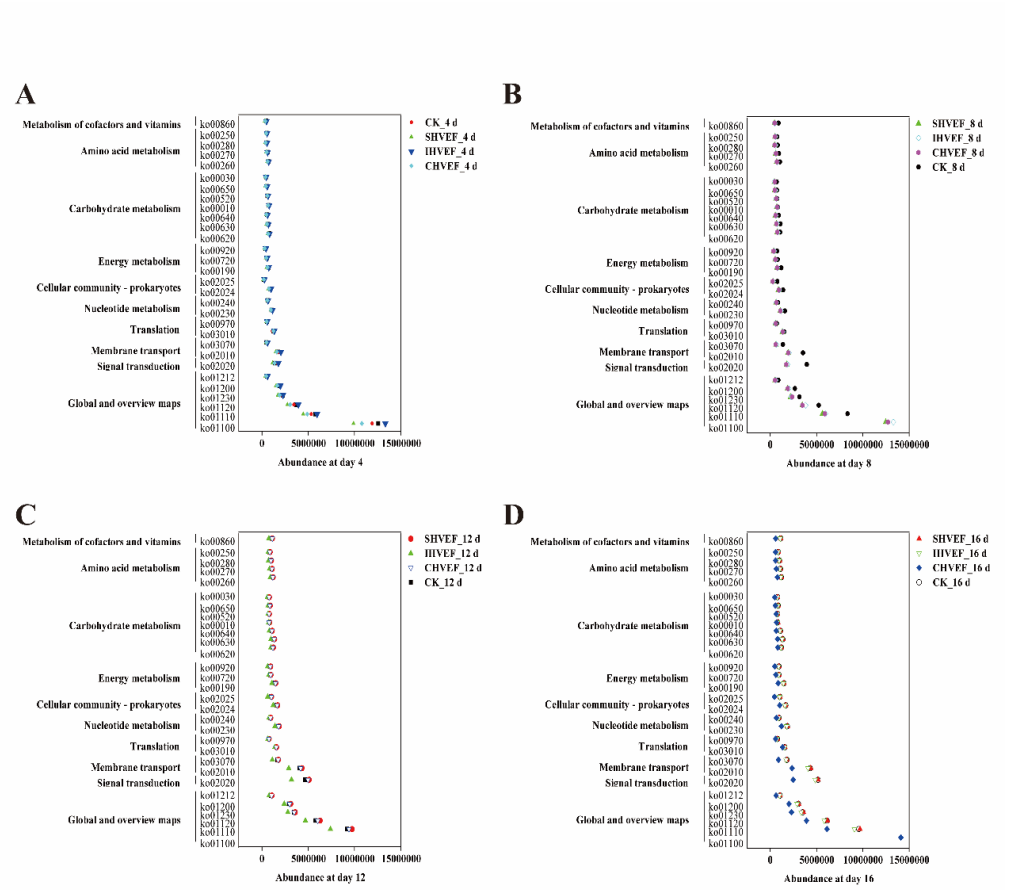

Figure 16. Relative abundance distribution of functional genes based on the KEGG pathway. (A): Relative abundance of day 4; (B): Relative abundance of day 8; (C): Relative abundance of day 12; (D): Relative abundance of day 16.

Values represent means ± SE (n=5).

4.7 Changes in WHC

The moisture content of the samples gradually decreased during storage time (Fig. 17A). A similar trend was observed for the effect of the EF treatments during the storage period. Compared with the CK group, the loss of moisture content of treatment group after application of the EF decreased on days 4, 8, and 16 of storage ($P < 0.05$).. On days 12 and 16 the moisture content of the CHVEF was significantly higher than that of the other treatment groups ($P < 0.05$). Investigating the moisture content in the meat is particularly important because variations in moisture content can result in a variety of changes in the quality of chilled fresh meat, including sensory qualities,

texture, storage stability, and processing characteristics (Pearce et al., 2011). In our study, the decreasing trend of pork moisture content slowed down after EF treatment, indicating that the EF has a positive impact on the WHC of meat. Possibly due to the partially bound water being impacted by charged particles, the hydrogen bond, and other water molecule structures, the binding ability with material molecules (protein) was strengthened, and the moisture content loss was reduced (Lin et al., 2017).

During the storage time, the storage loss of pork in each group gradually increased (Fig. 17B). At the later stage of storage (16 days), the sample stored at CHVEF and IHVEF had the lower storage loss while CK groups were higher in storage loss ($P < 0.05$), and there was no significant difference between CHVEF and IHVEF ($P > 0.05$). Studies have demonstrated that the disordered water molecule structures can be transformed into an ordered dendritic structure by the charge generated by the EF (Johari, 1981). HVEF probably introduced the charge produced by electricity to require the orderly activity of water molecules when the chilled fresh pork was exposed to an EF, thus reducing the water loss of meat (He et al., 2013). In addition, due to the EF being continuous and uniform. It may mean that a large number of ionized substances remained in the air during the closing of the EF of the IHVEF group, which still participated in the physiological and biochemical reactions in meat and affected the movement of water molecules.

The results of centrifugation loss with storage time were presented in Fig. 17C. The water loss of samples after high-speed centrifugation in the CK group tended to be higher than that in the other groups. Centrifugation loss of the CK group was significantly increased at 8 days compared to those treated by an EF. IHVEF group showed a positive effect on WHC in the early stage, although centrifugation loss increased rapidly at 16 days. The most significant was the CHVEF group, which maintains water molecules at all stages of the storage period attributed to reducing the loss of free water and immobilized water ($P < 0.05$). The results indicated that water molecules typically change their structural arrangements and arrange themselves in a specific order outside of an electric field, in agreement with previous research (He et al., 2014). Under the EF, the stability of water molecules in the muscle fibril gap improved and water loss decreased.

The results of cooking loss with storage time were presented in Fig. 17D. As seen by the exhibition of cooking loss of pork significantly increased in 4 days with the prolongation of the storage time may be induced by the chilled fresh pork passing the rigor stage (Domínguez et al., 2014). During the storage period of 12 and 16 days, the cooking loss was affected by the EF, IHVEF and CHVEF groups showed a significantly decreased cooking loss compared to the CK group ($P < 0.05$). As predicted by the previous research of Matsumoto et al.,(2002), HVEF treatments may cause the excellent WHC observed in this study. Xanthakis et al., (2013) gave a general view that the water dipoles were getting polarized and align from the native random state to the direction of the electric field vector. According to this, it may be explained why the HVEF could be combined with CFPS to reduce the cooking loss of samples.

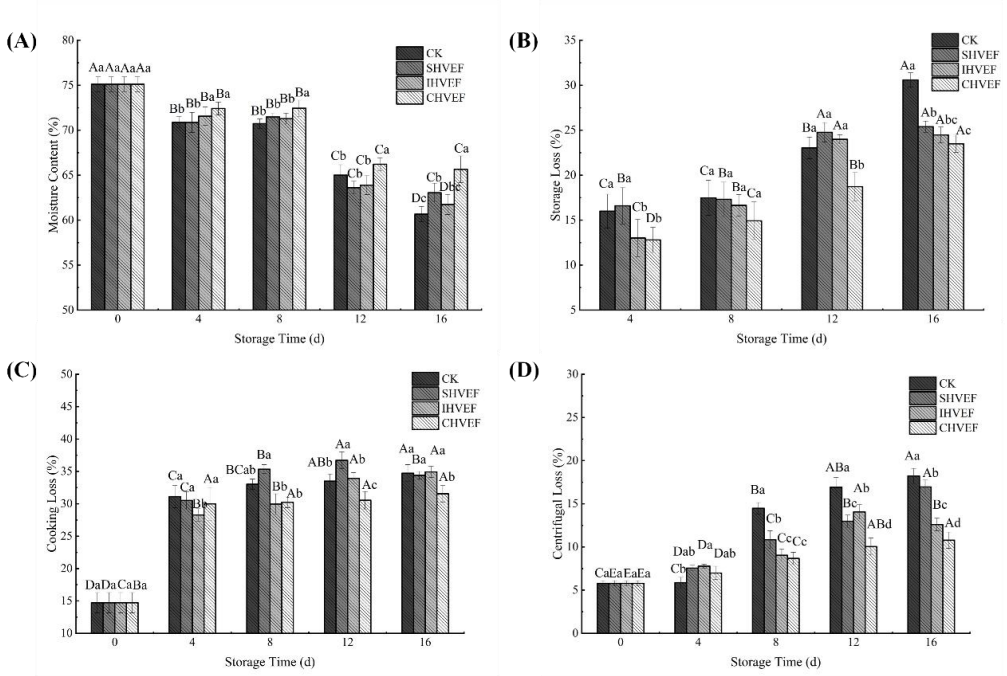

Figure 17. Effect of different EF actions on water holding capacity of chilled fresh pork.(A): moisture content; (B): storage loss; (C): centrifugal loss; (D): cooking loss.

Values represent means ± SE (n=5). A-D: Different letters represent the significance of WHC in the same treatment group at different storage days ($P < 0.05$). a-d: Different letters represent the significance of WHC in different treatment groups on the same storage day ($P < 0.05$).

4.8 Changes in T_2 transverse relaxation and H-proton density imaging spectra

Changes in water migration gradually manifested along with the extension of time (Fig. 18). The percentage of bound water relaxation area P_{2b} did not change significantly during the early storage time (4 days) ($P > 0.05$). At the 8 days of storage, the water in the CK group was obviously transferred, the percentage of immobilized water relaxation area P_{21} decreased significantly ($P < 0.05$), and the percentage of free water relaxation area P_{22} increased significantly ($P < 0.05$) (Table 2). This suggests that during storage, water migration from less mobile and bound water to free water increased. At 8, 12, and 16 days of storage, the P_{21} of the sample in the IHVEF and CHVEF were significantly higher than that of the CK group ($P < 0.05$), while P_{22} was

significantly lower ($P < 0.05$). On the 16 days, there were significant differences between IHVEF and CHVEF in P_{2b} and P_{21}, while there were no significant differences in P_{22} ($P < 0.05$). The muscle fiber structure of meat became loose during storage, and the immobilized water among filaments, myofibrils, and muscle cell membranes migrated to free water, resulting in water loss (Estévez et al., 2011). The results of this study suggested that the degree of water migration in samples treated with HVEF decreased, which may be indicated that HVEF may play an important role in reducing water migration during CFPS(Amiri et al., 2019). The sample of HVEF treated was not losing too much water due to a delay in the degradation of muscle fibers, thus maintaining higher immobilized water(Hu et al., 2021). The effect of the IHVEF was insignificantly weaker than that of the CHVEF but greater than that of the SHVEF and the CK groups. The extent of electrons released at intervals and during continuous release on water migration was not significant in the late storage period. This may be because the electrons released at intervals and continuously during the late storage period are fully linked with water molecules, and the migration of water molecules in two different states changes little (Pu et al., 2020). In the early stage of storage, there was no significant difference between the HVEF groups and CK ($P > 0.05$), indicating that the samples stored at a CFPS assisted by an EF had greater WHC in the later stage of storage. This result tied well with our earlier mentioned results regarding moisture content, centrifugal loss, and cooking loss.

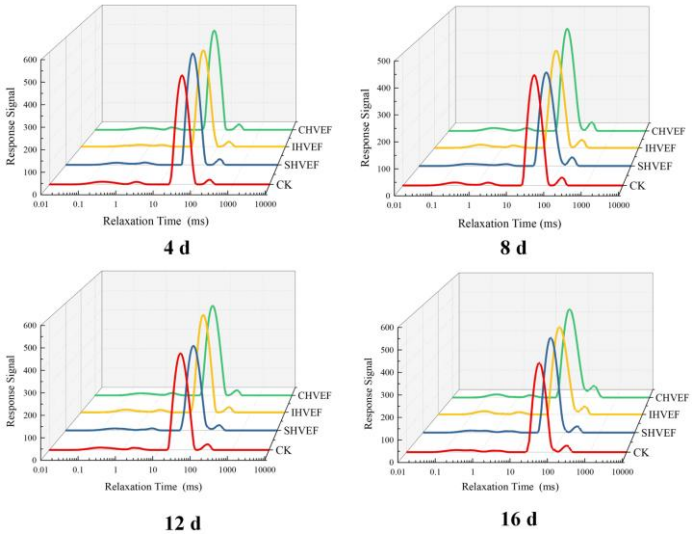

Figure 18. Effect of different EF actions on T_2 transverse relaxation peak response signal of chilled fresh pork.

Values represent means ± SE (n=5).

Table 2: Effect of different electrostatic field actions on T_2 transverse relaxation peak area percentage P_2 of chilled fresh pork

Index	Treatment	Storage time (d)				
		0	4	8	12	16
P_{2b}	CK	6.36 ± 0.65^{Aa}	5.05 ± 0.31^{Ba}	5.47 ± 0.28^{BCa}	5.66 ± 0.26^{BCa}	5.85 ± 0.09^{BCab}
	SHVEF	6.36 ± 0.65^{Aa}	4.81 ± 0.38^{Ba}	5.18 ± 0.17^{Ba}	5.17 ± 0.14^{Ba}	5.18 ± 0.12^{Bb}
	IHVEF	6.36 ± 0.65^{Aa}	4.27 ± 0.13^{Ca}	6.17 ± 0.22^{Aa}	5.25 ± 0.07^{Ba}	6.21 ± 0.26^{Aa}
	CHVEF	6.36 ± 0.65^{Aa}	5.13 ± 0.22^{Ba}	6.10 ± 0.41^{BCa}	5.97 ± 0.30^{BCa}	5.97 ± 0.31^{BCa}
	Mean ± SE	6.36±0.65	4.82±0.65	5.73±0.75	5.51±0.59	5.80±0.58
P_{21}	CK	92.99 ± 0.51^{Aa}	93.02 ± 0.61^{Aa}	88.69 ± 0.30^{Bb}	88.76 ± 0.23^{Bb}	88.67 ± 0.14^{Bc}
	SHVEF	92.99 ± 0.51^{Aa}	92.87 ± 0.45^{Aa}	90.95 ± 0.43^{Ba}	89.55 ± 0.31^{Cb}	89.55 ± 0.11^{Cbc}
	IHVEF	92.99 ± 0.51^{Aa}	93.24 ± 0.38^{Aa}	90.02 ± 0.37^{Bab}	92.07 ± 0.48^{Aa}	90.17 ± 1.46^{Bbab}
	CHVEF	92.99 ± 0.51^{Aa}	92.29 ± 0.19^{ABa}	90.25 ± 0.71^{Cab}	91.44 ± 0.21^{BCa}	91.44 ± 0.59^{BCa}
	Mean ± SE	92.99±0.51	92.86±1.00	89.98±1.34	90.46±1.44	89.96±1.12
P_{22}	CK	0.68 ± 0.19^{Ca}	1.92 ± 0.42^{Ba}	5.83 ± 0.55^{Aa}	5.57 ± 0.28^{Aa}	5.48 ± 0.22^{Aa}
	SHVEF	0.68 ± 0.19^{Da}	2.31 ± 0.23^{Ca}	3.86 ± 0.29^{Bb}	5.27 ± 0.39^{Aa}	5.27 ± 0.05^{Aa}
	IHVEF	0.68 ± 0.19^{Da}	2.48 ± 0.29^{Ca}	3.82 ± 0.47^{Ab}	2.67 ± 0.47^{BCb}	3.61 ± 0.21^{ABb}
	CHVEF	0.68 ± 0.19^{Ca}	2.57 ± 0.22^{Ba}	3.64 ± 0.33^{Ab}	2.58 ± 0.23^{Bb}	2.58 ± 0.41^{ABb}
	Mean ± SE	0.68±0.19	2.32±0.72	4.29±1.23	4.02±1.56	4.24±1.17

Values represent means ± SE (n=6). A-D: Different letters represent the significance of T_2 transverse relaxation peak area percentage P_2 for the same treatment group at different storage days ($P < 0.05$). a-d: Different letters represent the significance of T_2 transverse relaxation peak area percentage P_2 for different treatment groups on the same storage day ($P < 0.05$).

The H-proton density imaging spectra can intuitively reflect the distribution of H-protons in the meat. The more red areas in the image, the higher the H-proton density and the higher the moisture content of this part (Ouyang et al., 2022). The more blue areas, the lower the H-proton density and the lower the moisture content of this part (Fallah-Joshaqani et al., 2021). As shown in Fig. 19, the red color in the samples image of each treatment group gradually disappeared, which indicates that the moisture content of meat decreased during storage (Wang et al., 2021). On days 8, 12, and 16 of storage, the samples of the CK emerged with more yellow and green images, while there were still more red images in IHVEF and CHVEF, indicating that the water migration in the meat was reduced and the free water content was higher, which is in accordance with previous research (Ruiz-Cabrera et al., 2004).

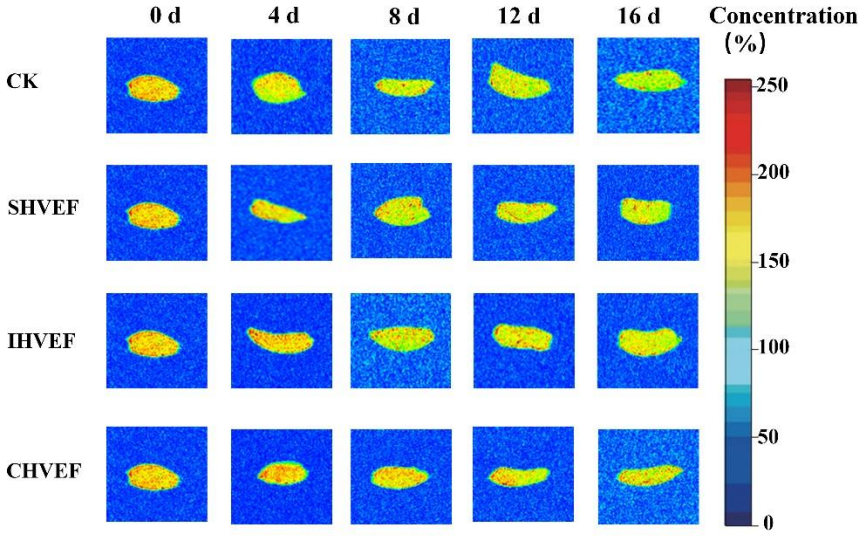

Figure 19. Effect of different EF actions on H-proton imaging spectra of chilled fresh pork.

Values represent means ± SE (n=5).

5. Conclusion

In conclusion, EF could effectively extend the storage period of chilled fresh pork to more than 16 days, and effectively reduce moisture loss during this storage period. Among them, IHVEF and CHVEF treatments are both well maintain the storage quality of meat. Compared to the CK group, samples from HVEF treatments had an acceptable pH value and a low degree of TVB-N and TVC during CFPS. At the same time, IHVEF and CHVEF treatment both have great potential in reducing bacterial loads, especially CHVEF had a better effect on the diminution of the bacteria community. Additionally, compared to the CK group, the relative abundance of dominant bacteria (*Pseudomonas*, *Lalilactobacillus*, and *Brochothrix*) was decreased greatly by CHVEF and IHVEF treatment. Regarding the results of storage loss, T_2

transverse relaxation, and H-proton imaging spectra, it has been found that IHVEF and CHVEF could effectively minimize the drip loss of chilled fresh pork stored at CFPS and reduced the migration of mobilized and bound water to free water. Furthermore, the outcomes of measuring moisture content, centrifugal loss, cooking loss indicated that the WHC of continuous EF treatment on chilled fresh pork was significantly higher than that of the interval EF treatment, implying that the continuous release of the EF has a superior effect on the storage and preservation of chilled fresh pork. Overall, this study showed that EF, especially continuous - used EF, could effectively maintain the freshness and WHC of chilled fresh pork by inhibiting the growth of bacteria and reducing the moisture loss during storage, indicating that HVEF had the potential to be used in meat preservation.

Acknowledgments

The authors want to appreciate the assistance of the Institute of Food Science and Technology, Chinese Academy of Agricultural Science.

References

Alahakoon, A. U., Oey, I., Bremer, P., & Silcock, P. (2019). Quality and safety considerations of incorporating post-pef ageing into the pulsed electric fields and sous vide processing chain. Food and Bioprocess Technology, 12(5), 852–864. https://doi.org/10.1007/s11947-019-02254-6

Alexandrakis, D., Brunton, N. P., Downey, G., & Scannell, A. G. M. (2012). Identification of spoilage marker metabolites in Irish chicken breast muscle using HPLC, GC–MS coupled with SPME and traditional chemical techniques. Food and Bioprocess Technology, 5(5), 1917–1923. https://doi.org/10.1007/s11947-010-0500-8

Amiri, A., Mousakhani-Ganjeh, A., Shafiekhani, S., Mandal, R., & Kenari, R. E. (2019). Effect of high voltage electrostatic field thawing on the functional and physicochemical properties of myofibrillar protein. Innovative Food Science & Emerging Technologies, 56, 102191. https://doi.org/10.1016/j.ifset.2019.102191

Andreevskaya, M., Jääskeläinen, E., Johansson, P., Ylinen, A., Paulin, L., Björkroth, J., & Auvinen, P. (2018). Food spoilage-associated Leuconostoc, Lactococcus, and Lactobacillus species display different survival strategies in response to competition. Applied and Environmental Microbiology, 84(13), e00554-18. https://doi.org/10.1128/AEM.00554-18

Borch, E., & Agerhem, H. (1992). Chemical, microbial and sensory changes during the anaerobic cold storage of beef inoculated with a homofermentative Lactobacillus sp. Or a Leuconostoc sp. International Journal of Food Microbiology, 15(1), 99–108. https://doi.org/10.1016/0168-1605(92)90139-T

Cai, L., Cao, A., Li, T., Wu, X., Xu, Y., & Li, J. (2015). Effect of the fumigating with essential oils on the microbiological characteristics and quality changes of refrigerated turbot (Scophthalmus maximus) fillets. Food and Bioprocess Technology, 8(4), 844–853. https://doi.org/10.1007/s11947-014-1453-0

Chaillou, S., Chaulot-Talmon, A., Caekebeke, H., Cardinal, M., Christieans, S., Denis, C., Hélène Desmonts, M., Dousset, X., Feurer, C., Hamon, E., Joffraud, J.-J., La Carbona, S., Leroi, F., Leroy, S., Lorre, S., Macé, S., Pilet, M.-F., Prévost, H.,

Rivollier, M., … Champomier-Vergès, M.-C. (2015). Origin and ecological selection of core and food-specific bacterial communities associated with meat and seafood spoilage. The ISME Journal, 9(5), 1105–1118. https://doi.org/10.1038/ismej.2014.202

Chauhan, S. S., & England, E. M. (2018). Postmortem glycolysis and glycogenolysis: Insights from species comparisons. Meat Science, 144, 118–126. https://doi.org/10.1016/j.meatsci.2018.06.021

Chen, X., Dong, P., Li, K., Zhu, L., Yang, X., Mao, Y., Niu, L., Hopkins, D. L., Luo, X., Liang, R., & Zhang, Y. (2022). Effect of the combination of superchilling and super-chilled storage on shelf-life and bacterial community dynamics of beef during long-term storage. Meat Science, 192, 108910. https://doi.org/10.1016/j.meatsci.2022.108910

Chen, X., Zhu, L., Liang, R., Mao, Y., Hopkins, D. L., Li, K., Dong, P., Yang, X., Niu, L., Zhang, Y., & Luo, X. (2020). Shelf-life and bacterial community dynamics of vacuum packaged beef during long-term super-chilled storage sourced from two Chinese abattoirs. Food Research International, 130, 108937. https://doi.org/10.1016/j.foodres.2019.108937

Chen, Y., Bassey, A. P., Bai, Y., Teng, S., Zhou, G., & Ye, K. (2022). Synergistic effect of static magnetic field and modified atmosphere packaging in controlling blown pack spoilage in meatballs. Foods, 11(10), Article 10. https://doi.org/10.3390/foods11101374

Dalvi-Isfahan, M., Hamdami, N., & Le-Bail, A. (2016). Effect of freezing under electrostatic field on the quality of lamb meat. Innovative Food Science & Emerging Technologies, 37, 68–73. https://doi.org/10.1016/j.ifset.2016.07.028

de la Cruz Quiroz, R., Rodriguez-Martinez, V., Velazquez, G., Perez, G. M., Fagotti, F., Welti-Chanes, J., & Torres, J. A. (2020). Residential refrigerator performance based on microbial indicators of ground beef preservation assessed using predictive microbiology tools. Food and Bioprocess Technology, 13(12), 2172–2185. https://doi.org/10.1007/s11947-020-02551-5

Dimakopoulou-Papazoglou, D., Lazaridou, A., Biliaderis, C. G., & Katsanidis, E. (2022). Effect of process temperature on the physical state of beef meat constituents – implications on diffusion kinetics during osmotic dehydration. Food and Bioprocess Technology, 15(3), 706–716. https://doi.org/10.1007/s11947-022-02778-4

Ding, A., Yang, Y., Sun, G., & Wu, D. (2016). Impact of applied voltage on methane generation and microbial activities in an anaerobic microbial electrolysis cell (MEC). Chemical Engineering Journal, 283, 260–265. https://doi.org/10.1016/j.cej.2015.07.054

Domínguez, R., Gómez, M., Fonseca, S., & Lorenzo, J. M. (2014). Influence of thermal treatment on formation of volatile compounds, cooking loss and lipid oxidation in foal meat. LWT - Food Science and Technology, 58(2), 439–445. https://doi.org/10.1016/j.lwt.2014.04.006

Estévez, M., Ventanas, S., Heinonen, M., & Puolanne, E. (2011). Protein carbonylation and water-holding capacity of pork subjected to frozen storage: Effect of muscle type, premincing, and packaging. Journal of Agricultural and Food Chemistry, 59(10), 5435–5443. https://doi.org/10.1634/stemcells.2004-0024

Fallah-Joshaqani, S., Hamdami, N., & Keramat, J. (2021). Qualitative attributes of button mushroom (Agaricus bisporus) frozen under high voltage electrostatic field. Journal of Food Engineering, 293, 110384. https://doi.org/10.1016/j.jfoodeng.2020.110384

Fernando A. G., da S. Jr., Jose Jarib, A.-E., Mateus M., da C., & Helinando P., de O. (2019). Low intensity electric field inactivation of gram-positive and gram-negative bacteria via metal-free polymeric composite. Materials Science and Engineering: C, 99, 827–837. https://doi.org/10.1016/j.msec.2019.02.027

Fidan, H., Esatbeyoglu, T., Simat, V., Trif, M., Tabanelli, G., Kostka, T., Montanari, C., Ibrahim, S. A., & Özogul, F. (2022). Recent developments of Lactic acid bacteria and their metabolites on foodborne pathogens and spoilage bacteria: Facts and gaps. Food Bioscience, 47, 101741. https://doi.org/10.1016/j.fbio.2022.101741

García, D., Gómez, N., Mañas, P., Raso, J., & Pagán, R. (2007). Pulsed electric fields cause bacterial envelopes permeabilization depending on the treatment intensity, the treatment medium pH and the microorganism investigated. International Journal of Food Microbiology, 113(2), 219–227. https://doi.org/10.1016/j.msec.2019.02.027

Gómez, B., Munekata, P. E. S., Gavahian, M., Barba, F. J., Martí-Quijal, F. J., Bolumar, T., Campagnol, P. C. B., Tomasevic, I., & Lorenzo, J. M. (2019). Application of pulsed electric fields in meat and fish processing industries: An overview. Food Research International, 123, 95–105. https://doi.org/10.1016/j.foodres.2019.04.047

Gonzalez, M. E., & Barrett, D. M. (2010). Thermal, high pressure, and electric field processing effects on plant cell membrane integrity and relevance to fruit and vegetable quality. Journal of Food Science, 75(7), R121–R130. https://doi.org/10.1111/j.1750-3841.2010.01763.x

Gu, X., Feng, L., Zhu, J., Li, Y., Tu, K., Dong, Q., & Pan, L. (2021). Application of gas sensors for modelling the dynamic growth of Pseudomonas in pork stored at different temperatures. Meat Science, 171, 108282. https://doi.org/10.1016/j.meatsci.2020.108282

Gumbart, J., Khalili-Araghi, F., Sotomayor, M., & Roux, B. (2012). Constant electric field simulations of the membrane potential illustrated with simple systems. Biochimica et Biophysica Acta (BBA) - Biomembranes, 1818(2), 294–302. https://doi.org/10.1016/j.bbamem.2011.09.030

Hautanen, J., Janka, K., Koskinen, J., Lehtimäki, M., & Kivistö, T. (1986). Optimization of filtration efficiency and ozone production of the electrostatic precipitator. Journal of Aerosol Science, 17(3), 622–626. https://doi.org/10.1016/0021-8502(86)90173-4

He, X., Liu, R., Satoru, N., Zheng, D., & Liu, H. (2013). Effect of high voltage electrostatic field treatment on thawing characteristics and post-thawing quality of frozen pork tenderloin meat. Journal of Food Engineering, 115(2), 245–250. https://doi.org/10.1016/j.jfoodeng.2012.10.023

He, Y., Gang, S., Koga, K., & Xu, L. (2014). Electrostatic field-exposed water in nanotube at constant axial pressure. Scientific Reports, 4(1), 1–5. https://doi.org/10.1038/srep06596

Hennefarth, M. R., & Alexandrova, A. N. (2022). Advances in optimizing enzyme

electrostatic preorganization. Current Opinion in Structural Biology, 72, 1–8. https://doi.org/10.1016/j.sbi.2021.06.006

Holman, B. W. B., Bekhit, A. E.-D. A., Waller, M., Bailes, K. L., Kerr, M. J., & Hopkins, D. L. (2021). The association between total volatile basic nitrogen (TVB-N) concentration and other biomarkers of quality and spoilage for vacuum packaged beef. Meat Science, 179, 108551. https://doi.org/10.1016/j.meatsci.2021.108551

Hopkins, D. L., Toohey, E. S., Warner, R. D., Kerr, M. J., Ven, R. van de, Hopkins, D. L., Toohey, E. S., Warner, R. D., Kerr, M. J., & Ven, R. van de. (2010). Measuring the shear force of lamb meat cooked from frozen samples: Comparison of two laboratories. Animal Production Science, 50(6), 382–385. https://doi.org/10.1071/AN09162

Hu, F., Qian, S., Huang, F., Han, D., Li, X., & Zhang, C. (2021). Combined impacts of low voltage electrostatic field and high humidity assisted-thawing on quality of pork steaks. LWT- Food Science and Technology, 150, 111987. https://doi.org/10.1016/j.lwt.2021.111987

Hu, R., Zhang, M., & Fang, Z. (2022). A novel synergistic freezing assisted by infrared pre-dehydration combined with magnetic Field: Effect on freezing efficiency and thawed product qualities of beef. Food and Bioprocess Technology, 15(6), 1392–1405. https://doi.org/10.1007/s11947-022-02825-0

Huang, H., Sun, W., Xiong, G., Shi, L., Jiao, C., Wu, W., Li, X., Qiao, Y., Liao, L., Ding, A., & others. (2020). Effects of HVEF treatment on microbial communities and physicochemical properties of catfish fillets during chilled storage. LWT - Food Science and Technology, 131, 109667. https://doi.org/10.1016/j.lwt.2020.109667

Huang, H., Xiong, G., Shi, L., Wu, W., Li, X., Qiao, Y., Liao, L., Ding, A., & Wang, L. (2021). Application of HVEF treatment in bacteriostasis against Acinetobacter radioresistens. Food Control, 124, 107914. https://doi.org/10.1016/j.foodcont.2021.107914

Huang, J., Que, F., Xiong, G., Qiao, Y., Wu, W., Wang, J., Ding, A., Liao, L., Shi, L., & Wang, L. (2023). Physicochemical and functional properties changes in myofibrillar protein extracted from channel catfish by a high-voltage electrostatic field. Food and Bioprocess Technology, 16(2), 395–403. https://doi.org/10.1007/s11947-022-02937-7

Hülsheger, H., Potel, J., & Niemann, E.-G. (1983). Electric field effects on bacteria and yeast cells. Radiation and Environmental Biophysics, 22(2), 149–162. https://doi: 10.1007/BF01338893

Hussain, M., Nauman, K., Asghar, B., Iqbal, S., & Rashid, M. A. (2021). Effect of low voltage electrical stimulation and chilling on microbial safety and quality attributes of Beetal Bucks and Lohi Rams carcass. Small Ruminant Research, 196, 106315. https://doi.org/10.1016/j.smallrumres.2020.106315

Ivanovic, J., Janjic, J., Đorđević, V., Dokmanović, M., Bošković, M., Marković, R., & Baltić, M. (2015). The effect of different packaging conditions, ph and Lactobacillus spp. On the growth of Yersinia enterocolitica in pork meat. Journal of Food Processing and Preservation, 39(6), 2773–2779. https://doi.org/10.1111/jfpp.12528

Johari, G. P. (1981). The dipolar correlation factor, the electrostatic field, the dipole moment, and the coulombic interaction energy of water molecules in clathrate

hydrates. The Journal of Chemical Physics, 74(2), 1326–1336.

Ko, W. C., Yang, S. Y., Chang, C. K., & Hsieh, C. W. (2016). Effects of adjustable parallel high voltage electrostatic field on the freshness of tilapia (Orechromis niloticus) during refrigeration. LWT - Food Science and Technology, 66, 151–157. https://doi.org/10.1016/j.lwt.2015.10.019

Leong, S. Y., Burritt, D. J., & Oey, I. (2016). Effect of combining pulsed electric fields with maceration time on merlot grapes in protecting CACO-2 cells from oxidative stress. Food and Bioprocess Technology, 9(1), 147–160. https://doi.org/10.1007/s11947-015-1604-y

Levkov, K., Vitkin, E., González, C. A., & Golberg, A. (2019). A laboratory IGBT-based high-voltage pulsed electric field generator for effective water diffusivity enhancement in chicken meat. Food and Bioprocess Technology, 12(12), 1993–2003. https://doi.org/10.1007/s11947-019-02360-5

Li, D., Jia, S., Zhang, L., Wang, Z., Pan, J., Zhu, B., & Luo, Y. (2017). Effect of using a high voltage electrostatic field on microbial communities, degradation of adenosine triphosphate, and water loss when thawing lightly-salted, frozen common carp (Cyprinus carpio). Journal of Food Engineering, 212, 226–233. https://doi.org/10.1016/j.jfoodeng.2017.06.003

Li, N., Zhang, Y., Wu, Q., Gu, Q., Chen, M., Zhang, Y., Sun, X., & Zhang, J. (2019). High-throughput sequencing analysis of bacterial community composition and quality characteristics in refrigerated pork during storage. Food Microbiology, 83, 86–94. https://doi.org/10.1016/j.fm.2019.04.013

Li, X., Zhang, Y., Li, Z., Li, M., Liu, Y., & Zhang, D. (2017). The effect of temperature in the range of −0.8 to 4°C on lamb meat color stability. Meat Science, 134, 28–33. https://doi.org/10.1016/j.meatsci.2017.07.010

Lin, Z., Yong, H., Zhang, C., Zhao, R., & Tang, S. (2017). Molecular dynamics simulation for the impact of an electrostatic field and impurity Mg2+ ions on hard water. Royal Society of Chemistry, 7(75), 47583–47591. https://doi.org/10.1039/C7RA09715H

Mai, X., Wang, W., Zhang, X., Wang, D., Liu, F., & Sun, Z. (2022). Mathematical modeling of the effects of temperature and modified atmosphere packaging on the growth kinetics of Pseudomonas Lundensis and Shewanella Putrefaciens in chilled chicken. Foods, 11(18), Article 18. https://doi.org/10.3390/foods11182824

Mason, C. K., Collins, M. A., & Thompson, K. (2005). Modified electroporation protocol for Lactobacilli isolated from the chicken crop facilitates transformation and the use of a genetic tool. Journal of Microbiological Methods, 60(3), 353–363. https://doi.org/10.1016/j.mimet.2004.10.013

Matsumoto, M., Saito, S., & Ohmine, I. (2002). Molecular dynamics simulation of the ice nucleation and growth process leading to water freezing. Nature, 416(6879), 409–413. https://doi.org/10.1038/416409a

Nowak, A., Rygala, A., Oltuszak-Walczak, E., & Walczak, P. (2012). The prevalence and some metabolic traits of Brochothrix thermosphacta in meat and meat products packaged in different ways. Journal of the Science of Food and Agriculture, 92(6), 1304–1310. https://doi.org/10.1002/jsfa.4701

Ohshima, T., Tanino, T., Guionet, A., Takahashi, K., & Takaki, K. (2021). Mechanism of

pulsed electric field enzyme activity change and pulsed discharge permeabilization of agricultural products. Japanese Journal of Applied Physics, 60(6), 060501. https://doi.org/10.35848/1347-4065/abf479

Ouyang, Q., Liu, L., Zareef, M., Wang, L., & Chen, Q. (2022). Application of portable visible and near-infrared spectroscopy for rapid detection of cooking loss rate in pork: Comparing spectra from frozen and thawed pork. LWT-Food Science and Technology, 160, 113304. https://doi.org/10.1016/j.lwt.2022.113304

Papadopoulou, O. S., Doulgeraki, A. I., Botta, C., Cocolin, L., & Nychas, G.-J. E. (2012a). Genotypic characterization of Brochothrix thermosphacta isolated during storage of minced pork under aerobic or modified atmosphere packaging conditions. Meat Science, 92(4), 735–738. https://doi.org/10.1016/j.meatsci.2012.06.030

Papadopoulou, O. S., Doulgeraki, A. I., Botta, C., Cocolin, L., & Nychas, G.-J. E. (2012b). Genotypic characterization of Brochothrix thermosphacta isolated during storage of minced pork under aerobic or modified atmosphere packaging conditions. Meat Science, 92(4), 735–738.

Pavlin, M., Leben, V., & Miklavčič, D. (2007). Electroporation in dense cell suspension—Theoretical and experimental analysis of ion diffusion and cell permeabilization. Biochimica et Biophysica Acta (BBA) - General Subjects, 1770(1), 12–23. https://doi.org/10.1016/j.bbagen.2006.06.014

Pearce, K. L., Rosenvold, K., Andersen, H. J., & Hopkins, D. L. (2011). Water distribution and mobility in meat during the conversion of muscle to meat and ageing and the impacts on fresh meat quality attributes—A review. Meat Science, 89(2), 111–124. https://doi.org/10.1016/j.meatsci.2011.04.007

Poojary, M., Roohinejad, S., Koubaa, M., Barba, F., Passamonti, P., Jambrak, A. R., Oey, I., & Greiner, R. (2016). Impact of pulsed electric fields on enzyme. In Handbook of Electroporation (pp. 1–21). Springer International Publishing. https://hal.science/hal-02614903

Pu P., Pu J., & Zhu Z. (2020). Study on the structure model of water molecule and the reasons of formation of some characteristics of liquid & solid water. American Journal of Modern Physics, 9(2), 11. https://doi.org/10.11648/j.ajmp.20200902.11

Qi, M., Yan, H., Zhang, Y., & Yuan, Y. (2022). Impact of high voltage prick electrostatic field (HVPEF) processing on the quality of ready-to-eat fresh salmon (Salmo salar) fillets during storage. Food Control, 137, 108918. https://doi.org/10.1016/j.foodcont.2022.108918

Qi, M., Zhao, R., Liu, Q., Yan, H., Zhang, Y., Wang, S., & Yuan, Y. (2021). Antibacterial activity and mechanism of high voltage electrostatic field (HVEF) against Staphylococcus aureus in medium plates and food systems. Food Control, 120, 107566. https://doi.org/10.1016/j.foodcont.2020.107566

Qian, S., Li, X., Wang, H., Mehmood, W., Zhong, M., Zhang, C., & Blecker, C. (2019). Effects of low voltage electrostatic field thawing on the changes in physicochemical properties of myofibrillar proteins of bovine Longissimus dorsi muscle. Journal of Food Engineering, 261, 140–149. https://doi.org/10.1016/j.jfoodeng.2019.06.013

Rahbari, M., Hamdami, N., Mirzaei, H., Jafari, S. M., Kashaninejad, M., & Khomeiri, M. (2018). Effects of high voltage electric field thawing on the characteristics of

chicken breast protein. Journal of Food Engineering, 216, 98–106. https://doi.org/10.1016/j.jfoodeng.2017.08.006

Robazza, W. da S., Teleken, J. T., Galvão, A. C., Miorelli, S., & Stolf, D. O. (2017). Application of a model based on the central limit theorem to predict growth of Pseudomonas spp. In fish meat. Food and Bioprocess Technology, 10(9), 1685–1694. https://doi.org/10.1007/s11947-017-1939-7

Ross, C. L. (2017). The use of electric, magnetic, and electromagnetic field for directed cell migration and adhesion in regenerative medicine. Biotechnology Progress, 33(1), 5–16. https://doi.org/10.1002/btpr.2371

Ruiz-Cabrera, M. A., Gou, P., Foucat, L., Renou, L. P., & Daudin, J. D. (2004). Water transfer analysis in pork meat supported by NMR imaging. Meat Science, 67(1), 169–178. https://doi.org/10.1016/j.meatsci.2003.10.005

Scheier, R., Bauer, A., & Schmidt, H. (2014). Early postmortem prediction of meat quality traits of porcine semimembranosus muscles using a portable Raman system. Food and Bioprocess Technology, 7(9), 2732–2741. https://doi.org/10.1007/s11947-013-1240-3

Seyfi, P., Golghand, M. R., Ghasemi, S., & Ghomi, H. (2020). The effect of mixed electric field on characteristic of ozone generation in a DBD plasma source. Journal of Theoretical and Applied Physics, 14(3), 195–202. https://doi.org/10.1007/s40094-020-00385-2

Song, W., Du, Y., Yang, C., Li, L., Wang, S., Liu, Y., & Wang, W. (2020). Development of PVA/EVA-based bilayer active film and its application to mutton. LWT - Food Science and Technology, 133, 110109. https://doi.org/10.1016/j.lwt.2020.110109

Sun, S., Zhao, J., Luo, Z., Lin, Q., Luo, F., & Yang, T. (2020). Systematic evaluation of the physicochemical properties and the volatile flavors of yak meat during chilled and controlled freezing-point storage. Journal of Food Science and Technology, 57(4), 1351–1361. https://doi.org/10.1007/s13197-019-04169-8

Sun, T. L., Zhang, P., Ren, Z. H., Zhang, P., & Yue, X. Q. (2013). Optimization of the combination of three natural preservatives in beef storage with controlled freezing point technique. Advanced Materials Research, 781–784, 1700–1707. Advances in Chemical Engineering III. https://doi.org/10.4028/www.scientific.net/AMR.781-784.1700

Suwandy, V., Carne, A., van de Ven, R., Bekhit, A. E.-D. A., & Hopkins, D. L. (2015). Effect of pulsed electric field treatment on the eating and keeping qualities of cold-boned beef loins: Impact of initial pH and fibre orientation. Food and Bioprocess Technology, 8(6), 1355–1365. https://doi.org/10.1007/s11947-015-1498-8

Tsong, T. Y. (1990). Electrical modulation of membrane proteins: Enforced conformational oscillations and biological energy and signal transductions. Annual Review of Biophysics and Biophysical Chemistry, 19(1), 83–106. https://doi.org/10.1146/annurev.bb.19.060190.000503

Valdivia-Nájar, C. G., Martín-Belloso, O., Giner-Seguí, J., & Soliva-Fortuny, R. (2017). Modeling the inactivation of Listeria innocua and Escherichia coli in fresh-cut tomato treated with pulsed light. Food and Bioprocess Technology, 10(2), 266–274. https://doi.org/10.1007/s11947-016-1806-y

Vanga, S. K., Wang, J., Jayaram, S., & Raghavan, V. (2021). Effects of pulsed electric

fields and ultrasound processing on proteins and enzymes: A review. Processes, 9(4), Article 4. https://doi.org/10.3390/pr9040722

Vasconcelos, H., Saraiva, C., & de Almeida, J. M. M. M. (2014). Evaluation of the spoilage of raw chicken breast fillets using fourier transform infrared spectroscopy in tandem with chemometrics. Food and Bioprocess Technology, 7(8), 2330–2341. https://doi.org/10.1007/s11947-014-1277-y

Wang, C., Chu, J., Fu, L., Wang, Y., Zhao, F., & Zhou, D. (2018). iTRAQ-based quantitative proteomics reveals the biochemical mechanism of cold stress adaption of razor clam during controlled freezing-point storage. Food Chemistry, 247, 73–80. https://doi.org/10.1016/j.foodchem.2017.12.004

Wang, L., Liu, Z., Dong, S., Zhao, Y., & Zeng, M. (2014). Effects of vacuum and modified atmosphere packaging on microbial flora and shelf-life of pacific white shrimp (Litopenaeus vannamei) during controlled freezing-point storage at −0.8°C. Food Science and Technology Research, 20(6), 1141–1152. https://doi.org/10.3136/fstr.20.1141

Wang, L., Wang, M., Zeng, X., & Liu, Z. (2016). Temperature-mediated variations in cellular membrane fatty acid composition of Staphylococcus aureus in resistance to pulsed electric fields. Biochimica et Biophysica Acta (BBA) - Biomembranes, 1858(8), 1791–1800. https://doi.org/10.1016/j.bbamem.2016.05.003

Wang, Q., Li, Y., Sun, D.-W., & Zhu, Z. (2018). Enhancing food processing by pulsed and high voltage electric fields: Principles and applications. Critical Reviews in Food Science and Nutrition, 58(13), 2285–2298. https://doi.org/10.1080/10408398.2018.1434609

Wang, X. Y., Xie, J., & Chen, X. J. (2021). Applications of non-invasive and novel methods of low-field nuclear magnetic resonance and magnetic resonance imaging in aquatic products. Frontiers in Nutrition, 8, 651804. https://doi.org/10.3389/fnut.2021.651804

Wang, Y., Yi, J., Yi, J., Dong, P., Hu, X., & Liao, X. (2013). Influence of pressurization rate and mode on inactivation of natural microorganisms in purple sweet potato nectar by high hydrostatic pressure. Food and Bioprocess Technology, 6(6), 1570–1579. https://doi.org/10.1007/s11947-012-0897-3

Wen, X., Liang, C., Zhang, D., Li, X., Chen, L., Zheng, X., Fang, F., Cheng, Z., Wang, D., & Hou, C. (2022). Effects of hot or cold boning on the freshness and bacterial community changes of lamb cuts during chilled storage. LWT - Food Science and Technology, 170, 114063. https://doi.org/10.1016/j.lwt.2022.114063

Wickramasinghe, N. N., Ravensdale, J., Coorey, R., Chandry, S. P., & Dykes, G. A. (2019). The predominance of Psychrotrophic Pseudomonads on aerobically stored chilled red meat. Comprehensive Reviews in Food Science and Food Safety, 18(5), 1622–1635. https://doi.org/10.1111/1541-4337.12483

Xanthakis, E., Havet, M., Chevallier, S., Abadie, J., & Le-Bail, A. (2013a). Effect of static electric field on ice crystal size reduction during freezing of pork meat. Innovative Food Science & Emerging Technologies, 20, 115–120. https://doi.org/10.1016/j.ifset.2013.06.011

Xanthakis, E., Havet, M., Chevallier, S., Abadie, J., & Le-Bail, A. (2013b). Effect of static electric field on ice crystal size reduction during freezing of pork meat. Innovative Food Science & Emerging Technologies, 20, 115–120.

https://doi.org/10.1016/j.ifset.2013.06.011

Xiao, Y., Liu, Y., Chen, C., Xie, T., & Li, P. (2020). Effect of Lactobacillus plantarum and Staphylococcus xylosus on flavour development and bacterial communities in chinese dry fermented sausages. Food Research International, 135, 109247. https://doi.org/10.1016/j.foodres.2020.109247

Xu, C.-C., Yu, H., Xie, P., Sun, B.-Z., Wang, X.-Y., & Zhang, S.-S. (2020). Influence of electrostatic field on the quality attributes and volatile flavor compounds of dry-cured beef during chill storage. Foods, 9(4), Article 4. https://doi.org/10.3390/foods9040478

Xu, M. M., Kaur, M., Pillidge, C. J., & Torley, P. J. (2023). Culture-dependent and culture-independent evaluation of the effect of protective cultures on spoilage-related bacteria in vacuum-packaged beef mince. Food and Bioprocess Technology, 16(2), 382–394. https://doi.org/10.1007/s11947-022-02948-4

Yan, L.-G., He, L., & Xi, J. (2017). High intensity pulsed electric field as an innovative technique for extraction of bioactive compounds—A review. Critical Reviews in Food Science and Nutrition, 57(13), 2877–2888. https://doi.org/0.1080/10408398.2015.1077193

Youssef, A. M., El-Sayed, H. S., El-Sayed, S. M., Fouly, M., & El-Aziz, M. E. A. (2023). Novel bionanocomposites based on cinnamon nanoemulsion and tio2-nps for preserving fresh chicken breast fillets. Food and Bioprocess Technology, 16(2), 356–367. https://doi.org/10.1007/s11947-022-02934-w

Yusupov, M., Van der Paal, J., Neyts, E. C., & Bogaerts, A. (2017). Synergistic effect of electric field and lipid oxidation on the permeability of cell membranes. Biochimica et Biophysica Acta (BBA) - General Subjects, 1861(4), 839–847. https://doi.org/10.1016/j.bbagen.2017.01.030

Zhao, X., Xing, T., Chen, X., Han, M., Deng, S., Xu, X., & Zhou, G. (2017). Changes of molecular forces during thermo-gelling of protein isolated from pse-like chicken breast by various isoelectric solubilization/precipitation extraction strategies. Food and Bioprocess Technology, 10(7), 1240–1247. https://doi.org/10.1007/s11947-017-1893-4

Zhu, N., Yu, N., Zhu, Y., Wei, Y., Zhang, H., & Sun, A. (2018). Inactivation of Pichia rhodanensis in relation to membrane and intracellular compounds due to microchip pulsed electric field (MPEF) treatment. Plos One, 13(6), e0198467. https://doi.org/0.1371/journal.pone.0198467

Zhu, Y., Zhang, K., Ma, L., Huo, N., Yang, H., & Hao, J. (2015). Sensory, physicochemical, and microbiological changes in vacuum packed channel catfish (Clarias lazera) patties during controlled freezing-point storage. Food Science and Biotechnology, 24(4), 1249–1256. https://doi.org/10.1007/s10068-015-0160-6

Chapter 4

Effects of different EF intensities assisted CFPS on WHC of chilled fresh meat during the early postmortem period

This chapter aimed to investigate how different EF intensities combined with CFPS affect the WHC of chilled fresh pork during the early postmortem period. Key objectives included evaluating EF impacts on actomyosin behavior, moisture distribution, and structural integrity. Cooking loss, T_2 transverse relaxation, myofibril fragmentation index (MFI), muscle microstructure (SEM), actomyosin particle size, secondary structure (FTIR), and actomyosin dissociation (SDS-PAGE) were analyzed. Results revealed that both low-voltage (LVEF) and high-voltage EF (HVEF) significantly reduced cooking loss compared to the control (CK), with HVEF exhibiting superior preservation of myofibril integrity. EF treatments enhanced hydrogen bonding, minimized immobilized water migration, and stabilized actomyosin interactions, thereby improving WHC. This chapter concluded that EF, particularly HVEF, optimizes WHC by modulating water distribution and actomyosin dynamics, offering a viable non-thermal strategy for meat preservation. These findings provide critical insights for advancing EF-based technologies in the meat industry to enhance storage quality and reduce moisture loss.

This chapter is adapted from:

Xu, Y., Leng, D., Li, X., Wang D., Chai X., Schroyen M., Zhang, D., Hou C. Effects of different electrostatic field intensities assisted controlled freezing point storage on water holding capacity of fresh meat during the early postmortem period. Food Chemistry 439, 138096 (2024).

https://doi.org/10.1016/j.foodchem.2023.138096

1. Abstract

In this study, the effect of different intensity EFs on the WHC of chilled fresh meat during the early postmortem period in CFPS were investigated. Significantly lower cooking loss were found in low voltage EF (LVEF) and high voltage EF (HVEF) compared to the control group (CK) ($P < 0.05$). The myofibril fragmentation index and microstructure results suggested that the sample under HVEF treatment remained relatively intact. It has been revealed that the changes in actomyosin properties under EF treatment groups were due to the combination and dissociation of actomyosin binding into myofilament concentration, which consequently affects the muscle WHC. The study further demonstrated that the EF, especially HVEF, might increase the WHC of chilled fresh meat by affecting the distribution of water molecules and physiochemical properties of actomyosin during the early postmortem period.

Keywords

EF, CFPS, Early postmortem period, WHC, Microstructure, Actomyosin.

2. Introduction

The fresh meat commonly comprises the majority of meat consumed in China. The glycolysis process, a physiological and biochemical reaction, naturally occurs in the muscle following slaughter, which plays a critical role in determining meat quality (Scheffler & Gerrard, 2007). The glycolytic process usually leads to the consumption of glycogen and ATP, causing an increase in lactic acid in muscles and a decrease in pH value. Meanwhile, the moisture content in the muscle undergone a serious of dynamic change after slaughter, thus influencing the storage quality of fresh meat during postmortem. The variation of WHC and the mechanism behind the phenomenon are well understood in earlier studies (Ma et al., 2023; Zhai et al., 2020). Melody et al. (2004) gave a view that the degradation of myofibrillar contributes to the decline in WHC during the early postmortem period. Similarly, Sabikun et al. (2019) demonstrated significant differences in moisture content during the early postmortem period, and pre-rigor muscles exhibited a higher WHC than post-rigor muscles. Furthermore, Ge et al. (2021) reported that the transition of water molecules leads to an increase in moisture loss in rigor mortis and post-rigor period. In addition, improving the WHC of fresh meat during the early postmortem period has been emphasized in current studies, from the internal mechanism to the external environment, cause this has a significant impact on the formation and determination of the quality of fresh meat after slaughter (Lin et al., 2022; Zhang et al., 2023).

Storage temperature has been proved as one of the crucial external environments in regulating the storage quality of fresh meat. CFPS has been identified as a viable option for the preservation of fresh meat, due to its efficiency in maintaining the WHC of meat (Park et al., 2022). The fact indicated that storing the meat at a specific temperature in the early postmortem period allows for the maintenance of desired storage quality of the fresh meat, greatly reducing moisture loss and extending the shelf life (Park et al., 2022). Mi et al. (2013) suggested that -2°C has attractive feature on the maintain of WHC compared with frozen storage. For a recent review, Lee et al. (2022) demonstrated that the pork loins stored at -3°C were performed superior than frozen samples in terms of WHC. Despite the effective WHC achieved, the narrow temperature range is consistently be the bottleneck that restricts the application in the chilled fresh meat preservation industry. The EF is an non-thermal technologies, which could provide a stable EF for a certain period and maintain the storage quality of fresh meat (Qi et al., 2022). Currently, EFs have been introduced to scientific research and a small part of industries for the preservation of fresh meat, such as reduce moisture loss, protein degradation, and color deterioration (Amiri et al., 2019; Wu et al., 2023). For example, the space EF system designed by DENBA+ TECHNOLOGY can activate cells for preservation. Our previous study demonstrated that the EF have a significant effect on reducing the moisture loss of chilled fresh meat during long-term CFPS. It has considerably enhanced WHC of post-rigor chilled fresh meat following consistently exposure to EF combined with CFPS, and developed different functional and physiochemical changes in myofibrillar (Xu et al., 2023).

However, few basic formations in the current literature regarding the underlying mechanism of different EF intensities assisted CFPS effect on the WHC of chilled fresh meat during the early postmortem period are available, mostly focus on the post-rigor period. Therefore, different intensities of EF assisted CFPS after slaughter for 5 d as a representative method in this study to investigate the WHC of muscle by comparing the change in properties such as cooking loss, moisture distribution, myofibril fragmentation index (MFI), muscle microstructure, partied size, and secondary structure of the actomyosin were determined. Furthermore, actomyosin degradation and dissociation were evaluated by SDS-PAGE and Western-Blot. The overall objective of this study was to investigate the impact of different EF intensities assisted CFPS on the WHC of the chilled fresh meat during the early postmortem period and attempted to evaluate the EF mechanism responsible for WHC in fresh meat from the combination and dissociation of actin and myosin.

3. Materials and methods

3.1 Materials

Ten *M. Longissimus thoracis et lumborum* (LTL) muscles were obtained from Beijing Ershang Meat Food Group Co., Ltd., taken from Landrace × Yorkshire × Duroc pigs aged six months and weighing an approximate 75 kg. The LTL muscles were then rapidly transported to the laboratory within 0.5 hours (0~4℃). Following this, each muscle was evenly sliced into 18 cuts (about 6 cm × 5 cm × 6 cm, 40 g) and packaged with PE film. Finally, the samples were randomly assigned to 3 treatment groups (Control group, CK; low voltage EF, LVEF; high voltage EF, HVEF). All the treatments group samples were placed in a -1.0 ± 0.5℃ humidity chamber (JYH-103, HENGWELL, Shanghai, China) for 0 h, 6 h, 12 h, 1d, 3 d, 5 d, respectively. The CK group received no EF, the LVEF group were exposed to a 4.0 kV (40 kV/m) EF intensity, and the HVEF group samples were exposed to a 12.0 kV EF intensity. To assess the effects of the EFs, the cooking loss, T_2 transverse relaxation, myofibrils microstructure (scanning electron microscope, SEM) and distribution of H-protons, myofibril fragmentation index, particle size of actomyosin, Fourier transform infrared spectroscopy spectrum (FTIR) and dissociation of actomyosin were measured in the respective samples.

3.2 The EF generation device

As in our previous study (Xu et al., 2023), a EF power supply (TCM6000i, TAISIMAN, Dalian, China), along with a 256 L humidity chamber (JYH-103, HENGWELL, Shanghai, China) were employed to form the EF generation device. The output terminals of the device were two copper plates with the samples placed between them, keeping a distance of 10 cm. The entire experimental system was set

up in a laboratory with a fixed temperature (-1.0 ± 0.5℃) and humidity (85.00 ± 0.50%).

3.3 Measurement of cooking loss

According to the report of Hopkins et al. (2010), the cooking loss were determined. The samples (20.00 ± 0.05 g) were put in sterile bags and cooked in a water bath at 71°C tested by the multi-channel temperature inspection instrument (LK-U, LANGUANG, Changzhou, China) before cooling down to room temperature and being weighted as M9. Wiped off the surface moisture and weighed as M10. Samples were measured simultaneously. The results were determined by the following Eq. (6):

$$\text{Cooking loss (\%)} = (M9-M10)/M9 \times 100 \quad (6)$$

3.4 Determination of T_2 transverse relaxation

The sample (3 cm × 1 cm × 1 cm) were placed in the hydrogen proton Nuclear Magnetic Resonance Imaging (NMI) (NMI20-040H-I, NIUMAG, Suzhou, China) tube. All the test parameters were according to the method of Xu et al. (2023) in order to analyze the migration of moisture content.

3.5 Distribution of H-protons measurement

Distribution of H-protons was assayed by NIUMAG NMR image processing system software (V1.0, NIUMAG, Shanghai, China). All the main parameters and relative analysis were referred to Xu et al. (2023).

3.6 Myofibril fragmentation index measurement

Samples were weighed about 1.00 ± 0.02 g and added 10 mL of MFI buffer (0.1 mol/L KCl, 0.02 mol/L Na2HPO4, 0.001 mol/L ethylene diamine tetraacetic acid (EDTA), 0.001 mmol/L MgCl2, pH 7.1), homogenize at 4°C, 1 200 r/min for 3 min, then centrifuged at 4°C, 3 000 × g for 15 min to collect precipitate. The pre-cooled MFI buffer (5 mL) were used to fully suspended the precipitate, filtered with a 200-mesh sieve and collect the filtrate. The protein content (M11) was measured by BCA method and adjusted to 1.0 mg/mL. The results were calculated by Eq. (7):

$$\text{MFI} = M11 \times 200 \quad (7)$$

3.7 SEM muscle microstructure measurement

Samples were taken about 5 mm × 3 mm × 3 mm along the fiber direction, and fix them with glutaraldehyde solution (2.5%) at 4℃. Take out the tissue block and rinse it repeatedly with phosphate buffer for 4 times each time, and then dehydrate with 30%, 50%, 70%, 80% and 90% ethanol solution gradient. The ethanol was replaced with isoamyl acetate, and dried in the oven at 30°C. The dried samples were fixed on

the sample table with conductive tape. The surface of the samples was sputtered and sprayed with gold. The results were observed by SEM (SU8010, Hitachi, Japan) and photographed.

3.8 Extraction of actin and actomyosin protein

The extraction of free actin and actomyosin was extracted as reported by Okitani et al. (2009). Sample were weighed about 2.00 ± 0.02 g and homogenized with 20 mL pre-cooled Weber-Edsall solution (0.6 mol/L KCl, 0.04 mol/L $NaHCO_3$, 0.01 mol/L Na_2CO_3, pH 7.2) for 2 times (30 s once, 10 s intervals, 1 200 r/min). The homogenate was placed in a 4°C liquid shake culture for 24 h. The 10 mL solution was taken as the total actin solution. The rest of 10 mL solution was diluted with 20 mL ultrapure water and then centrifuged at 4°C and 15 000 × g for 20 min to obtain the free actin solution. The precipitate was dissolved in Tris-KCl solution to obtain the actomyosin.

Part of the actomyosin solution was freeze-drying for FTIR spectroscopy. For SDS-PAGE analysis, the free actin solution and total actin solution of each sample was conducted into SDS-PAGE loading solution (Bai et al., 2020). The remaining actomyosin solution was diluted with Tris-KCL solution to a protein content of 1.0 mg/mL for subsequent experiments.

3.9 Particle size of the actomyosin protein determination

The zetasizer (Nano ZS90, Malvern Instruments Ltd., UK) was used to measure the particle size distribution of a protein solution (1.0 mg/mL). The average value was taken after three consecutive measurements.

3.10 Secondary structure of actomyosin protein determination

Tableting 1 mg freeze-drying samples obtained from 2.8, mix with 100 mg of potassium bromide. OMNIC software (Nicolet, Thermo Nicolet Corp., Madison, Wisconsin, USA) was used to limit the spectral band range to 1200~1700 cm-1 after grind and compress. Infrared spectra in transmission mode were recorded with a TENSOR 27 FTIR (BURUKER, Immanuelshofen, Baden-Wurttemberg, Germany) spectrometer.

3.11 Dissociation of the actomyosin protein determination

The 12% separating gels and 4% stacking gels were selected to determine the SDS-PAGE. After electrophoresis separation, the protein was printed to polyvinylidene fluoride (PVDF) membranes (Millipore, Billerica, MA) at 100 V. Subsequently, the transferred PVDF membrane was incubated overnight at 4°C with a primary antibody α-actin (ABclonal, catalog number A2319, 1:1000 dilution). Then, the membrane was incubated with a secondary antibody anti-rabbit-IgG-HRP (ABclonal, catalog number, AS014, 1:5000 dilution). Following the incubation, protein signals on the membranes

was visualized using the chromogenic agent DAB. The band intensity was analyzed according to the method of Bai et al. (2020). To ensure accuracy, select a random sample as the internal reference protein to reduce errors and the optical density values were obtained for subsequent data analysis. The dissociation of actomyosin was determined by the ratio of the optical density values of the free actin and total actin.

3.12 Statistical analysis

General Linear Model Program (IBM SPSS, 29.0, USA) was utilized to analyze cooking loss, T_2 transverse relaxation, myofibril fragmentation index, secondary structure, partied size, SEM of actomyosin protein and dissociation of actomyosin, respectively. Fixed effects were composed of different treatments, storage time, and their interaction, while carcass numbers was considered as the random factor. The significance level ($P < 0.05$) was conducted by Least significant differences (LSD) test. Results were presented as the mean $\pm$ standard errors.

4. Results and discussion

4.1 The change of WHC

The changes of cooking loss with storage time in different treatment groups were shown in Fig. 20. The cooking loss of the CK group increased considerably with the prolongation of postmortem time (0 ~ 12 h), reached the maximum at 12 h, then decreased at 1 d, and increased at the rest of storage period. The cooking loss of the HVEF and LVEF treatment groups were lower than that of the CK group after slaughter, resulted in a significantly reduction in moisture loss ($P < 0.05$). Simultaneously, the cooking loss of the HVEF treatment group was significantly different from those of the LVEF group, indicating that the HVEF has a unique appearance in WHC ($P < 0.05$). The blood circulation and energy support of the livestock were stopped after slaughter, while the complex physiochemical process of many muscle cells was still energetic in the pre-rigor, rigor mortis, and post-rigor stages (Ding et al., 2022). The changes in the moisture content continue to change obviously along with this process. Muscle fibers constantly contracted horizontally and longitudinally after slaughter was derived from glycolysis (Varghese & Mathew, 2017). The immobilized water inside the myofibrils was converted into free water and existed between the myofibrils, resulting in a WHC decrease in the CK group at 6 h. At 12 h, the samples in the CK group had the highest cooking loss and the worst WHC, which could be considered in the rigor mortis stage (Ge et al., 2021). The WHC in the CK group showed an upturned trend, as indicated by the observation of lactic acid depleted promote the muscles entered the post-rigor stage. Compared to the CK group, a lower cooking loss in LVEF and HVEF indicated relatively less muscle contraction intensity and stable water molecules occurred under the EF. Although the cooking loss peaked at 12 h, the moisture loss was much lower than in the CK group. Xie et al. (2023) has observed that the EF could strongly influence the WHC of meat. Usually, when the pH value of the solution deviates from the isoelectric point of the protein,

the protein undergoes a charge change, leading to a decrease in its solubility and easy precipitation. The EF alters the charge effect of proteins, forcing peptide chains to stretch and improving protein stability. Typically, when the pH value of the solution diverges from the protein's isoelectric point, the protein experiences an alteration in its charge, resulting in reduced solubility and increased precipitation. The EF modifies the charge impact on proteins, compelling peptide chains to elongates, thereby enhancing protein stability in solution and fostering interactions with water molecules. As a consequence, there was a decrease in water molecules loss (Roco et al., 2018). Additionally, previous study reported a change in myofibrils and actomyosin in chilled fresh meat in order to study the moisture content variation (Xie et al., 2023). The charges might accelerate the dissociation of actomyosin in the post-rigor phase and thus cause less deterioration of myofibrils in LVEF and HVEF treatment groups, which improved the WHC of muscle.

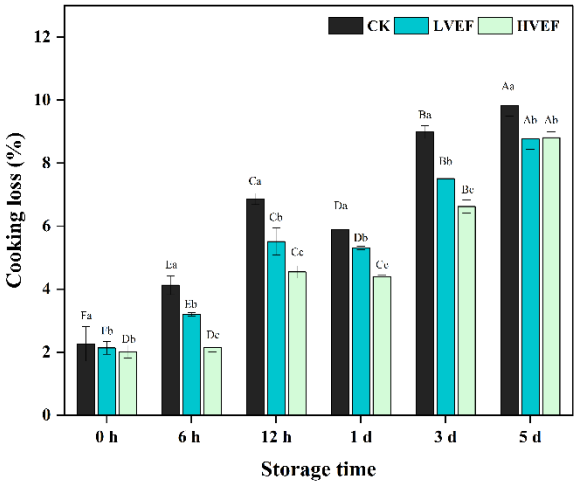

Figure 20. Changes in the cooking loss of fresh pork under different EF intensities assisted CFPS during early postmortem period.

Values represent means ± SE (n=10). A-D: The significance of the cooking loss at different storage times in the same treatment group ($P < 0.05$). a-d: The significance of cooking loss at the same storage time for different treatment groups ($P < 0.05$). Abbreviations: EF: electrostatic field; CFPS: controlled freezing point storage; CK: stored at -1.0 ± 0.5℃ with no EF; LVEF: stored at -1.0 ± 0.5℃ and treated with 4.0 kV high voltage EF; HVEF: stored at -1.0 ± 0.5℃ and treated with 12.0 kV high voltage EF.

The distribution of T_2 transverse relaxation water in different treatment groups was shown in Fig. 21. There exists a class of water populations in chilled fresh meat. T_2 transverse relaxation commonly shows three peaks, representing the bound water (T_{2b}), immobilized water (T_{21}), and free water (T_{22}), respectively (Hu et al., 2021). The third peak gradually increased with the extension of storage, possibly

corresponding to increased free water mobility and moisture content loss. The content of immobilized water in the samples treated with EF was significantly higher than that in the CK group at 6 h, 12 h, and 5 d (Table 3) ($P < 0.05$). In addition, the sample of HVEF has superior characteristics compare to the other groups as confirmed by the observation that lower moisture migration. The charged particles released by the EF manage the redistribution and movement of three populations. The relaxation time of the main peak indicated that the migration degree of the immobilized water in the EF group decreased, which illustrates increasing protein-water interactions under the EF (Lin et al., 2022). A pioneering study by Xie et al. (2023) illustrated that the migration of moisture content was related to the intensity of the EF. They believed that electric charges might induce the water molecular arranged orderly outside, leading to increased WHC during storage. In view of the rich functional charges of the EF, the protein conformation was changed irreversibly in the later stages of storage (Wang et al., 2023). The stability of protein molecules was formed between different types of cross-linking, resulting in a decrease in immobilized water migration (Amiri et al., 2019).

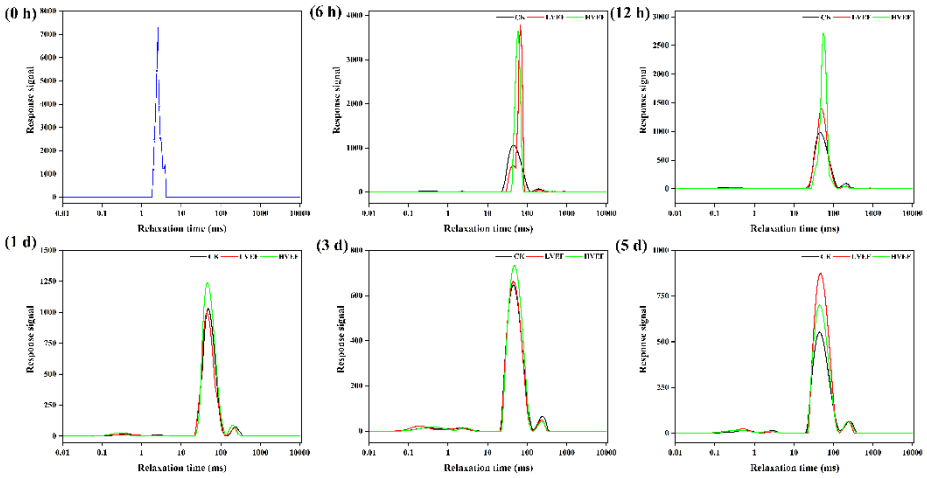

Figure 21. Changes in the T_2 transverse relaxation of fresh pork under different EF intensities assisted CFPS during early postmortem period.

Values represent means ± SE (n=10).

In addition, the changes of H-proton distribution in different treatment groups with storage time were studied. The H-proton imaging spectra provide a visual representation of H-proton distribution within chilled fresh meat. Regions with a reddish area in such images correspond to higher H-proton, indicating greater moisture content in those areas. Conversely, bluish regions represent lower H-proton,

suggesting less moisture content in those specific regions. The red region in the CK group gradually disappeared along with continuous storage time, thereby supporting the result of cooking loss that moisture content of meat samples decreased (Fig. 22). However, the sample images from the HVEF and LVEF groups exhibited a greater prevalence of red and yellow areas when stored at 1~5 d, which agreed with the suggestion from Xie et al. (2021). The samples treated with EF ordinary have better WHC due to the dipoles of water molecules tend to align along the external field (He et al., 2014). An investigation by Johari (1981) reported that the existence of an EF affected the arrangement and vibration of water molecules, just as demonstrated by this study, the greater WHC were observed in LVEF and HVEF groups. We have argued that the physiochemical deteriorations were accompanied by moisture loss during the early postmortem period. The chilled fresh meat images obtained from the CK group displayed a predominance of blue areas, which also proved this. In addition, the reddish area has been observed to be connected mainly in a specific area of the sample, indicates that a higher degree of alignment among the water molecules in response to the applied EF, which was primarily attributed to the electrostatic interaction energies between the water molecules. It has observed that LVEF-12 h, LVEF-3 d, HVEF-12 h, HVEF-1 d, and HVEF-3 d were showing an aggregation phenomenon of water molecules, which was validated the experimental results of cooking loss and T_2 transverse relaxation.

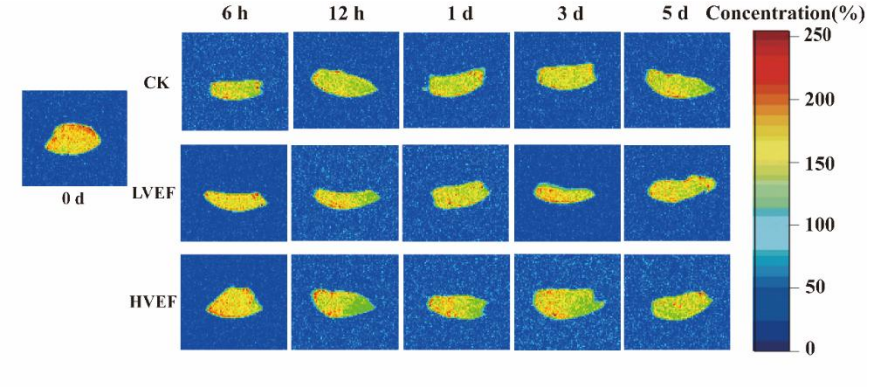

Figure 22. Changes in the distribution of H-proton of fresh pork under different EF intensities assisted CFPS during early postmortem period.

Values represent means ± SE (n=10).

Table 3: Changes in T_2 transverse relaxation peak area percentage P_2 of fresh pork under different EF intensities assisted CFPS during early postmortem period

Index	Treatment	Storage time (d)					
		0 h	6 h	12 h	1 d	3 d	5 d
P_{2b}	CK	——	3.18 ± 0.97^{Da}	3.94 ± 0.94^{Ba}	3.75 ± 0.93^{BCa}	5.22 ± 0.29^{Ac}	5.21 ± 0.36^{Aa}
	LVEF	——	0.52 ± 0.77^{Db}	2.95 ± 0.70^{Cb}	2.67 ± 1.11^{CDc}	6.36 ± 0.34^{Aa}	4.96 ± 0.57^{Bb}
	HVEF	——	——	0.58 ± 0.60^{BCc}	3.28 ± 0.55^{BCb}	5.67 ± 0.49^{BCb}	4.55 ± 0.46^{Ac}
	Mean ± SE	——	1.85±0.53	2.49±0.52	3.23±0.61	5.75±0.21	4.90±0.21
P_{21}	CK	100 ± 0.00^{Aa}	92.62 ± 0.44^{Ac}	91.93 ± 0.59^{Bc}	92.28 ± 1.10^{Ac}	90.33 ± 0.31^{Cb}	89.53 ± 0.43^{Dc}
	LVEF	100 ± 0.00^{Aa}	95.83 ± 1.20^{Ab}	94.74 ± 0.80^{Bb}	94.19 ± 1.31^{Ca}	90.56 ± 0.23^{Db}	90.30 ± 0.24^{Db}
	HVEF	100 ± 0.00^{Aa}	98.93 ± 0.36^{Aa}	97.27 ± 0.13^{Ba}	93.18 ± 0.53^{Cb}	92.08 ± 0.28^{Da}	92.40 ± 0.25^{Da}
	Mean ± SE	100±0.00	95.79±0.80	94.64±0.76	93.21±0.65	90.99±0.24	90.74±0.36
P_{22}	CK	——	4.19 ± 0.82^{BCa}	4.12 ± 0.62^{BCa}	3.97 ± 1.05^{Da}	4.44 ± 0.29^{Ba}	5.24 ± 0.23^{Aa}
	LVEF	——	3.65 ± 0.72^{Bb}	2.31 ± 0.28^{Db}	3.13 ± 0.72^{Cc}	3.07 ± 0.28^{Cb}	4.74 ± 0.36^{Ab}
	HVEF	——	1.28 ± 0.36^{Dc}	2.14 ± 0.73^{Cb}	3.58 ± 0.46^{Aab}	2.24 ± 0.16^{Cc}	3.04 ± 0.32^{Bc}
	Mean ± SE	——	3.04±0.47	2.85±0.40	3.14±0.32	3.25±0.26	4.34±0.32

Values represent means ± SE (n=10). A-D: The significance of the T_2 transverse relaxation peak area percentage P_2 at different storage times in the same treatment group ($P < 0.05$). a-d: The significance of T_2 transverse relaxation peak area percentage P_2 at the same storage time for different treatment groups ($P < 0.05$)

4.2 The change of MFI

The MFI of postmortem muscle increased throughout the storage time, peaking at 1 d in the CK group (Fig. 23A). This could be attributed to the ATP consumption during the postmortem rigor period, leading to the generation of actomyosin. Actomyosin has been defined as the main factor of muscle concentration and thus observed greater moisture loss during the pre-rigor phase (Roco et al., 2018). Consequently, the muscle went through a rigor mortis phase after 6 h. There was a noticeable disruption of bridges within the myofibrils, resulting in muscle expansion (Ertbjerg & Puolanne, 2017). This expansion signified the start of the post-rigor phase, which facilitated the dissociation of actomyosin and thus contributed to the change in WHC (Ertbjerg & Puolanne, 2017). Results showed that the MFI of the HVEF group was significantly lower than that of the CK group ($P < 0.05$). It has been suggested by Xie et al. (2023) that increased EF intensities showed a positive effect on myofibrillar protein, which maintained the muscle structural integrity and finally resulted in a lower rate of moisture loss. The result suggested that storage at electrostatic filed treatment result in comparatively smaller MFI, which enhance the storage quality as confirmed by a well-preserved myofibril structure. This phenomenon has been proposed in earlier studies (Wu et al., 2023). In agreement, Zhang et al. (2022) demonstrated that the higher integrity and stability of myofibrillar protein indicates a predominant myofibril. This may offer an explanation of why the smaller MFI was observed in the HVEF group. Consequently, the lower degree of myofibril contraction and crosslinking contributes to a reduced moisture loss in the muscle.

By conducting an analysis of cooking loss, moisture migration, and MFI, the muscle fibers from each treatment group stored for 0 h to 3 d were carefully chosen for microstructure examination. Both the MFI and SEM were important revealed for the integrity of myofibrils, which manifested the WHC of muscle. SEM was employed at a magnification of 1000 times to observe internal structural changes and fiber integrity to assess the change of muscle fibers at different groups. As shown in Fig. 23B, the muscle fibers exhibited a dense and compact structure with complete cross-sections and small pores at 0 h. In the CK group, the gaps between fresh muscle fibers gradually widened at 6 h, and the internal structure became looser with successive storage time, resulting in the formation of holes and sarcomeres. Commonly, the combination and dissociation of myosin and actin have been considered as the main factor of muscle concentration and loosen, thus observing greater moisture content change during the rigor phase after slaughter (Ertbjerg & Puolanne, 2017). The irreversible myofibril structure deteriorated, and the gap increased at 6 h, directly presenting a WHC decrease. While went through the pre-rigor phase, these holes and sarcomeres brought about the reduction of actomyosin content were responsible for the water molecular return according within 1 d~3 d. However, in the LVEF and HVEF groups, the majority of immobilized water was hold well with the myofibril, which is directly linked to the functional charge released by the EF. Although the samples in the LVEF and HVEF groups could still observe the gradual increase of muscle fiber gap and the loosening of the internal structure after storage for 12 h, the muscle fiber gap was smaller than that of the CK group, which was consistent with the results of WHC and MFI. It has been suggested by Dalvi-Isfahan et al. (2016) that

the bulk water could be remain within myofibrils is induced by the existence of the EF. The rebinding of actin and myosin induced the transverse contraction of the sarcomere, and the muscle fiber structure was gradually reset. The stability of the muscle fiber network structure was improved, which corresponded to the improvement of muscle WHC (Wu et al., 2023).

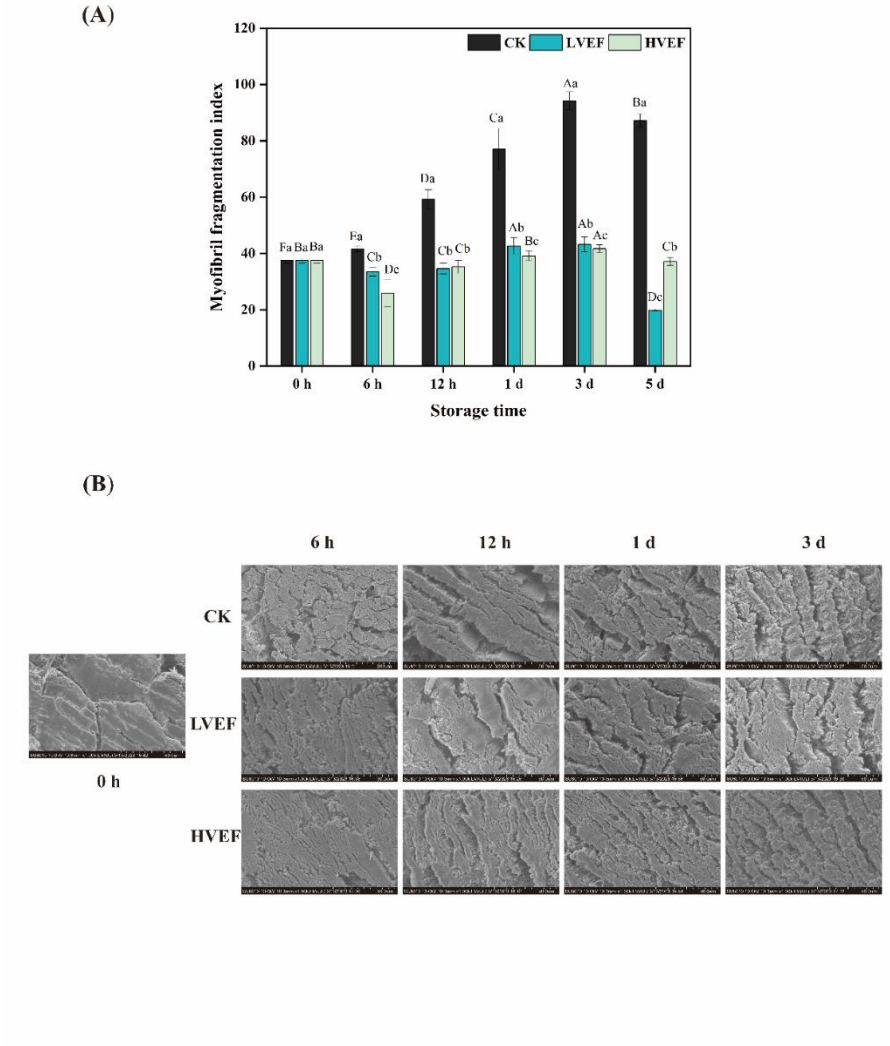

Figure 23. Changes in the microstructure of fresh pork muscle under different EF intensities assisted CFPS during early postmortem period. (A): Myofibril fragmentation index; (B): Scanning electron microscope of myofibrils microstructure.

Values represent means ± SE (n=10). A-D: The significance of the MFI at different storage times in the same treatment group ($P < 0.05$). a-d: The significance of MFI at the same storage time for different treatment groups ($P < 0.05$).

4.3 The change of average particle size of actomyosin

To further investigate the change of myofibrils in early postmortem period, the variation in average particle size of actomyosin among the different treatment groups was conducted in Fig. 24. The size of particle was believed to be a macroscopic indicator of protein structure during the early postmortem period. The size of actomyosin increased initially in the CK group and then decreased with the extension of storage time. The change of particle size during early postmortem period was considered a combination and dissociation of actin and myosin, which was consistent with protein collection. Notably, there existed a positive correlation between particle size and actomyosin formation. Furthermore, the particle size of actomyosin was affected not only by the degree of binding and dissociation of a single protein, but also by the connection between the protein molecules. During the initial postmortem period (6 h), there was a gradual increase in actomyosin size. Significantly, the actomyosin particle size was found to be greater in the LVEF and HVEF treatment groups than in the CK group, suggested that the EF promoting cross-linking between protein-protein and protein-water molecules during the early pre-rigor stage, which was mainly participated in the protein aggregation reaction in the same solution medium. (Wang et al., 2023). Protein fragmentation integrity was one of the representative indicators of WHC in muscle have been confirmed by previous studies (Wang et al., 2023). These cross-linked colloidal particles changed the capacitor rate, while changes in protein electrostatic interactions led to actomyosin molecules aggregation and consequent particle size increased (Xie et al., 2023). Similarly, Zhang et al. (2021) has been reported that structural integration of protein was influenced by electrostatic repulsive forces. The protective capacity of EF was observed on proteins, assemble of actomyosin was found in the result at 6 h may examined the relationship between these two parameters. On the other hand, increased particle size in the pre-rigor phase as evidence by the congregative and stable of muscle myofibrils, which was consistent with myofibrils microstructure results. Furthermore, at 12 h ~ 1 d, the average particle size of actomyosin treated with LVEF and HVEF was significantly lower than that of the CK group ($P < 0.05$), indicating that the EF treatment may prevent the actomyosin from connecting at the later of storage. The average particle size of actomyosin in the HVEF group was smaller than that of the LVEF and HVEF groups at 12 h and 1 d. Electrostatic repulsive force between actomyosin was reduced, leading to the size of actomyosin decreased and as a result, extend myofibrils and increased WHC were observed in LVEF and HVEF (Amiri et al., 2019; Xie et al., 2023). Although actomyosin particle size in the EF treatment group decreased at 3 d and 5 d, it remained higher than that of the CK group. This could be due to the moisture changes in each treatment group were primarily correlated with the stability and integrity of myofibrillar protein after 3 d, and the WHC changes mediated by muscle contraction resulting from actomyosin connection broken down. However, we need more evidence to support these results. Subsequently, we investigated the change of FTIR of actomyosin to estimate the variation of actomyosin.

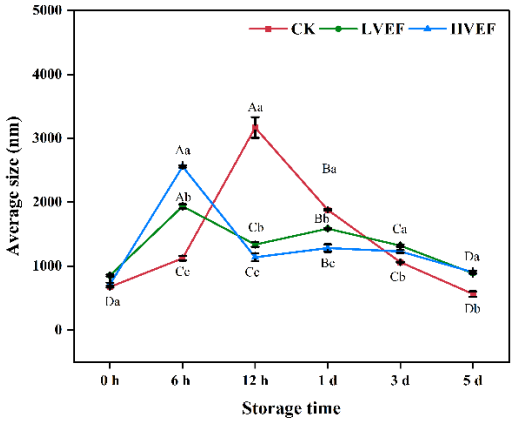

Figure 24. Changes in the average particle size of actomyosin of fresh pork under different EF intensities assisted CFPS during early postmortem period.

Values represent means ± SE (n=10). A-D: The significance of average particle size of actomyosin at different storage times in the same treatment group ($P < 0.05$). a-d: The significance of average particle size of actomyosin at the same storage time for different treatment groups ($P < 0.05$).

4.4 The change of FTIR of actomyosin

Fig. 25 showed the changed of FTIR of actomyosin in different treatment groups. The FTIR of actomyosin was reflected in protein fragment structural variation during the early postmortem period. The stability of protein secondary structures was affected by changes of protein molecules, especially the type of stability bonds. Generally, proteins have several distinct absorption bands in the infrared spectrum. The Amide A band (3400 cm^{-1}), for example, was usually associated with the interaction of protein and water molecules. The Amide I band (1600-1700 cm^{-1}) was usually associated with the changes in protein secondary structure. Furthermore, the Amide II band (1500-1600 cm^{-1}) and the Amide III band (1220-1320 cm^{-1}) were commonly associated with C=N and C-OH. The FTIR changes of the same treatment group were similar in different storage times. The Amide A band of the CK group exhibited a red shift, indicating a weakened hydrogen bond binding ability and substantial moisture loss, while the Amide A band of the LVEF and HVEF groups displayed a notable blue shift, implying an enhanced hydrogen bond binding ability between the protein and water molecules and as a result, the bulk water in muscle was strongly bond to protein leading to a better myofibrils integrity and higher WHC (Ouyang et al., 2022; Wu et al., 2023). It is noteworthy that charge distributions in an EF were typically determined and relatively stable (He et al., 2013). However, in practice, the charge distribution was usually following a self-distributed pattern defined by the material, and was susceptible to alteration due to changes in the surrounding charge (Qi et al., 2022). Proteins are inherently charged entities, and the optimization of surface interactions between charges could affect the stabilization of

proteins (Balcão & Vila, 2015). When subjected to an EF, the charge of protein encountered with alterations, consequently modifying the electrostatic repulsive force between protein and water molecules, making it difficult to migrate from myofibrils and resulting in mitigating moisture loss (Hu et al., 2021). In comparison to the results of LVEF and HVEF groups during the same storage period, the peak intensity of the Amide A band and Amide I band increased at 6 h and 1 d, accompanied by a significant blue shift at 12 h, 1 d, and 3 d. The HVEF group particularly exhibited stronger hydrogen bonding ability, which was closely related to the reduction of moisture loss. These changes in the spectra were attributed to alterations in hydrogen bonding and the influence of charge induced by the EF. The report of Rahbari et al. (2018) also showed that the main reason for the hydrogen bonding changed, possibly due to the high intensity of the EF. Consequently, the protein conformation was affected. The marked modifications were found with the spatial arrangement and molecular interactions (Balcão & Vila, 2015; Mozziconacci & Schöneich, 2015).

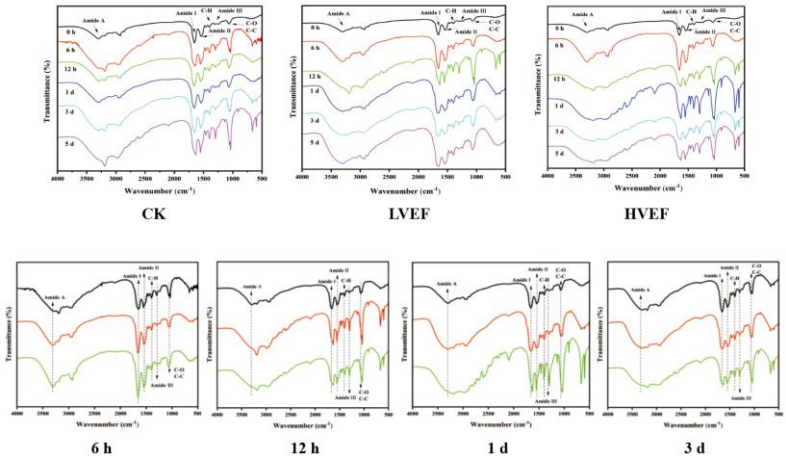

Figure 25. Changes in the FTIR of actomyosin of fresh pork under different EF intensities assisted CFPS during early postmortem period.

Values represent means ± SE (n=10).

4.5 The dissociation of actomyosin

Fig. 26 is the SDS-PAGE analysis of actomyosin in different treatment groups after slaughter. Actomyosin is bonded and dissociated continuously during the rigor phase and decisively alters the storage quality of chilled fresh meat. The condition of actomyosin is thus very interconnected with the WHC of meat (Ertbjerg & Puolanne, 2017). The electrophoretogram of Fig. 26 was a band of free actin. Through quantitative analysis (Fig. 26), it could be seen that the content of free actin in the CK group was lower than that in the LVEF and HVEF groups at 6 h~1 d, indicating that a large amount of actomyosin was combined. Since the muscles gradually enhance all energy, they become inflexible, and inextensibility refers to entering the rigor phase. The primary function of free actin was combined with the myosin to form the

actomyosin during the pre-rigor phase. Accordingly, the actomyosin was dissociated to form free actin, which refer to the onset of the post-rigor phase. Previous study has illustrated that the dissociation of actomyosin is closely related with biochemical events in muscle. The breakdown of ATP was the main feature of the rigor phase, which was also correlated with glycogen depletion (Ertbjerg & Puolanne, 2017). Under the action of the glycolysis process, the degradation of actomyosin was accelerated, which had a significant effect on improving muscle WHC and shortening the post-slaughter period. Additionally, the high density of the EF exposes muscle to relatively high electrical simulation, which accelerates the rigor phase during storage. The content of free actin in the EF was higher than that in CK groups at 6 h, while consistently increasing at 3 d (Fig. 26). This activity of many charges remains significant during the pre-rigor phase, when compared to the CK group, which in turn may accelerate the glycolysis process and thus result in the formation of an immense amount of actomyosin. This might explain why the size of actomyosin in EF groups at 6 h was larger than the CK group. Furthermore, the combination of actomyosin led to relatively integrated myofibrils, resulting in the majority of immobilized water trapped within myofibrils. After that, samples with dissociation of actomyosin in the post-rigor phase were performed better WHC. There was evidence of the less content of free actin showed in LVEF and HVEF treatment groups compared to the CK group, which means the EF still have a protective effect on actomyosin. Combined with the results of MFI and microstructure of myofibrils, the muscle at this time still remains concentration, which refer to the maintains of actomyosin interaction. The relative higher WHC and lower actomyosin content were observed in LVEF and HVEF group, this may relate to the EF involved in other physicochemical changes of muscle during the postmortem period. On one hand, it might be believed as and thereby change the elasticity of muscle undergoing post-rigor phase (Wu et al., 2023). On the other hand, the higher EF intensity HVEF presented a distinct physical stimulus, differing from heat and pressure (Rahbari et al., 2018), and thereby efficiently trigger the formation of dimers, polymers, and even insoluble protein precipitates (Liu et al., 2018; Jia et al., 2019). Consequently, the EF emerges as the predominant force driving protein aggregation and the subsequent formation of protein aggregates (Ha et al., 2021).

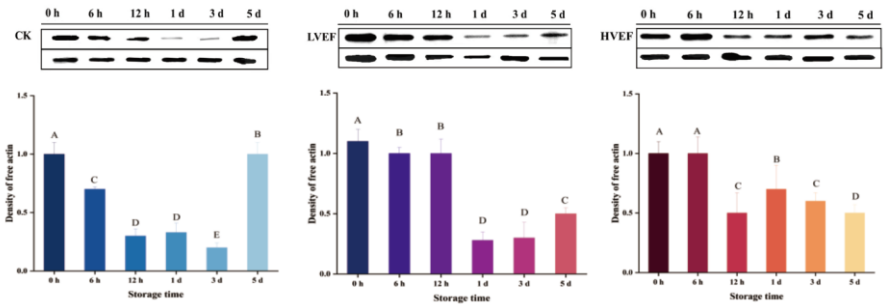

Figure 26. Changes in the density of free actin of fresh pork under different EF intensities assisted CFPS during early postmortem period.

Values represent means ± SE (n=10).

5. Conclusion

The application of EF with two different intensities assisted controlled freezing point, LVEF and HVEF, was found to significantly alter the WHC, myofibrils microstructure, and protein properties and dissociation in the early postmortem period. Both cooking loss and T_2 transverse relaxation results indicated that the immobilized water transfer to the free water was reduced in LVEF and HVEF treatment groups, leading to reduced moisture loss. MFI and SEM results showed that actomyosin could be the main factor affecting the integrity of myofibrils microstructure during early postmortem period and consequently, enhancing the WHC of chilled fresh meat. Results obtained from the analysis of particle size, FTIR and western blot of actomyosin indicated that the formation of actomyosin might play a dominant role in the contraction of myofibrils. Consequently, the HVEF treatment has an impact on the distribution and fluidity of intermuscular water molecules during early postmortem period. Additionally, it is suggested that the EF may facilitate the dissociation of actomyosin in the post-mortem period, thereby contributing to an increase in muscle WHC. Revealing the mechanism of EF preservation will contribute to the future advancement and implementation of a non-thermal processing technology, in the automated large-scale meat processing industry, thereby effectively attaining improved storage efficiency and minimal quality deteriorations.

Acknowledgments

This work was supported by the National Key R&D Program of China (No. 2022YFD2100500). The authors thank Chengjun Min and Yuxia Qi of the Beijing Ershang Meat Food Group Co., Ltd for their contributions to this work. The authors also appreciate the assistance by Mrs. Yanli Sun and Mrs. Ying Wang of the Electron Microscope Center and Mrs. Chunhong Li and Lan Tian of the National Key Laboratory of Argo-products Processing, Institute of Food Science and Technology, Chinese Academy of Agricultural Sciences.

References

Amiri, A., Mousakhani-Ganjeh, A., Shafiekhani, S., Mandal, R., Singh, A. P., & Kenari, R. E. (2019). Effect of high voltage electrostatic field thawing on the functional and physicochemical properties of myofibrillar proteins. Innovative Food Science & Emerging Technologies, 56, 102191. https://doi.org/10.1016/j.ifset.2019.102191

Bai, Y., Li, X., Zhang, D., Chen, L., Hou, C., Zheng, X., & Ren, C. (2020). Effects of phosphorylation on the activity of glycogen phosphorylase in mutton during incubation at 4 °C in vitro. Food Chemistry, 313, 126162. https://doi.org/10.1016/j.foodchem.2020.126162

Balcão, V. M., & Vila, M. M. D. C. (2015). Structural and functional stabilization of protein entities: State-of-the-art. Advanced Drug Delivery Reviews, 93, 25–41. https://doi.org/10.1016/j.addr.2014.10.005

Dalvi-Isfahan, M., Hamdami, N., & Le-Bail, A. (2016). Effect of freezing under electrostatic field on the quality of lamb meat. Innovative Food Science & Emerging Technologies, 37, 68–73. https://doi.org/10.1016/j.ifset.2016.07.028

Ding, Z., Wei, Q., Liu, C., Zhang, H., & Huang, F. (2022). The quality changes and proteomic analysis of cattle muscle postmortem during rigor mortis. Foods, 11(2), Article 2. https://doi.org/10.3390/foods11020217

Ertbjerg, P., & Puolanne, E. (2017). Muscle structure, sarcomere length and influences on meat quality: A review. Meat Science, 132, 139–152. https://doi.org/10.1016/j.meatsci.2017.04.261

Ge, Y., Zhang, D., Zhang, H., Li, X., Fang, F., Liang, C., & Wang, Z. (2021). Effect of postmortem phases on lamb meat quality: A physicochemical, microstructural and water mobility approach. Food Science of Animal Resources, 41(5), 802–815. https://doi.org/10.5851/kosfa.2021.e37

Ha, T. Q., Planje, I. J., White, J. R. G., Aragonès, A. C., & Díez-Pérez, I. (2021). Charge transport at the protein–electrode interface in the emerging field of BioMolecular Electronics. Current Opinion in Electrochemistry, 28, 100734. https://doi.org/10.1016/j.coelec.2021.100734

He, X., Liu, R., Nirasawa, S., Zheng, D., & Liu, H. (2013). Effect of high voltage electrostatic field treatment on thawing characteristics and post-thawing quality of frozen pork tenderloin meat. Journal of Food Engineering, 115(2), 245–250. https://doi.org/10.1016/j.jfoodeng.2012.10.023

He, Y., Sun, G., Koga, K., & Xu, L. (2014). Electrostatic field-exposed water in nanotube at constant axial pressure. Scientific Reports, 4(1), Article 1. https://doi.org/10.1038/srep06596

Hopkins, D. L., Toohey, E. S., Warner, R. D., Kerr, M. J., Ven, R. van de, Hopkins, D. L., Toohey, E. S., Warner, R. D., Kerr, M. J., & Ven, R. van de. (2010). Measuring the shear force of lamb meat cooked from frozen samples: Comparison of two laboratories. Animal Production Science, 50(6), 382–385. https://doi.org/10.1071/AN09162

Hu, F., Qian, S., Huang, F., Han, D., Li, X., & Zhang, C. (2021). Combined impacts of low voltage electrostatic field and high humidity assisted-thawing on quality of pork steaks. LWT, 150, 111987. https://doi.org/10.1016/j.lwt.2021.111987

Jia, G., Sha, K., Feng, X., & Liu, H. (2019). Post-thawing metabolite profile and amino acid oxidation of thawed pork tenderloin by HVEF-A short communication. Food Chemistry, 291, 16–21. https://doi.org/10.1016/j.foodchem.2019.03.154

Johari, G. P. (1981). The dipolar correlation factor, the electrostatic field, the dipole moment, and the Coulombic interaction energy of water molecules in clathrate hydrates. The Journal of Chemical Physics, 74(2), 1326–1336. https://doi.org/10.1063/1.441194

Lee, S., Park, D. H., Kim, E. J., Kim, H., Lee, Y., & Choi, M.-J. (2022). Development of temperature control algorithm for supercooling storage of pork loin and its feasibility for improving freshness and extending shelf life. Food Science of Animal Resources, 42(3), 467.

Lin, H., Zhao, S., Han, X., Guan, W., Liu, B., Chen, A., Sun, Y., & Wang, J. (2022). Effect of static magnetic field extended supercooling preservation on beef quality. Food Chemistry, 370, 131264. https://doi.org/10.1016/j.foodchem.2021.131264

Liu, Y.-F., Oey, I., Bremer, P., Silcock, P., & Carne, A. (2018). Proteolytic pattern, protein breakdown and peptide production of ovomucin-depleted egg white processed with heat or pulsed electric fields at different pH. Food Research International,

108, 465–474. https://doi.org/10.1016/j.foodres.2018.03.075

Ma, Y., Wang, Y., Wang, Z., Chen, B., Xie, Y., Kong, L., Zhou, H., & Xu, B. (2023). Mechanisms of chicken processing quality changes during the early postmortem time: The role of the changes in myofibrillar protein. International Journal of Food Science & Technology, 58(4), 1775–1786. https://doi.org/10.1111/ijfs.16286

Melody, J. L., Lonergan, S. M., Rowe, L. J., Huiatt, T. W., Mayes, M. S., & Huff-Lonergan, E. (2004). Early postmortem biochemical factors influence tenderness and water-holding capacity of three porcine muscles. Journal of Animal Science, 82(4), 1195–1205. https://doi.org/10.2527/2004.8241195x

Mi, H., Qian, C., Zhao, Y., Liu, C., & Mao, L. (2013). Comparison of superchilling and freezing on the microstructure, muscle quality and protein denaturation of grass carp (ctenopharyngodon Idellus). Journal of Food Processing and Preservation, 37(5), 546–554. https://doi.org/10.1111/j.1745-4549.2012.00678.x

Mozziconacci, O., & Schöneich, C. (2015). Chemical degradation of proteins in the solid state with a focus on photochemical reactions. Advanced Drug Delivery Reviews, 93, 2–13. https://doi.org/10.1016/j.addr.2014.11.016

Okitani, A., Ichinose, N., Itoh, J., Tsuji, Y., Oneda, Y., Hatae, K., Migita, K., & Matsuishi, M. (2009). Liberation of actin from actomyosin in meats heated to 65°C. Meat Science, 81(3), 446–450. https://doi.org/10.1016/j.meatsci.2008.09.008

Ouyang, Q., Liu, L., Zareef, M., Wang, L., & Chen, Q. (2022). Application of portable visible and near-infrared spectroscopy for rapid detection of cooking loss rate in pork: Comparing spectra from frozen and thawed pork. LWT, 160, 113304. https://doi.org/10.1016/j.lwt.2022.113304

Park, D. H., Lee, S., Kim, E. J., Jo, Y.-J., & Choi, M.-J. (2022). Development of a stepwise algorithm for supercooling storage of pork belly and chicken breast and its effect on freshness. Foods, 11(3), Article 3. https://doi.org/10.3390/foods11030380

Qi, M., Yan, H., Zhang, Y., & Yuan, Y. (2022). Impact of high voltage prick electrostatic field (HVPEF) processing on the quality of ready-to-eat fresh salmon (Salmo salar) fillets during storage. Food Control, 137, 108918. https://doi.org/10.1016/j.foodcont.2022.108918

Rahbari, M., Hamdami, N., Mirzaei, H., Jafari, S. M., Kashaninejad, M., & Khomeiri, M. (2018). Effects of high voltage electric field thawing on the characteristics of chicken breast protein. Journal of Food Engineering, 216, 98–106. https://doi.org/10.1016/j.jfoodeng.2017.08.006

Roco, T., Torres, M. J., Briones-Labarca, V., Reyes, J. E., Tabilo-Munizaga, G., Stucken, K., Lemus-Mondaca, R., & Pérez-Won, M. (2018). Effect of high hydrostatic pressure treatment on physical parameters, ultrastructure and shelf life of pre- and post-rigor mortis palm ruff (Seriolella violacea) under chilled storage. Food Research International, 108, 192–202. https://doi.org/10.1016/j.foodres.2018.03.009

Sabikun, N., Bakhsh, A., Ismail, I., Hwang, Y.-H., Rahman, M. S., & Joo, S.-T. (2019). Changes in physicochemical characteristics and oxidative stability of pre- and post-rigor frozen chicken muscles during cold storage. Journal of Food Science and Technology, 56(11), 4809–4816. https://doi.org/10.1007/s13197-019-03941-0

Varghese, T., & Mathew, S. (2017). Assessment of the textural variation of iced stored Anabas testudineus (Bloch, 1792) muscle tissue with emphasis on their collagen and myofibrillar protein content. Journal of Food Science and Technology, 54(8), 2512–2518. https://doi.org/10.1007/s13197-017-2695-4

Wang, Y., Yuan, J., Li, K., Chen, X., Wang, Y., & Bai, Y. (2023). Evaluation of chickpea protein isolate as a partial replacement for phosphate in pork meat batters: Techno-functional properties and molecular characteristic modifications. Food Chemistry, 404, 134585. https://doi.org/10.1016/j.foodchem.2022.134585

Wu, G., Yang, C., Bruce, H. L., Roy, B. C., Li, X., & Zhang, C. (2023). Effects of alternating electric field assisted freezing-thawing-aging sequence on longissimus dorsi muscle microstructure and protein characteristics. Food Chemistry, 409, 135266. https://doi.org/10.1016/j.foodchem.2022.135266

Wu, Z.-X., Bai, Y.-H., Wang, Z.-Y., Fan, Y.-C., Song, L., Liu, Y.-X., Li, D.-Y., Jiang, P.-F., & Zhou, D.-Y. (2023). Effect of boiling on texture of scallop adductor muscles and its mechanism based on label-free quantitative proteomic technique. Food Chemistry, 414, 135723. https://doi.org/10.1016/J.FOODCHEM.2023.135723

Xie, Y., Zhou, K., Chen, B., Ma, Y., Tang, C., Li, P., Wang, Z., Xu, F., Li, C., Zhou, H., & Xu, B. (2023). Mechanism of low-voltage electrostatic fields on the water-holding capacity in frozen beef steak: Insights from myofilament lattice arrays. Food Chemistry, 428, 136786. https://doi.org/10.1016/j.foodchem.2023.136786

Xie, Y., Zhou, K., Chen, B., Wang, Y., Nie, W., Wu, S., Wang, W., Li, P., & Xu, B. (2021). Applying low voltage electrostatic field in the freezing process of beef steak reduced the loss of juiciness and textural properties. Innovative Food Science & Emerging Technologies, 68, 102600. https://doi.org/10.1016/j.ifset.2021.102600

Xu, Y., Zhang, D., Xie, F., Li, X., Schroyen, M., Chen, L., & Hou, C. (2023). Changes in water holding capacity of chilled fresh pork in controlled freezing-point storage assisted by different modes of electrostatic field action. Meat Science, 204, 109269. https://doi.org/10.1016/j.meatsci.2023.109269

Zhai, C., Djimsa, B. A., Prenni, J. E., Woerner, D. R., Belk, K. E., & Nair, M. N. (2020). Tandem mass tag labeling to characterize muscle-specific proteome changes in beef during early postmortem period. Journal of Proteomics, 222, 103794. https://doi.org/10.1016/j.jprot.2020.103794

Zhang, H., Cao, Y., Dong, X., Li, X., & Zhang, C. (2023). Effect of different postmortem ageing conditions on physicochemical properties, structure and water-holding capacity of pork. International Journal of Food Science & Technology, 58(3), 1662–1672. https://doi.org/10.1111/ijfs.16182

Zhang, Y., Kim, Y. H. B., Puolanne, E., & Ertbjerg, P. (2022). Role of freezing-induced myofibrillar protein denaturation in the generation of thaw loss: A review. Meat Science, 190, 108841. https://doi.org/10.1016/j.meatsci.2022.108841

Zhang, Y., Magro, A., Puolanne, E., Zotte, A. D., & Ertbjerg, P. (2021). Myofibrillar protein characteristics of fast or slow frozen pork during subsequent storage at −3 °C. Meat Science, 176, 108468. https://doi.org/10.1016/j.meatsci.2021.108468

Chapter 5

Structure and functional properties of myosin induced by EFs at different pH values

This chapter aimed to investigate the effects of EF on the structural and functional properties of myosin under varying pH conditions (9.0, 7.0, 5.0, and 3.0), with the goal of elucidating its potential application in meat preservation. Key parameters, including surface hydrophobicity, sulfhydryl (-SH) content, zeta potential, particle size, secondary structure (FTIR), microstructure (SEM), water-holding capacity (WHC), and texture profile analysis (TPA) of myosin gels, were systematically analyzed. The results indicated that EF treatment significantly reduced surface hydrophobicity and preserved higher -SH content, suggesting an attenuation of oxidative denaturation. EF also inhibited protein aggregation, as evidenced by reduced particle size, and contributed to the stabilization of α-helix structures, particularly under extreme pH conditions. Moreover, EF treatment improved gel WHC by enhancing water–protein interactions and promoted the formation of denser, firmer gel networks with more uniform microstructures. These findings suggest that EF treatment effectively maintains the structural integrity and functional properties of myosin across a range of pH conditions, likely through charge redistribution and strengthened electrostatic interactions. This study provides new insights into the potential of EF technology for improving meat quality during storage.

This chapter is adapted from:

Xu, Y., Leng, D., Schroyen M., Li, X., Wang D., Zhang, D., Hou C. Structure and functional properties of myosin induced by electrostatic fields at different pH values. Innovative Food Science & Emerging Technologies, 102, 104004 (2025).

https://doi.org/10.1016/j.ifset.2025.104004

1. Abstract

In this study, the effects of EF on myosin structure and function at different pH values were investigated. The results demonstrated that a higher surface hydrophobicity and lower sulfhydryl group content of the EF group compared to Control group ($P < 0.05$). The particle size, secondary structure, and microstructure investigations revealed that the EF group had decreased protein aggregation and a more stable protein structure. Furthermore, the application of EF improved the water holding capacity (WHC) of myosin gel by enhancing interaction between water molecules and protein, reducing the loss of free and immobilized water. In addition, the structure of the gel formed by EF was more stable, showing higher gel hardness and dense microstructure. The study further revealed that the internal mechanism of EF to maintain the quality of fresh meat may be related to maintaining the structural and functional activity of myosin.

Keywords

EF, Myosin, pH value, Protein structure, Protein function.

2. Introduction

There is a dynamic variation of pH value in postmortem muscles, which inevitably leads to modifications in the muscle protein (Liu et al., 2018). According to studies, protein in its native state often carries a negative charge and is comparatively stable close to the isoelectric point (pI) (Han et al., 2022; Sun et al., 2024). However, alterations in charged groups and electrostatic interactions between proteins could be impacted by external and internal variation pH value conditions, thus altering protein structure and function. As reported by Yu et al., (2024), pH value alters the distribution of electrostatic charges on the protein surface, which in turn affects the structure of the protein. Other investigations have also confirmed that the change of hydrogen bond stability triggers the weakening of protein interaction, which ultimately leads to the loss of α-helix (Zhang et al.,2024). Therefore, exploring new technologies with high effective value to adjust the distribution of charge on the protein surface, maintaining the structure and function of protein in different pH value conditions, and ultimately promoting its better function is a crucial aspect of improving meat quality.

Previous studies have shown the positive methods that reduce the degradation of proteins at different pH values, such as the addition of non-meat proteins, including proline (Zhou & Yang, 2020), lard-based diacylglycerol, or egg white proteins (Walayat et al., 2020; Zhao et al., 2020). Additionally, the external techniques, including pulsed ultrasonic treatment (Sun et al., 2021) and low and high pressure processing (Chen et al., 2023; Guo et al., 2019) have been successfully applied to mitigated the destruction of protein structure and characteristics. EF has been demonstrated as a promising non-thermal method for maintaining the storage quality of fresh meat (Xie et al., 2023). Different from the technologies mentioned above, the EF does not bring other additional substances to affect the sense of the material, nor does it cause a cavitation effect to damage the material structure. It has the advantages of efficiency of energy transfer and less energy consumption in applications, which was make it attractive to researchers and entrepreneurs in the preservation field (Wang et al., 2018). Studies have shown that the charge released by the EF has a positive effect on the electrostatic interaction between macromolecular substances and the adjustment of the surface net charge distribution (Rodrigues et al., 2019; Xie et al., 2023). Proteins, as macromolecular substances, exhibit substantial surface charge densities that constitute a fundamental mechanism underlying the role of EFs in maintaining their structural and functional integrity (Pereira et al., 2024). This phenomenon has been substantiated by Rodrigues et al., (2020), who proposed that while protein biological functions are closely associated with their structural conformations, external EFs may induce conformational modifications through electrostatic interactions. In general, the EF exerts multifaceted effects on the meat protein system, mainly through the electrostatic shielding effect to maintain the structure, delay oxidation, and mitigate protein denaturation and aggregation. Furthermore, the modification of charge distribution collectively strengthens protein and water interactions through optimized hydrogen bonding networks and electrostatic attraction forces, ultimately enhancing the functional properties of the protein. Xie, et al., (2021) demonstrated that external EFs mitigate protein oxidative

damage through a dual mechanism involving charge release and modulation of interprotein electrostatic forces. Also, Rodrigues et al., (2019) demonstrated that the regulation of protein surface potentials and intermolecular interactions by EFs provides a controllable strategy for charge redistribution and optimization of functional protein properties. Additionally, some researchers suggested that EFs could inhibit protein oxidation and preserve structural integrity by facilitating directional charge arrangement (Qian et al., 2019). Similarly, based on our earlier research, we found that EF influences the process of actomyosin combination and dissociation by released charges, regulates the contraction and relaxation of muscle fibers, and ultimately regulates the degree of muscle tenderization during the postmortem (Xu et al., 2024). Numerous studies have investigated the effects of EFs on water molecule dynamics. EFs optimize ice crystal formation through charge-mediated nucleation control, thereby regulating water migration in meat and enhancing muscle WHC (Lin et al., 2025; Wang et al., 2024; Xie et al., 2021). Research on the effects of EFs on the integrity and function of muscle proteins remains limited, with most studies focusing on whole meat treatment rather than independent investigations of proteins in meat. Considering the strong association between electrostatic interactions and the structural and functional properties of proteins, it is reasonable to hypothesize that EFs exert a positive effect on proteins (Rodrigues et al., 2020). This approach may be regarded as a promising technique for maintaining the structural integrity of protein at different pH value conditions.

Therefore, the following experiments were conducted for this study: myosin was selected as the target protein to establish myosin models at 4 different pH value conditions (9.0, 7.0, 5.0, 3.0), due to it is the main component of the myofibrillar lattice (Xie et al., 2023). The changes of secondary structure, microstructure, oxidation properties, texture properties and thermal processing properties of myosin with and without the application of an EF were comprehensively analyzed. This study attempts to explain how the EF maintains the integrity of myosin at different pH values from the perspective of maintaining the structure and function of protein, thereby enhancing the storage quality of meat. We supposed that this work could contribute to a better comprehension of the potential principle of the function of EFs in the preservation of meat and put forward a fresh insight into the preservation of meat.

3. Materials and methods

3.1 The preparation of Myosin solution

Myosin was obtained by purifying commercial myosin isolates (M1636, SIGMA-ALDRICH, SHANGHAI, CHINA). Purity and conformation meet the requirements. Myosin protein solution (MYPs) of 10% v/v, 10 mg protein/mL was prepared by preparing 50 mmol/L K_3PO_4 buffer (3 mmol/L Na_3PO_4) with pH of 9.0, 7.0, 5.0, and 3.0. The solution was stirred for 2 h to ensure that it was completely dissolved, and then checked the pH value. The pH values of the MYPs measured at 25 ± 0.5°C were 9.0, 7.0, 5.0, and 3.0, respectively. And adjust the pH value with hydrochloric acid or sodium hydroxide if needed.

3.2 The treatment of EF

10 mL volume of MYPs was placed in a 90 mm disposable plate (after ultraviolet disinfection), and the solution was stationary for 10 min to make the surface of the solution stable. Then, MYPs were treated at -1 ± 0.2℃ under 12 kV (120 kV/m) EF for 6 h, the parameters of the procedure were selected from our previous studies (Xu et al., 2024). The distance between the solution surface and the discharge plate of EF was 5 ± 0.2 cm. MYPs treated without EF were used as the Control group, and those treated with EF were used as the EF group. After the treatment, the sample was collected and transferred to a glass tube and equilibrated at 4℃ for 24 h.

3.3 The preparation of the MYPs samples

The MYPs powder was prepared by vacuum freeze-drying (LGJ-10, BEIJING FOUR-RING SCIENCE INSTRUMENT PLANT LTD., BEIJING, CHINA) to evaluate the protein secondary structure (FTIR) and microstructure (SEM). After pre-freezing at -20℃ for 2 h, freeze-drying temperature was -65℃ for 24 h and pressure was 15 MPa. The obtained protein powder sample was immediately transferred to -80℃ for storage and named myosin protein solution powder (MYPp). The remaining MYPs samples were used to determine surface hydrophobicity, sulfhydryl group content (-SH), protein Zeta-potential and particle size distribution, protein degradation degree (SDS-PAGE), and fluorescence spectrum. MYPs gel was prepared by MYPs after heating and its WHC (T_2 relaxation time, H - proton content, and centrifugal loss), texture profile analysis (TPA), and microstructure were determined.

3.4 Surface hydrophobicity

The 1 mL of 2 mg/mL MYPs was homogenized with 40 μL of 1 mg/mL bromophenol blue solution, followed by incubation under 25 ± 0.5℃ for 15 min. The MYPs were centrifuged at 3000 × g for 15 min, 4℃. The supernatant was taken and measured at 595 nm. (M13) Take 1 mL of 20 mmol/L phosphate buffer (0.6 mol/L NaCl, pH 6.5) instead of MYPs as the Control group (M12). Characterize the surface hydrophobicity with the connection volume of bromophenol blue. The results were calculated by Eq. (8):

$$\text{MYPs surface hydrophobicity (μg)} = (M12 - M13)/M12 \times 40 \quad (8)$$

Where, 40 is the volume of bromophenol blue.

3.5 Sulfhydryl group contents

According to the method of Liu et al., (2023), 5 mL of urea-triglycine buffer (pH 8.0) and 0.02 mL of 5,5' - dithiobis-2-nitrobenzoic acid reagent (4 mg/mL) were combined with 0.5 mL of MYPs. The mixes were measured at 412 nm following a 30 min dark incubation period at 25 ± 0.5℃. The results were calculated by Eq. (9):

$$\text{-SH（μmol/g protein）} = 73.53 \times A412 \times D/C \quad (9)$$

Where, A412 is the absorbance at a wavelength of 412 nm; D is the dilution factor (6.04); C is the sample concentration (mg/mL); and -SH is the total quantity of sulfhydryl group (μmol/g).

3.6 Zeta-potential and particle size distribution

The determination procedure referred to Xu et al., (2024), briefly, the 1 mL of 1 mg/mL MYPs suspension was loaded in a machine. Zeta-potential and particle size distribution of MYPS was measured by a Zeta Potential Analyzer (NANO ZS90, MALVERN INSTRUMENTS LTD., UK).

3.7 SDS-PAGE

SDS-PAGE was performed by previously method (Chen et al., 2023): The same volume of loading buffer was mixed with 1 mg/mL MYPs, which were then heated for 5 min in boiling water. Each sample (5 μL) was added to a gel containing 4% concentrate and 12% separation. It was initially operated at 80 V and then run at 120 V. The 0.1% (w/v) Coomassie Blue R250 was used to stain the gel overnight, decolorized with decolorizing solution at 25 ± 0.5℃ until clear bands appeared, and finally observed in Bio-Rad imaging system (BIO-RAD, HERCULES, CALIFORNIA, USA).

3.8 Fluorescence spectrum

The procedure was carried out according to Deng et al., (2025) with minor modification, the 0.2 mg/mL MYPs were collected to measure the fluorescence spectrum (HITACHI F-4600, SHIMADZU, JAPAN). Excitation wavelength: 283 nm. The emission light was obtained at 300 ~ 400 nm. Scan speed: 1 000 nm/min.

3.9 Secondary structure components

Received MYPp 1 mg from 2.1.3. The secondary structure components of MYPp were monitored with an FTIR spectrophotometer (TENSOR 27 FTIR, BURUKER, IMMANUELSHOFEN, BADEN-WURTTEMBERG, GERMANY). FTIR spectra were scanned and recorded at 500 ~ 4000 cm−1. Plot after recording fixed values. The Amide I region could primarily be associated with the overlapping bands, including α-helix (1646 ~ 1664 cm^{-1}), random coil (1637 ~ 1645 cm^{-1}), β-sheet (1664 ~ 1681 cm^{-1}), and β-turn (1615 ~ 1637 and 1682 ~ 1700 cm^{-1}).

3.10 Preparation of MYPs gel

The MYPs gel was prepared according to the study of Xu et al., (2023). The MYPs were collected and put into a closed glass bottle, then it was heated from 25℃ to 80℃ within 55 min, and kept heated at 80℃ for 30 min. After the end of the time, it was cooled in ice water to 25 ± 0.5℃, and stored at 4℃ overnight to determine the following indexes.

3.11 WHC

The T_2 relaxation time and H-proton density of the gel were measured referred to the method of Xu et al., (2023) with minor modifications. The 2.0 ± 0.05 g gel was placed in a tube for determination. The main parameters of T_2 include: Proton resonance frequency 20 MHz, TW (ms) = 4 500, TE (ms) = 0.5, NS = 4, NECH=18000. The main parameters of H-proton density include: repetition time of 2000 MS, performing 4 repetition times, longitudinal relaxation time of 20 MS, and spin echo time of 20 MS.

The centrifugal loss was also according to Xu et al., (2023) with some modification. The 2.00 ± 0.05 g protein gel was centrifuged at 8000 ×g at 4℃ for 10 min, and the residual moisture was removed after centrifugation. The centrifugal loss (%) was expressed as the percentage of the mass of the gel after centrifugation relative to that before centrifugation.

3.12 Texture profile analysis (TPA)

The gel was cut into cylinders with a diameter of 2 cm and a height of 2 cm and placed in a glass tube. The P/0.5 probe (Diameter: 0.5 mm) of the texture analyzer (TA-XT PLUS®, STABLE MICRO SYSTEM, UK) was selected to determine the TPA. The pre-measurement rate of 2 mm/s, the mid-measurement rate of 1 mm/s, and the post-measurement rate of 1 mm/s, the pressing distance was 4 mm of the gel height, initiating force was 5 g.

3.13 SEM

MYPp was obtained from 2.1.3 and fixed on the observation platform with gold. The morphology of the MYPp was evaluated by SEM (SU8010, HITACHI, JAPAN). The images were obtained at the magnification of 1000 ×.

The sample was cut from the central area of the gel and vacuum freeze-dried. The morphology of the MYPs was evaluated by the same SEM machine. All images were obtained at the magnification of 2000 ×.

3.14 Statistical analysis

The overall test was carried out twice, and the indicators in each test were repeated for 3 times, and the data were expressed as mean ± SE. One-way ANOVA was analyzed using SPSS Statistics 26.0 software and Duncan's method to determine the significance between the data ($P < 0.05$). Origin 2021 was used to produce the figures.

4. Results and discussion

4.1 Surface hydrophobicity and sulfhydryl group contents of MYPs

It was observed that the surface hydrophobicity of MYPs was lowest at pH 7.0 and reached a maximum at pH 9.0 (Fig. 27). Zhang et al., (2019) proposed the same conclusion that the surface hydrophobicity of pH value was the lowest near the pI. Changes in pH value altered the molecular flexibility and structure of the protein, resulting in an enhanced exposure of hydrophobic groups on the surface of protein subunits (Yu et al., 2024). The surface hydrophobicity was higher at pH 3.0 and 9.0, and proteins were substantially more hydrophobic in alkaline environments than in acidic ones, which might be attributed to the alkaline impact might led to an expansion of protein molecules, causing the interaction of hydrophobic groups that related to the protein assemble (Liu et al., 2024). Moreover, the surface hydrophobicity of the EF group was lower than that of the Control group at pH 7.0 and 5.0, suggesting that the EFs had a great influence on the solubility, ionization, and charge characteristics of proteins (Liu et al., 2018). The large and tiny molecule fragments, peptides, and amino acids were common forms of proteins under EFs that were not favorable for the exposure and formation of hydrophobic groups, resulting in a decline in the surface

hydrophobicity of the protein and an enhancement in dispersion, which was consistent with the research conclusions of Liu et al., (2018) and Zhou et al., (2015).

As shown in Fig. 27, the contents of sulfhydryl groups in both groups were significantly lower than pH 7.0 under acidic and alkaline conditions ($P < 0.05$). The EF treated protein sulfhydryl group had a larger concentration than the other two groups at pH 9.0 and 5.0 ($P < 0.05$). The myosin molecule consists of about 42 hydrophobic groups, including sulfur amino acids, cysteine, and methionine with high oxidation sensitivity were altered in the process of protein oxidation (Walayat et al., 2024). It was known that these sulfhydryl groups were easily oxidized to generate disulfide bonds, which might promote the cross-linking in protein and allow the new sulfhydryl groups generated without limitation (Chen et al., 2024). Therefore, the degree of protein oxidation was directly correlated with sulfhydryl group content. Yu et al., (2024) suggested that a pH environment near the pI leads to a higher sulfhydryl content and a lower protein oxidation degree. Walayat et al., (2024) also concluded consistent with the results. They suggested that sulfhydryl groups undergo deprotonation at extreme pH values to generate mercaptan compounds, and that the oxidation of sulfhydryl groups was accelerated more quickly in acidic and alkaline conditions. While the higher sulfhydryl group content of MYPs in the EF indicated that the EF effectively prevented myosin from degenerating, reduced the exposure of sulfhydryl groups in myosin, and improved the stability of the protein structure, which was in line with the findings of Yang et al., (2024).

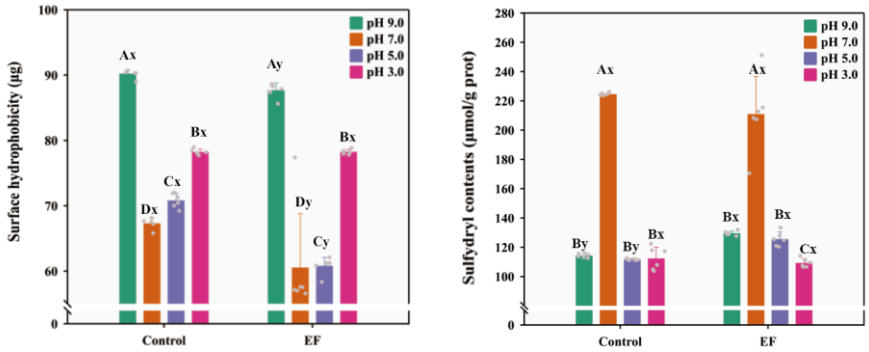

Figure 27. Effect of EF treatment on the surface hydrophobicity and sulfhydryl group content of myosin at different pH values.

Values represent means ± SE (n=6). Abbreviations: EF: electrostatic field; Control: controlled freezing point storage; MYPs: myosin protein solution. A-D: The significance of the surface hydrophobicity and sulfhydryl group content at different pH values in the same treatment group ($P < 0.05$). x-y: The significance of surface hydrophobicity and sulfhydryl group content at the same pH value for different treatment groups ($P < 0.05$).

4.2 Zeta-potential and particle size of MYPs

As shown in Fig. 28, obvious Zeta-potential initially decreased and subsequently increased were observed in the two groups. When the pH value was close to the pI

(pH 5.5), there was basically no electrostatic repulsion between proteins (Yu et al., 2024). Following treatment with the EF on MYPs, the exposed groups on the surface were changed completely, with an obvious unbalance between positive charges and negative charges of the protein (Liu et al., 2024). At pH 9.0, 7.0 and 5.0, the Zeta-potential of the EF group was higher than that of the Control group. Hartvig et al., (2011) suggested that the enhancement of electrostatic interactions induces changes in the double electron layer on the protein surface. This might explain why the application of an EF increases the repulsion between proteins, promoting a more uniform dispersion of myosin in the solution and resulting in a more stable solution system during this phase (Rodrigues et al., 2019). Nevertheless, the presence of a strong acid (pH 3.0) must also be considered, a lower value in the EF group was recorded in Fig. 28, indicating that the positive charges located on the protein surface that determine the pI, such as NH3+, were insensitive to the influence of the EF. Therefore, molecules condensed or aggregated due to hydrophobic contact, and the dispersion in solution was inadequate lead to a relative higher value in EF group.

The particle size of MYPs in the Control group decreased from 1949.67 nm to 603.20 nm within pH 9.0~5.0 and increased to 1696.67 nm in pH 3.0, while in the EF group, the particle size was significantly lower than Control group in each point (Fig. 28). The average particle size of myosin in solution reflects protein aggregation, specifically, the smaller the particle size, the lower the degree of protein aggregation (Chen et al., 2024). According to the acid-base environment of the solution was close to the pI (pH 5.5) of myosin protein (Yu et al., 2024), the electrostatic repulsion between myosin molecules was changed, and contributed to the surface hydrophobicity of MYPs significantly decreased, which was assistant with the result of 3.1. In turn, the EF provided an increase of electrostatic repulsion of charge between the surface of myosin and resulted in the fracture of ionic bonds (Hartvig et al., 2011). In such a case, the single matrix of myosin could be separated from the polymer, ultimately dictating the average particle size of myosin in solution (Müller et al., 2022). Xie et al., (2013) believe that the coupling of the dipole with the external EF is mainly due to the position rearrangement of the local atomic charge of the protein. This further supported the limiting effect of the EF on the conformational change of proteins in solution, consistent with the observation of the Zeta potential.

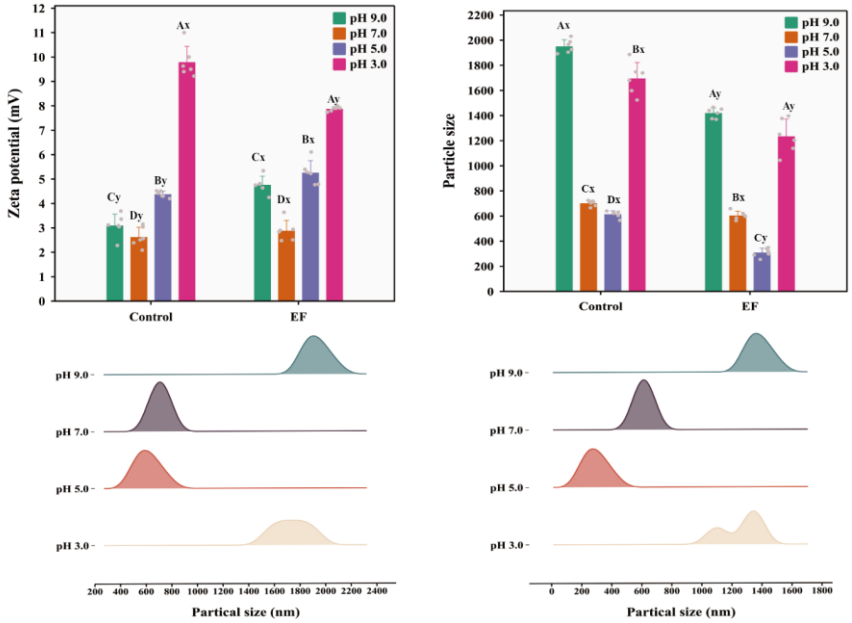

Figure 28. Effect of EF treatment on the Zeta - potential and particle size of myosin at different pH values.

Values represent means ± SE (n=6). A-D: The significance of Zeta – potential and particle size at different pH values in the same treatment group ($P < 0.05$). x-y: The significance of Zeta – potential and particle size at the same pH value for different treatment groups ($P < 0.05$).

4.3 Secondary structure of MYPp

As shown in Fig. 29, in the pH range of 3.0 ~ 9.0, the α-helix continuously decreased and the β-sheet significantly increased ($P < 0.05$). The largest percentage of α-helix (36.27%) and lowest percentage of β-sheet (34.02%) were found in MYPp at pH 7.0. It was worth noting that the lowest value of α-helix (0%) and the highest content of β-sheet (92.02%) were observed at pH 3.0, suggesting that acidic circumstances had a negative effect on the MYPp, which was also in line with the results of Wen et al., (2024). Similarly, the EF group showed a tendency of decreasing content of α-helix with the pH value decreased from 7.0 to 3.0. The MYPp under EF exhibited a higher content of α-helix at pH 9.0, 7.0, and 5.0 than the Control group. The changes in α-helix and β-sheet content were attributed to alterations in the number of intramolecular and intermolecular hydrogen bonds in myosin, induced by electrostatic repulsion (Yu et al., 2024). This phenomenon was exemplified in the study on surface hydrophobicity. Therefore, it could be speculated that the appearance of an EF leads to a change in electrostatic repulsion, reduces the enhancement and aggregation of

protein-protein cross-linking, and strengthens the bond between the protein and the water molecules (Liu et al., 2024).

Furthermore, the vibration peak of MYPp was analyzed using infrared spectroscopy (Fig. 29). The amount of tryptophan residues was exposed outside the protein molecule to produce hydrophobic residues as the external environment shifts to acidic and alkaline circumstances, resulting in the hydrophobicity of the protein increased, which was in line with the surface hydrophobicity results. It was possible that the β-sheet structural unfold caused by the EF allowed the creation of α-helix and promoted hydrogen bonding to possess a decreasing hydrophobicity and a stabilized structure of the protein (Xie et al., 2023).

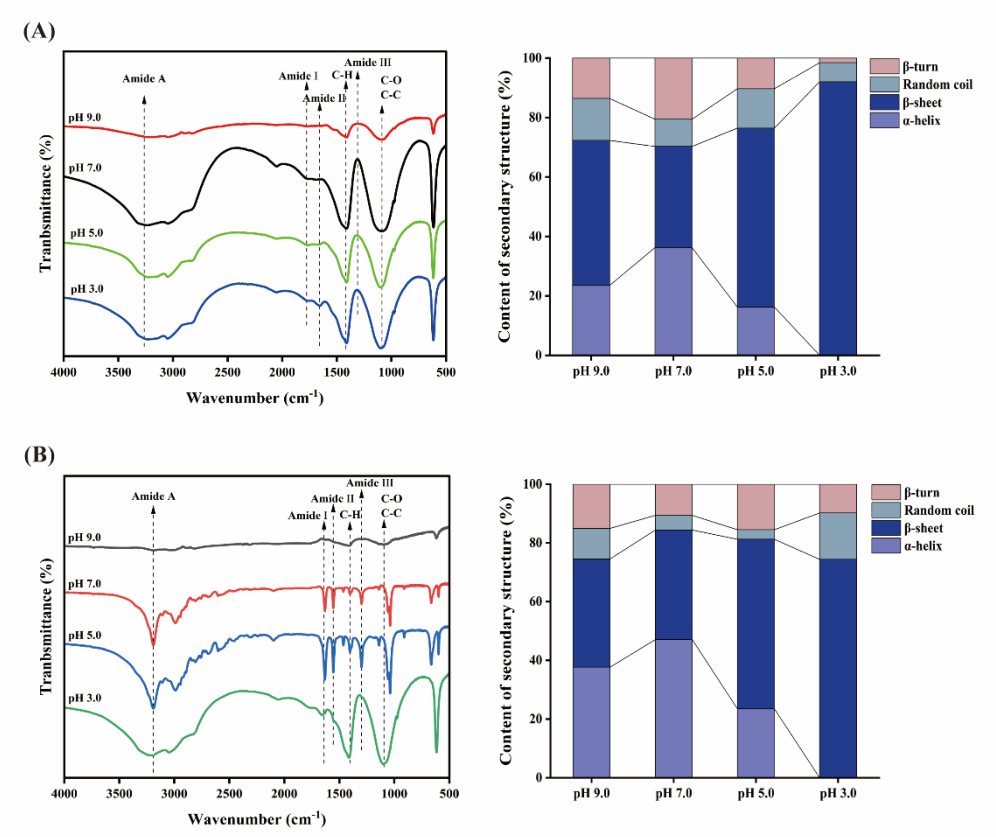

Figure 29. Effect of EF treatment on the secondary structure and infrared spectroscopy of myosin at different pH values.

Values represent means ± SE (n=6). (A): Control group; (B): EF group.

4.4 SDS-PAGE of MYPs and Microstructure of MYPp

As shown in Fig. 30, the darker the band color, the more stable the protein structure. The degradation of myosin heavy chain, tropomyosin, and myosin light chain 1 and 2 increased at pH 9.0 and 5.0. The bands appeared the shallowest at pH 3.0, suggesting that the protein may have been completely degraded. The protein of the EF group still maintained high activity at different pH values, especially at pH 3.0, the protein bands were more complete than the Control group. Research by Wen et al., (2024) suggested that the extreme pH value breaks the secondary bonds of protein such as ionic bonds, hydrogen bonds, and hydrophobic interaction. Therefore, it could be assumed that the function of intermolecular covalent cross-linking bonds in proteins was weakened at this point, and thus the protein degradation made the bands shallow or disappear. The oxidation of specific protein groups, such as sulfhydryl, methylthioyl, and α-carbon radicals, could alter the charge, conformation, and chemical properties of the protein, ultimately affecting its structure and function (Li et al., 2024). The bands of protein in the EF group were deeper at pH 9.0, 5.0, and 3.0, indicating that the degree of protein oxidation was lower than that in the Control group. The formation of disulfide bonds was reduced and the structure of the protein was stable in the highest and lowest pH value environment.

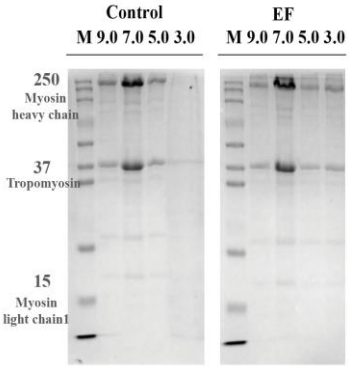

Figure 30. Effect of EF treatment on the SDS-PAGE of myosin at different pH values.

Values represent means ± SE (n=6).

As shown in Fig. 31, myosin was close to each other at pH 9.0 due to the enhanced interaction between molecules, and the protein structure was relatively ordered to form a large and fusiform-like protein structure. At pH 7.0, myosin aggregated but distributed evenly, while at pH 5.0, there are a few little protein clumps, most of the proteins exist in the form of small molecules, and the protein particles were small and scattered. When the pH value decreased to 3.0, small molecules formed new, relatively rough and disordered granular aggregates, accompanied by the presence of slightly thick protein filamentous aggregates. The different pH values affected the interaction of tertiary and quaternary structures between the myosin head, leading to internal disulfide bonds and hydrophobic groups were exposed (Fig. 30). Those large volume proteins were likely to form aggregates with the help of electrostatic repulsion,

Van der Waals force and so on, which could be produced by the intermolecular interactions (Yu et al., 2024). A few proteins soluble aggregates appeared in the EF group, which was consistent with the results of Hartvig et al., (2011) and Xie et al., (2023). The addition of EF changes the ionization and static charge values of protein molecules, which promotes the ordering of myosin molecules and makes the solution system more stable.

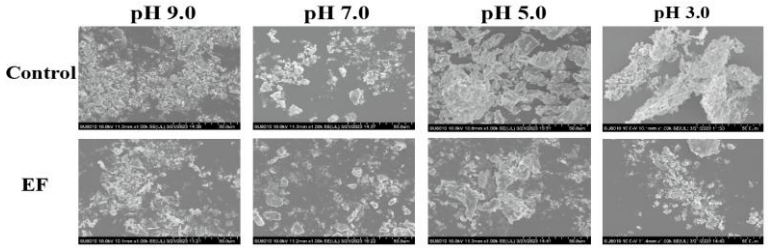

Figure 31. Effect of EF treatment on the microstructure of myosin at different pH values.

Values represent means ± SE (n=6).

4.5 Fluorescence spectra of MYPs

The fluorescence intensity of proteins in both groups peaked at pH 5.0 and decreased at pH 3.0, as indicated by Fig. 32. The tryptophan residues encased in the hydrophobic structure of protein exhibited increased fluorescence intensity upon stimulation when myosin was folded. The results were aligned with the reports of the Yu et al., (2024) investigation, and the authors presumed a connection between the alteration in protein structure and the decrease in fluorescence intensity. Reduced fluorescence intensity occurred when tryptophan was exposed to the surface of protein molecules due to partial or complete unfolding of myosin at pH 9.0 and 3.0. In addition, the fluorescence intensity of the EF group was higher than that of the Control group at each pH value. This could be attributed to the EF shielding the tryptophan residues on the surface of the protein. This further indicated that EF treatment had a certain delay effect on myosin oxidation, which was also confirmed by the study of Jia et al., (2018), illustrating that the endogenous fluorescence intensity of proteins under EF was higher.

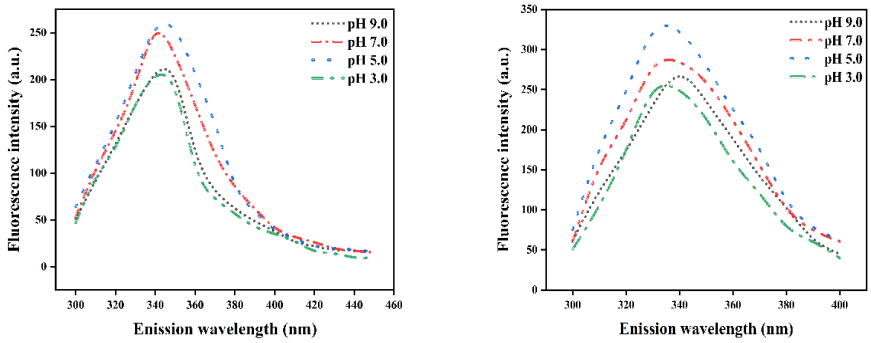

Figure 32. Effect of EF treatment on the fluorescence intensity of myosin at different pH values.

Values represent means ± SE (n=6). Control group at left, EF group at right.

4.6 The WHC of MYPs gel

The peak area ratio (T_{21}) of immobilized water was the highest at pH 5.0, and the lowest at pH 9.0 and 3.0 (Fig. 33). This reflected that the immobilized water content decreased mainly because it was difficult for water and macromolecules to combine when MYPs were far from the pI (pH 5.5), resulting in poor WHC of the gel. It has been proposed that the extreme pH value was not conducive to the formation of gels (Sun et al., 2021). When observing the surface of the gel, it was noticed that the texture of the gel was rough and dry at pH 9.0. Furthermore, a significant amount of water escaped from the gel at pH 3.0, confirming that the free water content at pH 3.0 was insignificantly higher than at pH 9.0. Conversely, the gel structure was dense and uniform at pH 5.0, which was favorable for the maintenance of water molecules. In addition, the content of immobilized was significantly lower than the EF group for gels in the Control group, which could be ascribed to the effect of the EF on the net charge on the protein surface, leading to the stable water molecules trapped in large cavities in the myosin gel network (Guo et al., 2019). The increase of net charge enhances the hydration and electrostatic interaction between protein and water molecules in MYPs gel and results in a stable network formation (Sun et al., 2021).

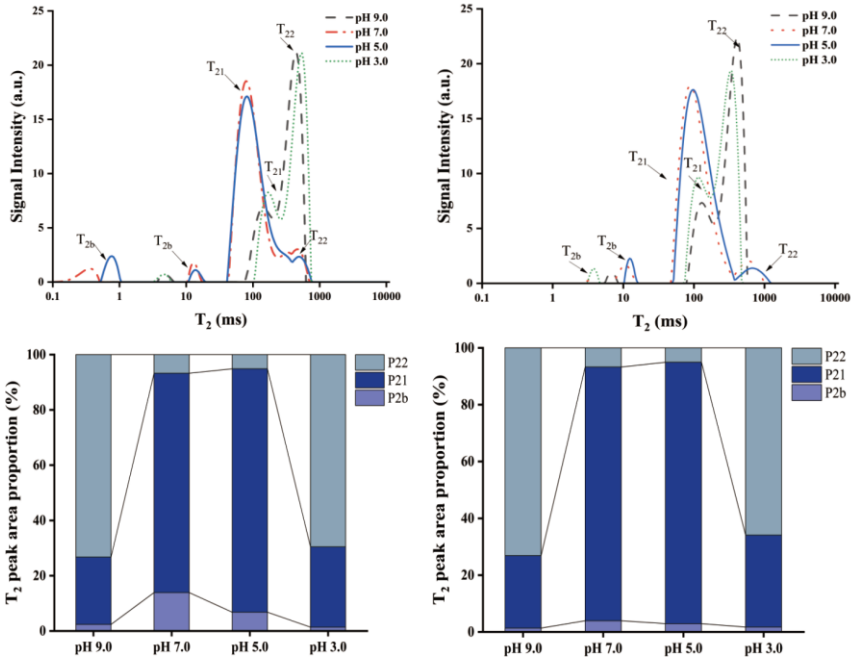

Figure 33. Effect of EF treatment on WHC of myosin gel at different pH values.

Values represent means ± SE (n=6).

The gel image turned purple during the imaging scan at pH 9.0, suggesting that the water molecules of the Control group were poorly maintained (Fig. 34). It was suggested that when the protein was close to the pI and the bond between the water molecules and protein was reasonably stable, thus H-proton were better occupied in the image at pH 7.0 and 5.0 (Zhang et al., 2019). In addition, the image exhibited a significant quantity of blue region at pH 3.0, which indicated a significant amount of water was lost since acidic conditions cause changes in the charged groups on the surface of the protein (Liu et al., 2008). As the EF progressed, the H-proton in gel exhibited an aggregation trend, with intensity continuously increasing and the color changing from yellow to red at pH 7.0~5.0. Additionally, the gel of the EF group was more complete at pH 9.0 and the gel surface of the EF group was less hydrated at pH 3.0.

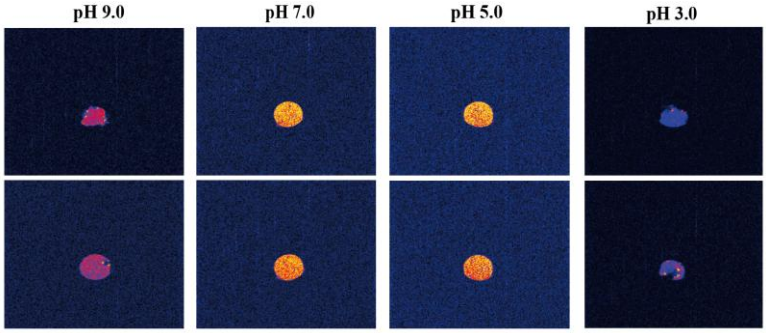

Figure 34. Effect of EF treatment on H-proton of myosin gel at different pH values.

As illustrated in Fig. 35, the centrifugal loss of both the Control group and EF group exhibited a decreased trend followed by an increase within the range of pH 9.0~3.0 ($P < 0.05$). The significant changes did not occur until pH 3.0, indicating that the protein has deviated from the pI could achieve a decrease in the static charged group on the protein, which led to the loss of immobilized water and free water (Zhao et al., 2020). EF gels exhibited a lower centrifugal loss at pH 3.0, indicating that a positive effect might occur on the binding of protein molecules induced by the EF, thus leading to a well-formed gel (Yu et al., 2024). Zhang et al.,(2024) believed that the increased hydrogen bonding and net charge could be the main trigger of the enhanced WHC of protein gels. As the net charge increased under the EF treatment, the protein aggregation decreased, allowing the myosin protein to form a structure that maintained the immobilized water and free water inside the gels.

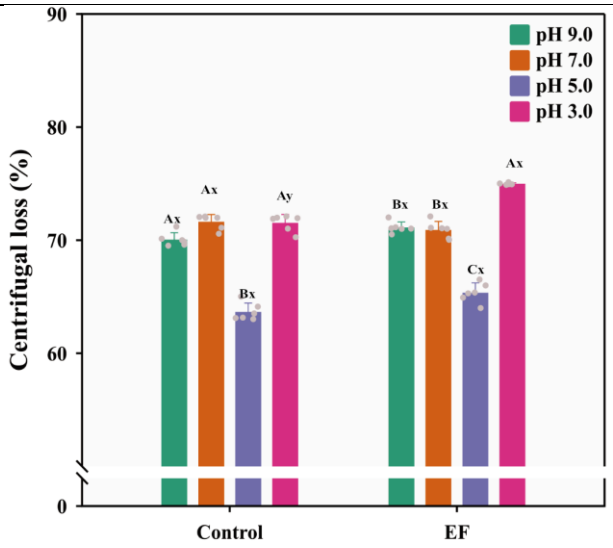

Figure 35. Effect of EF treatment on centrifugal loss of myosin gel at different pH values.

A-D: The significance of the centrifugal loss at different pH values in the same treatment group ($P < 0.05$). x-y: The significance of centrifugal loss at the same pH value for different treatment groups ($P < 0.05$).

4.7 The TPA of MYPs gel

Unlike subjective sensory panels, TPA provides objective, numerical data that minimizes human variability, ensuring accuracy and reproducibility. By applying a two-bite compression cycle, it effectively simulates the primary mechanical actions in the mouth. This approach is exceptionally well-suited for analyzing heat-induced protein gels. The process of thermal denaturation and subsequent aggregation leads to the formation of a three-dimensional network. The measured TPA parameters are direct manifestations of this network's microstructure. For instance, a harder gel typically indicates a denser protein network with stronger cross-links. The altering pH value influences the protein structure, thereby modifying the gel texture characteristics. As shown in Table 4, the gumminess, chewiness, and whiteness were changed insignificantly at pH 9.0~5.0 ($P > 0.05$). At pH 3.0, the protein was under acidic conditions and far away from the pI, the net positive charge of the protein increased significantly. The charge was exposed to the weak electrostatic repulsion, leading to the aggregation and denaturation of protein. It was negative for the protein to form a stable and ordered network, contributing to the variation of gumminess, chewiness, and whiteness.

Hardness, defined as the peak force during the first compression cycle, reflects the strength of the gel matrix and the force required to cause it to yield. In the context of a heat-induced protein gel, this is directly related to the density and strength of the cross-links formed between denatured protein molecules. After the protein was made

into a gel, the variation trend of gel hardness at each pH value was decrease of pH value (9.0 ~3.0), the gel hardness of the gel increased first and then decreased (Fig. 36). The gel had a highly rough exterior at pH 9.0 and was extensively fractured following determination, while the look of gel was comparatively smooth at pH 5.0. The increase of gel hardness may be due to the stable maintenance of immobilized water in the network of gel caused by the decreased degree of protein degradation. The result was in agreement with Liu et al., (2010) who suggested the effect on the gel properties of protein, with the decrease of pH value, the gelation rate and gel hardness of protein increased in the range of pH 9.0~5.5. The gel hardness dropped once more when the pH value dropped to 3.0, and a significant amount of water appeared on the gel surface, likely because of a significant loss of free water. The variation trend of the EF group was similar to the Control group, while the gel hardness was significantly higher than that of the Control group, meanwhile, relatively a smoother appearance of the gel surface was observed. The numerical changes manifested by the quantified gel indicate the existence of a flexible and reversible protein network. The higher hardness of the EF group indicates that it has an elastic structure and can effectively retain water. The appearance of an EF moderately enhanced the number and intensity of charge on protein, thereby increasing the binding of protein to protein and protein to water molecule (Wen et al., 2024). It was conducive to forming a dense and uniform gel structure, resulting in improved gel hardness.

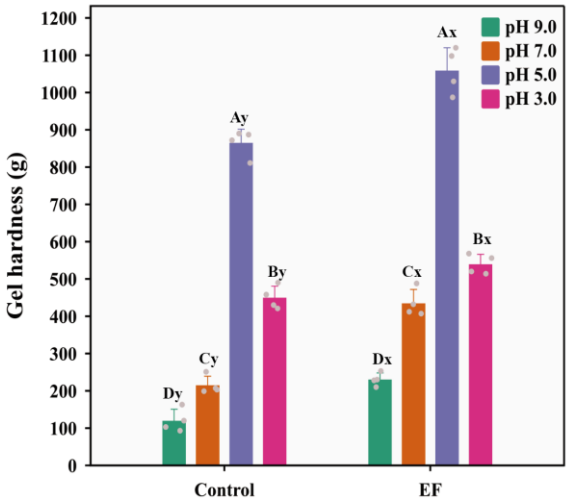

Figure 36. Effect of EF treatment on gel hardness of myosin gel at different pH values.

A-D: The significance of the gel hardness at different pH values in the same treatment group ($P < 0.05$). x-y: The significance of gel hardness at the same pH value for different treatment groups ($P < 0.05$).

Table 4: Effect of EF on texture properties of myosin gels at different pH values

pH	Treatment	Springiness	Gumminess	Chewiness	Whiteness
9.0	Control	0.413±0.003 ^{Bx}	0.436±0.001 ^{Bx}	18.26±0.08 ^{Cx}	62.78±0.11 ^{Dx}
	EF	0.437±0.005 ^{Bx}	0.439±0.018 ^{Bx}	19.00±0.03 ^{Cx}	60.77±0.14 ^{Cx}
7.0	Control	0.667±0.007 ^{Ax}	0.519±0.008 ^{Ax}	59.04±0.09 ^{Ax}	71.81±0.17 ^{Bx}
	EF	0.687±0.007 ^{Ax}	0.521±0.002 ^{Ax}	57.99±0.04 ^{Ax}	70.57±0.16 ^{Bx}
5.0	Control	0.328±0.011 ^{Cx}	0.291±0.002 ^{Cx}	41.72±0.09 ^{Bx}	90.51±0.16 ^{Ax}
	EF	0.360±0.004 ^{Cx}	0.288±0.002 ^{Cx}	41.49±0.13 ^{Bx}	88.91±0.10 ^{Ax}
3.0	Control	0.255±0.001 ^{Dx}	0.172±0.001 ^{Dy}	16.45±0.16 ^{Dx}	67.92±0.09 ^{Cx}
	EF	0.245±0.003 ^{Dx}	0.239±0.001 ^{Cx}	12.62±0.13 ^{Dy}	52.63±0.11 ^{Dy}

Values represent means ± SE (n=6). A-D: The significance of the springiness, gumminess, chewiness, and whiteness at different pH values in the same treatment group ($P < 0.05$). x-y: The significance of springiness, gumminess, chewiness, and whiteness at the same pH value for different treatment groups ($P < 0.05$).

4.8 The microstructure of MYPs gel

The SEM in the gel structure was shown in Fig. 37. The cross-linking between protein gel networks was weak at pH 9.0, and the many aggregates of varying sizes were interlaced with each other. At pH 7.0~5.0, which is near the pI of protein, the gel formed a relatively ordered, high density and small and uniform pore size gel network structure. At pH 3.0, the gel micelles appear rough and irregularly shaped, while the gel pore size was large and uneven. Slightly thick protein filamentous aggregates around the pores could be observed within the microstructure, and it is worth noting that there were several rod-shaped or spherical protein particles at the M position. The dense protein structure could be observed in neutral conditions, while the presence of extreme pH value might be more effective than neutral in influencing

the electrostatic interaction between myosin molecules, which is also proved by Yu et al., (2024). Noticeably, the gels in EF group had a relatively flat structure at pH 9.0~5.0, which could account for the higher WHC in in the structure. Even though some visible uneven pores appeared on the surface at pH 3.0, possibly due to the minimal net surface charge on the proteins caused by an EF, thus reducing the aggregation of filamentous polymer (Zhang et al., 2024). This caused the myosin molecules to occupy more space within the gel to form an ordered three-dimensional network structure, further supporting the theory that the EF protects the molecular structure of the protein.

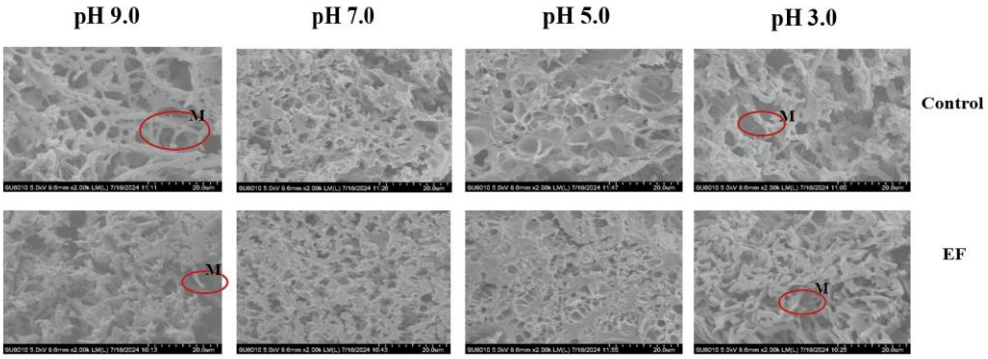

Figure 37. Effect of EF treatment on microstructure of myosin gel at different pH values.

Values represent means ± SE (n=6).

5. Conclusion

The EF had a major impact on the structure and function of myosin at various pH values. The results of surface hydrophobicity and sulfhydryl group content demonstrated that the process of oxidative denaturation of myosin could be delayed by the EF at pH 9.0 and 3.0. As indicated by the results of particle size and Zeta-potential, secondary structure, microstructure changes, and protein degradation, the EF could enhance the electrostatic interaction between proteins by releasing electric charges, thereby improving the structural and functional characteristics of proteins damaged by the highest and lowest pH value. The findings of T_2 relaxation and centrifugal loss of myosin gel demonstrated that the EF decreased the amount of immobilized water that was transferred to free water, leading to a reduced moisture loss, which proved that the EF enhanced the connection between the protein and the water molecule. As evidenced by the hardness analysis and SEM results of the myosin gel, a stronger and dense structure formed by the myosin gel could be encouraged by the EF, which would help to better maintain the water molecule in the gel. Therefore, it could be concluded that the EF protects the structure and function of myosin at different pH values. This may be beneficial to the future explanation of the mechanism of enhancing muscle quality in the EF.

Acknowledgments

This work was supported by the Key R&D Program of Shandong Province, China (2023CXGC010708). The authors appreciate the assistance by Mrs. Yanli Sun and Mrs. Ying Wang of the Electron Microscope Center and Mrs. Chunhong Li and Lan Tian of the National Key Laboratory of Argo-products Processing, Institute of Food Science and Technology, Chinese Academy of Agricultural Sciences.

References

Chen, C., Liu, Z., Xiong, W., Yao, Y., Li, J., & Wang, L. (2024). Effect of alkaline treatment duration on rapeseed protein during pH-shift process: Unveiling physicochemical properties and enhanced emulsifying performance. Food Chemistry, 459, 140280. https://doi.org/10.1016/j.foodchem.2024.140280

Chen, H., Zou, Y., Zhou, A., Liu, X., & Benjakul, S. (2023). Elucidating the molecular mechanism of water migration in myosin gels of Nemipterus virgatus during low pressure coupled with heat treatment. International Journal of Biological Macromolecules, 253, 126815. https://doi.org/10.1016/j.ijbiomac.2023.126815

Deng, Y., Wang, R., Xu, M., Li, X., Zhang, Y., Gooneratne, R., & Li, J. (2025). Elucidating the binding mechanism of silver carp myosin to T-2 toxin using multi-spectroscopic analysis, molecular docking and molecular dynamics simulation. LWT, 117532. https://doi.org/10.1016/j.lwt.2025.117532

Guo, Z., Li, Z., Wang, J., & Zheng, B. (2019). Gelation properties and thermal gelling mechanism of golden threadfin bream myosin containing CaCl2 induced by high pressure processing. Food Hydrocolloids, 95, 43–52. https://doi.org/10.1016/j.foodhyd.2019.04.017

Han, G., Li, Y., Liu, Q., Chen, Q., Liu, H., & Kong, B. (2022). Improved water solubility of myofibrillar proteins by ultrasound combined with glycation: A study of myosin molecular behavior. Ultrasonics Sonochemistry, 89, 106140. https://doi.org/10.1016/j.ultsonch.2022.106140

Hartvig, R. A., van de Weert, M., Østergaard, J., Jorgensen, L., & Jensen, H. (2011). Protein adsorption at charged surfaces: The role of electrostatic interactions and interfacial charge regulation. Langmuir, 27(6), 2634–2643. https://doi.org/10.1021/la104720n

Jia, G., Nirasawa, S., Ji, X., Luo, Y., & Liu, H. (2018). Physicochemical changes in myofibrillar proteins extracted from pork tenderloin thawed by a high-voltage electrostatic field. Food Chemistry, 240, 910–916. https://doi.org/10.1016/j.foodchem.2017.07.138

Li, S., Zhang, K., Wu, Y., Chen, Q., Li, M., Kong, B., & Zhang, C. (2024). Role of ultrasonic freezing-treated pork dumpling filling during frozen storage: Insights from protein oxidation, aggregation, and functional properties. International Journal of Refrigeration, 165, 223–232. https://doi.org/10.1016/j.ijrefrig.2024.05.035

Lin, H., Wang, J., Chisoro, P., Wu, G., Zhao, S., Hu, X., Yang, C., Liu, Y., Jia, W., Li, Q., Zhang, C., Blecker, C., & Li, X. (2025). Changes in freezing parameters and temperature distribution of beef induced by AC electric field: Alleviation on freezing damage and myowater loss. Journal of Food Engineering, 387, 112343.

https://doi.org/10.1016/j.jfoodeng.2024.112343

Liu, M., Wei, Y., Li, X., Quek, S. Y., Zhao, J., Zhong, H., Zhang, D., & Liu, Y. (2018). Quantitative phosphoproteomic analysis of caprine muscle with high and low meat quality. Meat Science, 141, 103–111. https://doi.org/10.1016/j.meatsci.2018.01.001

Liu, P., Hou, M., Yue, Y., Tong, Y., Zhang, T., Lu, Z., & Yang, L. (2023). Effects of ultrahigh magnetic field on the structure and properties of whey protein. LWT, 177, 114590. https://doi.org/10.1016/j.lwt.2023.114590

Liu, Q., Yang, Q., Wang, Y., Jiang, Y., & Chen, H. (2024). Pretreatment with low-frequency magnetic fields can improve the functional properties of pea globulin amyloid-like fibrils. Food Chemistry, 439, 138135. https://doi.org/10.1016/j.foodchem.2023.138135

Liu, R., Zhao, S., Liu, Y., Yang, H., Xiong, S., Xie, B., & Qin, L. (2010). Effect of pH on the gel properties and secondary structure of fish myosin. Food Chemistry, 121(1), 196–202. https://doi.org/10.1016/j.foodchem.2009.12.030

Liu, R., Zhao, S., Xiong, S., Xie, B., & Qin, L. (2008). Role of secondary structures in the gelation of porcine myosin at different pH values. Meat Science, 80(3), 632–639. https://doi.org/10.1016/j.meatsci.2008.02.014

Liu, Y.-F., Oey, I., Bremer, P., Silcock, P., & Carne, A. (2018). Proteolytic pattern, protein breakdown and peptide production of ovomucin-depleted egg white processed with heat or pulsed electric fields at different pH. Food Research International, 108, 465–474. https://doi.org/10.1016/j.foodres.2018.03.075

Müller, W. A., Sarkis, J. R., Marczak, L. D. F., & Muniz, A. R. (2022). Molecular dynamics study of the effects of static and oscillating electric fields in ovalbumin. Innovative Food Science & Emerging Technologies, 75, 102911. https://doi.org/10.1016/j.ifset.2021.102911

Pereira, R. N., Rodrigues, R., Avelar, Z., Leite, A. C., Leal, R., Pereira, R. S., & Vicente, A. (2024). Electrical fields in the processing of protein-based foods. Foods, 13(4), Article 4. https://doi.org/10.3390/foods13040577

Qian, S., Li, X., Wang, H., Mehmood, W., Zhong, M., Zhang, C., & Blecker, C. (2019). Effects of low voltage electrostatic field thawing on the changes in physicochemical properties of myofibrillar proteins of bovine Longissimus dorsi muscle. Journal of Food Engineering, 261, 140–149. https://doi.org/10.1016/j.jfoodeng.2019.06.013

Rodrigues, R. M., Avelar, Z., Machado, L., Pereira, R. N., & Vicente, A. A. (2020). Electric field effects on proteins – Novel perspectives on food and potential health implications. Food Research International, 137, 109709. https://doi.org/10.1016/j.foodres.2020.109709

Rodrigues, R. M., Vicente, A. A., Petersen, S. B., & Pereira, R. N. (2019). Electric field effects on β-lactoglobulin thermal unfolding as a function of pH – Impact on protein functionality. Innovative Food Science & Emerging Technologies, 52, 1–7. https://doi.org/10.1016/j.ifset.2018.11.010

Sun, H., Zhang, Y., & Sun, J. (2024). Dietary inulin supplementation improves the physicochemical and gel properties of duck myofibrillar protein: Insights into the effect of muscle fiber types. Food Hydrocolloids, 150, 109722. https://doi.org/10.1016/j.foodhyd.2023.109722

Sun, Y., Ma, L., Fu, Y., Dai, H., & Zhang, Y. (2021). The improvement of gel and physicochemical properties of porcine myosin under low salt concentrations by pulsed ultrasound treatment and its mechanism. Food Research International, 141, 110056. https://doi.org/10.1016/j.foodres.2020.110056

Walayat, N., Wei, R., Su, Z., Lorenzo, J. M., & Nawaz, A. (2024). Effect of tea polysaccharides on fluctuated frozen storage impaired total sulfhydryl level and structural attributes of silver carp surimi proteins. Food Hydrocolloids, 157, 110448. https://doi.org/10.1016/j.foodhyd.2024.110448

Walayat, N., Xiong, Z., Xiong, H., Moreno, H. M., Niaz, N., Ahmad, M. N., Hassan, A., Nawaz, A., Ahmad, I., & Wang, P.-K. (2020). Cryoprotective effect of egg white proteins and xylooligosaccharides mixture on oxidative and structural changes in myofibrillar proteins of Culter alburnus during frozen storage. International Journal of Biological Macromolecules, 158, 865–874. https://doi.org/10.1016/j.ijbiomac.2020.04.093

Wang, Q., Li, Y., Sun, D.-W., & Zhu, Z. (2018). Enhancing food processing by pulsed and high voltage electric fields: Principles and applications. Critical Reviews in Food Science and Nutrition, 58(13), 2285–2298. https://doi.org/10.1080/10408398.2018.1434609

Wang, W., Lin, H., Guan, W., Song, Y., He, X., & Zhang, D. (2024). Effect of static magnetic field-assisted thawing on the quality, water status, and myofibrillar protein characteristics of frozen beef steaks. Food Chemistry, 436, 137709. https://doi.org/10.1016/j.foodchem.2023.137709

Wen, H., Zhang, D., Ning, Z., Li, Z., Zhang, Y., Liu, J., Yu, T., & Zhang, T. (2024). Effect of benzoic acid-based and cinnamic acid-based polyphenols on foaming properties of ovalbumin at acidic, neutral and alkaline pH conditions. Food Hydrocolloids, 153, 109998. https://doi.org/10.1016/j.foodhyd.2024.109998

Wen, X., Mu, Z., Gantumur, M.-A., Bilawal, A., Jiang, Z., & Zhang, L. (2024). Characterization of whey protein isolate aggregation induced by different acidic substances: Triggered by disulfide bond formation and recombination. Food Hydrocolloids, 157, 110414. https://doi.org/10.1016/j.foodhyd.2024.110414

Xie, Y., Chen, B., Guo, J., Nie, W., Zhou, H., Li, P., Zhou, K., & Xu, B. (2021). Effects of low voltage electrostatic field on the microstructural damage and protein structural changes in prepared beef steak during the freezing process. Meat Science, 179, 108527. https://doi.org/10.1016/j.meatsci.2021.108527

Xie, Y., Liao, C., & Zhou, J. (2013). Effects of external electric fields on lysozyme adsorption by molecular dynamics simulations. Biophysical Chemistry, 179, 26–34. https://doi.org/10.1016/j.bpc.2013.05.002

Xie, Y., Zhou, K., Chen, B., Ma, Y., Tang, C., Li, P., Wang, Z., Xu, F., Li, C., Zhou, H., & Xu, B. (2023). Mechanism of low-voltage electrostatic fields on the water-holding capacity in frozen beef steak: Insights from myofilament lattice arrays. Food Chemistry, 428, 136786. https://doi.org/10.1016/j.foodchem.2023.136786

Xie, Y., Zhou, K., Chen, B., Wang, Y., Nie, W., Wu, S., Wang, W., Li, P., & Xu, B. (2021). Applying low voltage electrostatic field in the freezing process of beef steak reduced the loss of juiciness and textural properties. Innovative Food Science & Emerging Technologies, 68, 102600. https://doi.org/10.1016/j.ifset.2021.102600

Xu, Y., Leng, D., Li, X., Wang, D., Chai, X., Schroyen, M., Zhang, D., & Hou, C. (2024).

Effects of different electrostatic field intensities assisted controlled freezing point storage on water holding capacity of fresh meat during the early postmortem period. Food Chemistry, 439, 138096. https://doi.org/10.1016/j.foodchem.2023.138096

Xu, Y., Zhang, D., Xie, F., Li, X., Schroyen, M., Chen, L., & Hou, C. (2023). Changes in water holding capacity of chilled fresh pork in controlled freezing-point storage assisted by different modes of electrostatic field action. Meat Science, 204, 109269. https://doi.org/10.1016/j.meatsci.2023.109269

Yang, C., Wu, G., Liu, Y., Li, Y., Zhang, C., Liu, C., & Li, X. (2024). Low-voltage electrostatic field enhances the frozen force of −12 ℃ to suppress oxidative denaturation of the lamb protein during the subsequent frozen storage process after finishing initial freezing. Food Chemistry, 438, 138055. https://doi.org/10.1016/j.foodchem.2023.138055

Yu, C., Chen, L., Xu, M., Ouyang, K., Chen, H., Lin, S., & Wang, W. (2024). The effect of pH and heating on the aggregation behavior and gel properties of beef myosin. LWT, 191, 115615. https://doi.org/10.1016/j.lwt.2023.115615

Yu, Q., Hong, H., Liu, Y., Monto, A. R., Gao, R., & Bao, Y. (2024). Oxidation affects pH buffering capacity of myofibrillar proteins via modification of histidine residue and structure of myofibrillar proteins. International Journal of Biological Macromolecules, 260, 129532. https://doi.org/10.1016/j.ijbiomac.2024.129532

Yu, S., Yan, J.-K., Jin, M.-Y., Li, L.-Q., Yu, Y.-H., & Xu, L. (2024). Preparation, physicochemical and functional characterization of pectic polysaccharides from fresh passion fruit peel by magnetic-induced electric field-assisted three-phase partitioning. Food Hydrocolloids, 156, 110292. https://doi.org/10.1016/j.foodhyd.2024.110292

Zhang, A., Chen, S., Wang, Y., Zhou, G., Wang, L., Wang, X., & Xu, N. (2019). Effect of different homogenization pressure on soy protein isolate-vitamin D3 complex. Process Biochemistry, 87, 145–150. https://doi.org/10.1016/j.procbio.2019.09.011

Zhang, Y., Lyu, H., Wang, Y., Bai, G., Wang, J., Teng, W., Wang, W., & Cao, J. (2024). Optimizing the formation of myosin/high-density lipoprotein composite gels: PH-dependent effects on heat-induced aggregation. International Journal of Biological Macromolecules, 268, 131786. https://doi.org/10.1016/j.ijbiomac.2024.131786

Zhao, X., Han, G., Sun, Q., Liu, H., Liu, Q., & Kong, B. (2020). Influence of lard-based diacylglycerol on the rheological and physicochemical properties of thermally induced pork myofibrillar protein gels at different pH levels. LWT, 117, 108708. https://doi.org/10.1016/j.lwt.2019.108708

Zhou, F., Zhao, M., Cui, C., & Sun, W. (2015). Influence of linoleic acid-induced oxidative modifications on physicochemical changes and in vitro digestibility of porcine myofibrillar proteins. LWT, 61(2), 414–421. https://doi.org/10.1016/j.lwt.2014.12.037

Zhou, Y., & Yang, H. (2020). Enhancing tilapia fish myosin solubility using proline in low ionic strength solution. Food Chemistry, 320, 126665. https://doi.org/10.1016/j.foodchem.2020.126665

Chapter 6

General Discussion, Perspectives and Conclusion

1. Main result of EF assisted CFPS

1.1 EF improves storage quality of chilled fresh pork

In this PhD, we examined the effect of EF assisted CFPS on the storage quality of chilled fresh meat, with a focus on WHC of meat.Our research, as detailed in the preceding chapters, has demonstrated that EF application significantly enhances meat preservation quality through multiple mechanisms. Our studies have indicated that EF assisted preservation effectively inhibits the growth and reproduction of microorganisms, reduces moisture loss, and extends shelf life. These findings collectively substantiate the technological viability of EF intervention in both experimental and commercial meat preservation. However, the underlying molecular mechanisms of EF's preservative effect on meat still need to be explored.

1.2 Reduced moisture Loss and economic benefits

In our current research on the WHC of fresh meat using EF-assisted CFPS, the findings reveal a notable improvement compared to traditional CFPS methods. The incorporation of EF has significantly enhanced moisture retention, reducing moisture loss by approximately 7%. Globally, the meat industry incurs billions in annual losses due to moisture evaporation. Conservative estimates suggest these losses exceed $2 billion. Therefore, the 7% reduction in water loss achieved by EF-assisted CFPS represents a monumental economic opportunity, potentially saving the industry hundreds of millions of dollars worldwide. This advancement not only underscores the efficacy of EF in optimizing meat quality but also carries substantial economic implications by minimizing product weight loss and improving yield. Such a reduction in moisture loss can lead to lower production costs, reduced waste, and enhanced product appeal in the market. The promising feedback from this study supports the broader commercial adoption of EF, paving the way for more sustainable and efficient practices in the food industry.

2. EF regulates WHC by influencing the content of microorganisms on the meat surface

2.1 Antimicrobial capacity of EF

Chapter 3 demonstrates that HVEF significantly inhibits microbial proliferation and stabilizes water molecule dynamics in chilled pork, extending its shelf life to 16 days. HVEF suppresses bacterial growth while reducing the TVC and TVB-N content and maintaining WHC of the meat, offering a non-thermal preservation strategy to enhance meat quality and safety. During the spoilage process of animal-based foods, microorganisms multiply in large numbers, resulting in an increase in the content of TVC on the surface of the meat. Meanwhile, during the microbial degradation of proteins, the alkaline nitrogenous compounds generated through decomposition are volatile. The greater the concentration of these substances, the more severe the destruction of amino acids (Qi, et al., 2022). In chapter 3, the significant reduction of the content of TVC and TVB-N (Fig. 3) represents that EF has an impact on microorganisms. Multiple studies have confirmed that the emergence of EF can effectively inactivate microorganisms. The core mechanism is to destroy the integrity

of the microorganisms through multi-target physical and chemical actions (Batista Napotnik et al., 2021; Ross, 2017).

Specifically, EF can achieve efficient inhibition of microorganisms through the synergistic effects of multiple pathways such as electro-physical destruction, oxidative stress, metabolic inhibition and gene regulation (Li et al., 2013). In terms of electro-physical damage, researchers have found that the normal transmembrane potential of microorganisms is affected by the potential difference generated by EF, causing the membrane potential to collapse and ultimately leading to cell death (Hülsheger et al., 1983). Another study has shown that external EF enhances antibacterial activity by electrochemically and rapidly inactivate pathogens while also inhibiting biofilm formation (Fernando et al., 2019). Furthermore, high-intensity EF induces the formation of irreversible pores in the lipid bilayer of microbial cell membranes. The leakage and loss of intracellular contents such as proteins, nucleic acids and ions leads to an imbalance in osmotic pressure and eventually results in cell death (Ross, 2017). The study of Yusupov et al., (2017) revealed that lipid oxidation combined with EF application synergistically reduces electroporation thresholds and accelerates pore formation, which ultimately leads to internal material loss and cell destruction. In addition to directly damaging the cell membranes of microorganisms, some studies have shown that the addition of EF can promote the production of reactive oxygen species (ROS) within cells, disrupt the redox balance, and induce apoptosis. Meanwhile, it triggers the release of free radicals (OH) on the electrode surface, attacking microbial membrane proteins and DNA, and causing oxidative stress (Vanga et al., 2021). EF stimulates the production of reactive oxygen species in the cell, which exceeds the clearance capacity of the antioxidant system and causes oxidative damage (Qi, et al., 2022). Pan et al., (2025) demonstrated that HVEF inactivates E. coli through membrane integrity disruption, oxidative stress induction, characterized by reduced superoxide dismutase activity (SOD) and elevated ROS/malondialdehyde levels, and apoptosis initiation, establishing a mechanistic link between EF exposure and bacterial lethality. Additionally, Chavez-Manini et al., (2024) concluded that the bactericidal efficacy of the electric current positively correlates with exposure duration and intensity. Moreover, electrode materials critically influence microbial inactivation as well, primarily through redox reactions. Metallic electrodes induce oxidative damage to cell membranes and alter gene expression, whereas carbon electrodes exhibit distinct mechanisms with reduced oxidative impacts, suggesting material-dependent pathways in microbial inhibition.

Also the KEGG and GO analyses confirmed that the HVEF significantly influences microbial metabolic pathways during meat storage. Comparative pathway expression analyses revealed temporal variations: after 4 days, HVEF-treated samples exhibited upregulated activity in secondary metabolite biosynthesis and environmental adaptation pathways, whereas prolonged storage (8~16 days) demonstrated suppressed expression in oxidative physiology, biofilm formation, and nutrient transport systems (ABC transporters, two-component systems). This phenomenon can be understood as follows: Short-term exposure (4 days) upregulates secondary metabolite synthesis genes, forcing microbial resources to tilt towards non-growth-related metabolisms. The long-term effect (8~16 days) blocks metabolic collaboration and adaptive responses by inhibiting quorum sensing and biofilm formation pathways

(Fig. 7). Notably, HVEF enhanced amino acid biosynthesis while attenuating carbohydrate and energy metabolism, potentially limiting microbial carbon substrate utilization critical for off-flavor generation. These modulatory effects on cofactor/vitamin metabolism, nucleotide turnover, and signal transduction pathways elucidate HVEF's preservation mechanism through metabolic pathway interference, reducing spoilage-associated enzymatic activities and microbial community interactions. Studies have shown that EF can interfere with the metabolic activity of microorganisms through multiple targets, ultimately causing metabolic arrest and programmed death of microorganisms, thereby delaying meat spoilage (Liu et al., 2023). HVEF significantly downregulates genes related to carbohydrate metabolism, energy metabolism and amino acid metabolism, limits the synthesis of ATP and the utilization of carbon sources, and weakens the energy supply and biosynthesis capabilities of microorganisms (Qi, Liu, Liu, et al., 2022). Their study demonstrates that high voltage alternating EF (HAEF) treatments effectively inhibit microbial proliferation in stored shrimp by modulating lipid-related metabolic pathways. Metabolomics revealed HAEF-induced perturbations in sphingolipid metabolism, ascorbate/aldarate metabolism, and lipid oxidation, with oxidized ceramide and docosahexaenoic acid (DHA) identified as key biomarkers (Fan et al., 2025). These findings elucidate the antimicrobial mechanism of HAEF through targeted metabolic pathway interference, providing insights for optimizing EF applications in meat preservation.

2.2 EF reduces microbial activity and enhances muscle WHC

In chapter 3 and 4, we found that EF significantly reduced moisture loss in meat by aligning water molecules through charge polarization and enhancing molecules binding. This improved WHC, evidenced by lower storage, centrifugation, and cooking losses ($P < 0.05$), attributed to ordered molecular structures under continuous EF exposure. It is generally believed that the reproduction and metabolism of microorganisms can directly or indirectly affect the storage quality of meat through multiple pathways. First, microbial metabolism breaks down nutrients in meat, such as proteins, fats, and sugars. Subsequently, metabolic byproducts such as organic acids, alcohols, and gases are produced. These byproducts can alter the meat environment, for example by lowering the pH or generating salts, thereby reducing the WHC (Guo et al., 2024). During this process, proteins responsible for maintaining cellular water balance or protecting muscle structure may undergo alterations. Impaired expression or function of these proteins, along with the exposure of hydrophobic regions, can lead to protein aggregation or degradation, thereby hindering the transport of water molecules (Holman et al., 2025). Furthermore, extracellular enzymes secreted and produced by microorganisms can degrade the membrane structure of muscle cells. This disruption of cell membrane integrity leads to the release of intracellular water to the meat surface, resulting in drip loss (Fan et al., 2025).

Therefore, the variation of the water content in meat is influenced by the microbial load, and controlling microbial growth is key to maintaining meat moisture and quality. Spoilage bacteria such as Pseudomonas and Escherichia coli decompose proteins during their growth and reproduction, producing mucus, amine compounds

and hydrogen sulfide, which makes the meat surface slippery. At the same time, water accumulates in the form of an exudate, leading to the coexistence of localized dry and moist areas. During the actual measurement process, it was observed that the meat samples without EF treatment exhibited severe localized moisture loss on the surface, with the affected areas showing a relatively sticky and slippery texture. In contrast, EF-treated samples demonstrated superior visual and textural qualities. Specifically, in the analysis of our results (Fig. 6), it was found that HVEF treatments, and particularly CHVEF, significantly inhibited Pseudomonas growth in chilled pork by disrupting bacterial cell membranes via transmembrane voltage-induced pore formation, reducing its abundance by 32.5~44.26% during storage. This suppression mitigated spoilage effects, such as slime formation and moisture loss, preserving meat quality and preventing discoloration. The prolonged EF exposure disrupts the metabolic activities of Pseudomonas, inhibiting its ability to contribute to spoilage. The inactivation of spoilage bacteria by HVEF reduces the damage of microorganisms to the meat structure, particularly with respect to moisture loss. A study by Li et al. (2017) has shown that the efficacy of HVEF in thawing frozen common carp meat significantly reduced moisture loss. HVEF attenuated microbial proliferation by inactivating spoilage bacteria, thereby mitigating microbial driven water deterioration during low temperature storage while modulating enzyme activities to preserve meat quality (Li et al., 2017). It has also been shown that HVEF treatment inactivated spoilage bacteria in catfish fillets during 4℃ storage, significantly reducing microbial activity and water loss, thereby extending shelf life by 2 days while preserving moisture retention and tissue integrity (Huang et al., 2020).

Moreover, the regulatory effect between the water molecule migration and bacterial growth inhibition is reciprocal. The directional migration of water molecules reduces local water activity (Aw), thereby inhibiting bacterial growth (Passot et al., 2012). Aw refers to the degree of freedom with which microorganisms can utilize water in meat: the lower the Aw value, the less water is available for microbial use. As the microbial environment becomes increasingly unfavorable, the microbial load correspondingly decreases (Sogabe et al., 2022). The studies of Bover-Cid et al. (2015, 2017), revealed that high pressure processing (HPP) regulates the growth and reproduction of microorganisms by affecting the aw of meat (Bover-Cid et al., 2015, 2017). These studies demonstrated that inactivated bacteria in meat occurs primarily through aw modulation. A lower Aw induces piezo protection, limiting log reduction, whereas a higher Aw optimizes bacterial inactivation. This highlights the pivotal role of aw in governing HPP efficacy against spoilage bacteria. Both HPP and HVEF technologies disrupt hydrogen bonding networks, modifyAw, and affect phase transitions, thereby reducing free water availability and impairing microbial viability through membrane destabilization or metabolic interference (Pandey, 2025). Therefore, we speculate that EF can also affect the survival state of microorganisms after adjusting Aw by regulating the directional migration of water molecules.

3. The influence of the charges released by the EF on water molecules

3.1 The self-structure of water molecules

Water molecules are formed by weak hydrogen-bonds (HB) to form large molecular clusters. Their spatial structure is V-shaped, and the centers of positive and negative charges cannot coincide, therefore water molecules are electrically polar molecules (Chowdhury et al., 2019). This kind of water molecule cluster generally has a crystalline structure with relatively large gaps (Zheligovskaya & Lyakhov, 2024). This structure represents a dynamic combination that remains stable only for a relatively short period. New water molecules are continuously incorporated into a given cluster, while others simultaneously dissociate from it. Consequently, the structure is highly sensitive to external changes.

3.2 The influence of EF on the self-structure of water molecules

In the water-related results of chapter 3, it was found that during the storage of fresh meat, both the cooking loss and the centrifugation loss decreased significantly in the case of EF assisted CFPS (Fig. 8). This indicates that the water molecules in chilled fresh meat are influenced by EF, causing a portion of the free water, which is prone to loss, to convert to bound water. This transformation temporarily retains moisture and effectively reduces drip loss. A study by Kirov (2025) has shown that changes in temperature, pressure, and field strength can alter the structure of water molecule clusters, including hydrogen bonds (HBs) (Kirov, 2025). This observation can help explain the observed increase in WHC discussed in chapter 3. Ajide & English, (2023) elucidated the role of EF in modulating water's molecular dynamics, dipolar alignment, and HB network reorganization. What can be determined is that EF-induced dipolar alignment intensifies with higher field intensities and lower frequencies. This enhanced alignment directly influences the polarization of water molecules, amplifying their response to external fields. Static fields reduce HB lengths and angles, whereas oscillating fields induce their elongation, reflecting field-dependent structural perturbations. The distortion of HB geometry and compromised network integrity under EF stimuli highlight the dominance of kinetic energy over directional field interactions. These structural changes can alter the thermodynamic and transport properties of water, such as viscosity and diffusion rates. These findings collectively demonstrate that the field parameters critically govern the structural adaptability of water molecules, dipolar responsiveness, and HB kinetics (Gabyshev, 2025). Ruan (2008) demonstrated that the geometric structure of water molecules and related factors have a strong dependence on the intensity of EF. Under both forward and reverse EF conditions, electrons are easily excited, leading to the repeated formation and dissociation of water molecules, which decompose into OH^- and H^+ ions. Xie et al., (2021) suggested that structural changes in water molecules themselves could explain the improvement in meat WHC resulting from EF treatment. It has been illustrated that LVEF assisted freezing accelerates ice nucleation, homogenizes crystal distribution, and suppresses the transition of immobilized water to free water. By

enhancing freezing kinetics and changing the structure of the water molecules, this process effectively preserved beef juiciness.

The findings reported by Ruan also support another conclusion: the dissociation of water molecules under the influence of EF disrupts the initially ordered HB arrangements, increases the dynamic disorder of liquid water, and impedes the formation of a stable six-membered ring structure, thereby inhibiting ice crystal nucleation. A concern in Ruan's study is that the temperature range suitable for the CFPS method is relatively narrow, making ice crystal formation highly probable under external factors such as temperature fluctuations. However, the application of EF has effectively mitigated this issue. By suppressing the likelihood of water molecules in meat forming ice crystals, EF significantly enhances the preservation efficacy of CFPS for fresh meat. This view is also supported by the research of An et al., (2024), who argue that EF critically modulate bulk water crystallization: low intensities suppress freezing even at 100~200 K, while higher fields induce HB reorganization into hexagonal ice structures, with accelerated cooling amplifying short-range ordering, demonstrating field-driven control over phase transitions and ice nucleation dynamics. The water molecules under the action of EF remain in a disordered state at low temperatures and avoid homogeneous nucleation. This conclusion is obviously beneficial for maintaining the supercooled state during low temperature storage (Braslavsky et al., 2019). This observation might explain why the addition of EF enhances the WHC of CFPS. The range of acceptable storage temperature for CFPS is narrow, which to some extent increases the risk of ice crystal nucleation. The addition of the EF induces structural dissociation of water molecules. The HBs in water molecules are disrupted, and the internal structure is destabilized, causing large water molecule clusters to break down into smaller clusters or individual molecules, thereby inhibiting the growth of ice crystals. Similarly, this mechanism has been directly observed by molecular dynamics simulations (Deng et al., 2024). The results demonstrated that applied EF significantly reduce heterogeneous nucleation energy barriers by promoting single ice structure formation, effectively suppressing random ice nucleation and offering insights for optimizing CFPS processes.

3.3 EF promotes the ordered arrangement of water molecules

In chapter 3 and 4, we described that, compared with the control group, the transfer of immobilized water to free water in the meat of EF assisted CFPS was suppressed, resulting in lower loss of free water. As a result, chilled fresh pork in the EF group showed better WHC properties. Research shows that under the action of EF, energy-carrying ions or electrons undergo energy deposition, mass deposition and charge exchange with water molecules in water containing materials (Gabyshev, 2025). At this point, the water molecule can be regarded as two equivalent and equipotential small spheres, one positively charged and the other negatively charged. Under EF, the positive component drives hydrogen atoms to migrate toward regions of lower electric potential, while the negative component induces oxygen atoms to move toward regions of higher electric potential. This inherent separation of charges, fundamental to the molecule's dipole moment, is the driving force behind its alignment. As a result of these oppositely directed forces acting on the charged components of the water

molecule, the molecules undergo deflection and vibration within the EF (Phan et al., 2025). These mechanical disturbances directly convert electrical energy into molecular kinetic energy, increasing the system's overall activity. The electric field force induces repeated and continuous polarization of water molecules, leading to their distortion, deformation, reorientation, vibration, and alignment in a specific direction, referred to as the ordering of water molecules (He et al., 2020). In the control group, a large amount of immobilized water was converted into free water and subsequently lost during storage. The presence of EF effectively alleviated this phenomenon. Under the influence of the external EF, water molecules within the muscle became polarized and arranged in an orderly manner. The direction of polarization is determined by the orientation of the EF at the moment when the water molecules exit its influence (Zheng, 2016). The findings of Xie et al., (2023) further support this explanation. They saw that LVEF assisted freezing enhanced WHC of beef by maintaining regular myofilament lattice arrangement and inhibiting immobilized-to-free water migration, thereby preserving 36% more moisture through stabilized myofibrillar structure. In addition, another intuitive manifestation of the ordered arrangement of water molecules is in H-proton imaging (Fig. 10 and 11). In our study, it is demonstrated that the addition of EF outperformed the control group in maintaining moisture distribution, as H-proton imaging revealed sustained red/yellow areas (higher moisture) and aggregated water molecules at a relatively concentrated location, attributed to enhanced dipole alignment and electrostatic interactions, highlighting the superiority of HVEF efficacy in reducing moisture migration and enhancing the orderly arrangement of water molecules. When analyzing the possible causes, we noted the research of Lin et al., (2024). They employed molecular dynamics simulations to elucidate how external electric fields drive water molecule aggregation by altering multi-body ionic interactions, revealing structural disparities between anionic/cationic polyelectrolytes. It may have advanced the fundamental insights of EF into the motility behavior of water molecules.

In several studies, researchers have utilized the directional driving effect of EF on water molecules and applied and explored it in various research areas, including wastewater adsorption treatment and the separation of water and oil substances (Fan & Yin, 2024; Li et al., 2022). EF also exhibits a certain adsorption effect on both positive and negative ions. However, due to the dynamic motion of water molecules, the duration over which the EF can exert its influence is limited. Consequently, the adsorption phenomenon associated with the EF-water molecule interactions is considered a secondary effect. The primary effect of the EF is the alignment of water molecules, and this ordered arrangement demonstrates relatively high stability (Li et al., 2021). The research by Heidarinejad & Babaei, (2015) shows that the number of ions in water increases with extended EF treatment time. The ions produced in water following EF treatment exhibit strong paramagnetic properties and exhibit long-term storage stability. This view supports the possibility that EF can be retained over prolonged periods. In the later stage of storage, the intense movement of water molecules slows down, which is specifically reflected in the result of the moisture content that does not undergo a drastic decrease (Fig. 8), which proves that the meat treated by EF has better moisture stability.

It is worth noting that water molecules possess a moment of inertia, corresponding to an intrinsic rotational frequency on the order of several hundred megahertz or higher. However, since the EF is an electric field generated by stationary charges and remains constant over time, the inertia of water molecules can be ignored. As a result, their response to the field is not hindered by inertial effects (Zhou et al., 2024). Therefore, the effect of the EF on the directional orientation of water molecules is extremely rapid, which significantly shortens the processing time and avoids overheating or undesirable side reactions associated with continuous energy input. It also highlights the core advantages of EF, namely precise energy delivery, instantaneous responsiveness, and energy efficiency.

4. The influence of the charge released by EF on proteins

Studies have confirmed that proteins can bind water molecules. The major proteins in meat, including myofibrillar and sarcoplasmic proteins, all interact with water molecules. Myofibrillar proteins, which constitute muscle fibers, form a microenvironment through their regular arrangement and retain moisture via capillary action and ionic osmotic pressure. Sarcoplasmic proteins, containing numerous hydrophilic groups, adsorb water molecules through HBs and electrostatic interactions. Research has shown that myofibrillar proteins are primarily responsible for retaining immobilized water, while sarcoplasmic proteins maintain free water. Both types of proteins are involved in regulating the moisture balance in muscle tissues (Puolanne, 2022). Therefore, when analyzing the mechanism by which EF affects water molecules in meat, it is essential to evaluate whether EF can indirectly influence the binding capacity between water molecules and macromolecular substances, thereby affecting the WHC of meat.

4.1 The influence of EF on the binding ability of protein to water molecules

As demonstrated in the analysis of muscle fiber structure in chapters 3 and 4, the myofibrillar fragmentation index (MFI) of meat treated with EF assisted CFPS was lower than that of the control group. The application of EF contributed to a more ordered structural arrangement in fresh meat, effectively reducing moisture loss from the gaps between muscle fibers. The immobilized water is primarily located within highly organized myofibrillar structures. The most notable observation is the formation of inter-fiber gaps, through which water escapes due to capillary action (Xie et al., 2023).

The principal protein component of muscle fibers is myofibrillar protein, composed mainly of myosin and actin, which together facilitate muscle contraction through coordinated structural interactions. Its arrangement state and interaction directly determine the WHC of meat. Preservation of protein structural integrity, through mechanisms including inhibition of denaturation and regulation of interprotein cross-linking, constitutes the fundamental mechanism underlying moisture retention (Im et al., 2024). Structural denaturation of myofibrillar proteins exposes hydrophobic domains and weakens both HB and electrostatic interactions with water molecules. This reduction in interactions leads to protein aggregation and the subsequent

exclusion of water molecules, thereby accelerating moisture loss (Ma et al., 2024). A regular arrangement of myosin and actin supports the stability of the myofilament lattice through capillary action and electrostatic fixation of immobilized water. The denaturation of protein disrupts the actomyosin lattice architecture, resulting in irreversible muscle segment contraction, increased hardness, narrowed myofibrillary spaces, and accelerated loss of free water.

In chapter 4, postmortem muscle exhibited increased myofibrillar fragmentation index (MFI) due to ATP depletion and actomyosin formation, leading to structural disruption (widened fiber gaps, loosened lattice) and moisture loss. The HVEF treatment significantly reduced MFI by preserving myofibrillar integrity through electrostatic interactions, minimizing sarcomere contraction and actomyosin dissociation. SEM revealed denser fibers with smaller pores in HVEF groups, correlating with enhanced WHC as immobilized water remained bound within the stabilized myofibrillar network. This aligns with a reduced cooking loss and a maintained sarcomere Z-line integrity, demonstrating that EFs mitigate structural degradation of muscle, thereby retaining water via regulated myosin-actin interactions and suppressed free water migration. The same view was supported by Wu et al., (2023), who believed that EF preserves muscle fiber integrity and minimizes myofibrillar protein structural alterations, thereby enhancing moisture content by stabilizing protein-water interactions compared to conventional freeze-thawing. The research of Xie et al.,(2021) confirmed this point. Their research found that LVEF assisted freezing minimized freezing-induced structural damage in beef by reducing muscle fiber gaps and enhancing compactness. LVEF assisted freezing repaired Z-line fractures, shortened sarcomere elongation, and stabilized A-band alignment, preserving myofibrillar integrity critical for WHC. Reduced carbonyl and increased sulfhydryl content indicated suppressed protein oxidation, while Raman/fluorescence spectroscopy confirmed minimized secondary/tertiary structural changes. These structural stabilizations mitigated ice crystal disruption to the myofilament lattice, thereby maintaining immobilized water binding via intact protein-water interactions. By preserving both muscle fiber architecture and protein conformation, LVEF assisted freezing reduced free water migration, directly linking improved microstructural and molecular stability to enhanced WHC during freezing. All these results reveal an underlying mechanism: in an EF, the plates that discharge in the upward and downward directions do so through an output voltage. During this process, electric potential is continuously generated and returned as positive charges move toward negative charges. Water molecules within the EF undergo repeated vibrations around their equilibrium positions. Compared to conditions without an EF, the water molecules exhibit increased activity and enhanced molecular motion. As a result, the complex chain-like and cluster-like macromolecular associations of water, $(H_2O)n$, are dissociated into individual water molecules, forming relatively stable dihydrate molecules $(H_2O)_2$. This leads to an increase in Aw and changes the binding states of certain water molecule groups with proteins (Zhou et al., 2024). For instance, the main peptide chain groups and some non-polar residues on protein molecules can bind to water molecules through HBs, resulting in ion-dipole interactions, dipole-induced dipole interactions, and hydrophobic interactions. Consequently, the conformation of the protein changes, thereby affecting several of its functional properties, such as

hydrophobicity, solubility, and gelation characteristics (Abbasi et al., 2019). Therefore, when the binding state between water molecules and proteins changes, the ability of proteins to retain water molecules is also altered. This theory suggests that WHC is not only directly influenced by the EF acting on water molecules, but also indirectly affected by changes in the conformational state of proteins. In both research and application, the WHC of meat can be regulated by optimizing the interactions between proteins and water molecules, enhancing protein stability, preserving the structural integrity of muscle fibers, and ultimately improving the WHC of meat (Zuo et al., 2016).

The ionic species generated by applied EF induce dielectrophoretic interactions with water molecules, subsequently modulating the dynamics of protein-water binding. To determine whether EF exerts a direct effect on proteins, chapter 5 employs a purified myosin solution model (Fig. 14). This selection rationale derives from inherent hydrophilicity of myosin and the presence of polar amino acid residues in its globular head domain, which facilitate HB mediated water binding. The experiments of chapter 5 using myosin solutions revealed that EF induces structural stabilization effects, particularly under extreme pH conditions. These findings demonstrate the feasibility of EF-mediated protein modification strategies for the targeted modulation of functional properties. Wang et al., (2023) directly treated soybean 7S globulin with EF and found that soybean 7S protein could be aggregated orderly by moderate EF. Surface hydrophobicity was improved and total sulfhydryl groups declined by reducing the β-sheet content, and, optimizing foaming properties, highlighting EF's efficacy in preserving and functionally enhancing protein aggregates compared to conventional methods. The conclusion that EF has a direct effect on proteins was confirmed by Yang et al.,(2024). They have demonstrated that LVEF-assisted freezing effectively preserved lamb muscle microstructure integrity and significantly inhibited protein oxidative denaturation during frozen storage, evidenced by reduced carbonyl content, lower surface hydrophobicity, and higher sulfhydryl retention compared to non LVEF treatments. Notably, LVEF maintained secondary/tertiary protein structures and functional properties equivalent to conventional -18°C freezing ($P>0.05$), confirming its efficacy in suppressing protein oxidation. Similarly, in another study, Yang et al., (2024) revealed that constant-current pulsed EF thawing enhances pork water retention by minimizing migration and thawing loss, while preserving myofibrillar protein integrity via suppressed oxidative denaturation, thereby maintaining solubility, thermal stability, and microstructure akin to fresh meat versus conventional methods. In our study presented in chapter 5, the effects of EF on protein structure and function were analyzed by directly applying EF to proteins. The results provide strong evidence that EF can not only regulate the WHC of meat by directly affecting water molecules, but also regulate the ability of proteins to bind water through alterations in their structure and function, resulting in increased protein stability. Furthermore, EF significantly increases the electrostatic interactions between proteins (Lin et al., 2024). This conclusion is undoubtedly valuable for explaining the mechanism by which EF enhances muscle WHC.

In addition, several researchers employed molecular dynamics simulations to reveal the change of protein (Hajjari & Sharif, 2021; Khursandov et al., 2024; Muhammedkutty et al., 2025). For example, the study of Müller et al., (2022) revealed

that EF enhance ovalbumin's thermal stability in secondary structures, increasing molecular size, dipole moment, and surface area while reducing HBs, aligning with experimental non-thermal effects and supporting tailored protein modification for improved functionality. Li et al., (2022) revealed through molecular dynamics simulations that pulsed EF enhanced catalytic efficiency of trypsin by increasing HBs, expanding the solvent-accessible surface area, reducing radius of gyration and random coil content, while improving substrate affinity via active site modifications, consistent with experimental activity gains.

5. The influence of parameters and action modes of EFs on water molecules

In addition to the two influences mentioned above, this study identified two interesting phenomena. First, as presented in chapter 4, the effects of LVEF and HVEF on WHC in muscle were compared. The results demonstrated that HVEF significantly reduced cooking loss, enhanced the retention of immobilized water, and reduced the migration of free water compared to LVEF and control groups ($P < 0.05$). These effects were attributed to stabilized charge release and strengthened electrostatic interactions with water molecules, demonstrating the superior efficacy of HVEF in maintaining moisture distribution during storage (Fig. 11 and 12). Previous studies have shown that the charges released by an EF generally affect electrically polar molecules (Xie et al., 2025). As a polar molecule, when water molecules are energized by an EF, certain HBs are weakened, while the intermolecular forces in specific orientations are strengthened. Therefore, a denser and ordered short-range structure is formed, and the rearrangement of the intermolecular HB network is more significant. Under the influence of EF, water molecules undergo dynamic reorganization of water clusters, in which macro-clusters continuously dissociate and migrate, while simultaneously recombining with micro-clusters, exhibiting fluctuations near their equilibrium positions. The dielectric constant of water (ε=78) is significantly higher than that of most other solutions. When an external EF is applied, the field intensity within water is reduced by several orders of magnitude compared to that in an insulating layer. Additionally, as positive and negative ions in water gradually adsorb onto the electrodes, the effect of the EF is substantially diminished. Therefore, to induce a certain level of molecular ordering under EF, a relatively high field intensity and sufficient exposure duration are required (Abbasi et al., 2019). For example, it has been demonstrated that HVEF significantly enhances frozen pork thawing efficiency compared to air thawing, with higher voltages (10 kV) reducing thawing time by 37.5% while maintaining meat quality (He et al., 2013). This theory is also supported by Jia et al., (2017), that demonstrates that higher-voltage HVEF (-20 kV) significantly enhances thawing efficiency in frozen rabbit meat while optimally preserving quality, evidenced by superior WHC, minimal myofibrillar protein denaturation, and stable water mobility, highlighting dual efficacy of HVEF in accelerating thawing and maintaining meat integrity.

Apart from water molecules, EF with a higher intensity also has a relatively significant influence on other macromolecular substances. It has been demonstrated that high-intensity constant-current pulsed EF (CC-T) suppressed myoglobin oxidation and myofibrillar protein denaturation by inhibiting disulfide/carbonyl bond

formation, preserving solubility, thermal stability, and intact muscle fiber microstructure, outperforming conventional thawing methods in protein integrity and water retention (Yang et al., 2024). In addition, the study of Wang et al., (2025) revealed that higher-intensity pulsed EF effectively stabilize soybean protein isolate (SPI) aggregates by inducing structural unfolding, subunit dissociation, and sustained exposure of hydrophobic/sulfhydryl groups, enabling irreversible reaggregation via disulfide bonds and hydrophobic interactions. Enhanced oxidation from EF-generated free radicals accelerates disulfide crosslinking, promoting stable aggregates with improved functional integrity, surpassing reversible low-intensity pulsed EF effects, offering more precise control over targeted protein structure. LVEF and HVEF have their own advantages and limitations, and their applications remain a topic of considerable debate in both research and practice. LVEF is characterized by low energy consumption, low equipment costs, and safe operation, making it suitable for the mild treatment of proteins or biomaterials, such as avoiding excessive denaturation. However, its effective range is limited, and its regulatory efficiency in modulating molecular aggregation or interfacial behavior is relatively low. In contrast, HVEF offers several advantages: its strong EF force can significantly accelerate the directional migration of molecules (such as water molecule rearrangement and protein conformational transitions), enhance the interfacial disruption ability (such as improved thawing efficiency), and effectively inhibit microbial activity (Wang et al., 2018). For example, HVEF (such as 10~25 kV) significantly enhances functional properties or preservation effects by rapidly disrupting the HB network or inducing protein structure optimization (such as reduced β-sheet content and enhanced surface hydrophobicity). In chapter 4, it was proven that a higher field strength (HVEF) generates stronger polarization effects and non-thermal effects, enabling the desired outcomes to be achieved in a shorter time while offering improved penetration and uniformity in complex systems. However, these advantages must be balanced against increased energy consumption and equipment complexity.

Another notable observation from the study presented in chapter 3 is the investigation of the effects of four different modes on the migration of water molecules in fresh meat. Among these, SHVEF and IHVEF respectively represent a single short-time treatment and an interval short-time treatment, both of which were found to maintain good WHC. Similarly, Liu et al., (2025) used the synergistic effect of pulsed EF with demulsifiers, which enhanced interfacial destabilization while maintaining structural efficiency, enabling swift water separation within 10 min. This phenomenon is most likely attributed to the formation of HBs. The orientation polarization of water molecules exhibits a ‘memory effect’, whereby water molecules can still maintain local order for a certain period after the removal of the electric field (EF), thereby maintaining their activity temporarily. Additionally, residual bound charges may appear at the interface (Li et al., 2024). A similar observation was reported in the study of Bi et al., (2024), which has illustrated the effect of short time EF treatment (100 ps) on water molecules. The study demonstrated that EF rapidly disrupts water molecular aggregation by weakening HBs and shortening bond lifetimes, enhancing mobility and inducing droplet coalescence via interfacial tension reduction. This finding highlights the fact that EF treatment applied in short periods

or at intervals remains effective, thereby offering undoubtedly reduced energy consumption.

6. Limitations

Despite its promise, EF preservation technology faces several practical limitations in meat applications. Firstly, its efficacy is highly dependent on specific environmental conditions, particularly stable preserve environment. In a typical cold chain with frequent door openings, maintaining these ideal parameters for consistent EF performance is challenging, potentially leading to uneven preservation. To overcome this, integrating EF systems with advanced, well-sealed cold storage infrastructure is essential to minimize environmental fluctuations.

Secondly, the penetration depth of the electrostatic field into the meat matrix is inherently limited. While surface sterilization is effective, the field strength attenuates rapidly, leaving deeper tissue and potential internal contamination unaddressed. This restricts its application to thin cuts or surfaces. A promising solution involves combining EF with other preservation techniques, which can synergistically protect the entire product.

Finally, the initial capital investment and operational energy costs for industrial-scale EF systems can be substantial, posing an economic barrier for widespread adoption, especially for biger producers. The return on investment must be clearly demonstrated against traditional methods. Future efforts should focus on optimizing electrode design and system energy efficiency, alongside conducting long-term cost-benefit analyses to prove its commercial viability.

7. Perspectives

The promising results from the studies performed in this PhD lay a foundation for advancing EF technology in meat preservation. Future research should address the following areas to optimize efficacy, scalability, and industrial adoption:

7.1 Mechanistic insights at molecular and cellular levels

While EF disrupts bacterial membranes, further studies on species specific responses and biofilm penetration are needed. For example, it could elucidate the molecular mechanisms of EF-induced stress responses in spoilage microorganisms by integrating metabolomic and genomic profiling. Cultured mid-log phase bacterial cells will be divided into EF-treated and control groups, with EF exposure applied using a EF to simulate industrial preservation conditions. Cells will be harvested immediately post-treatment (T0) and after recovery periods (T2h, T4h) to capture dynamic stress adaptation. Metabolomic profiling will involve quenching cellular metabolism with cold methanol, followed by liquid-liquid extraction of intracellular metabolites. Untargeted metabolomics will be conducted via LC-MS/MS, focusing on stress-related metabolites such as osmoprotectants, antioxidants, energy currencies (ATP/ADP), and membrane lipids. Data will be analyzed using MetaboAnalyst for multivariate statistics (PCA) and pathway enrichment via KEGG. Concurrently, RNA sequencing could profile transcriptional changes in EF-treated versus control cells at

T0 and T2h. Functional annotation will map these genes to GO terms and KEGG pathways, such as protein folding, ROS detoxification, and fatty acid biosynthesis. Integration of metabolomic and genomic datasets via weighted gene co-expression network analysis will correlate metabolite dynamics with gene expression patterns, identifying hub molecules and pathways driving stress adaptation.

In addition, advanced techniques like molecular dynamics simulations (MD) could reveal how EF stabilizes water molecules within myofibrillar networks. Investigating the impact of EF on ice crystal formation during freezing may further enhance WHC. For instance, it could investigate the mechanisms by which EF treatment stabilizes water molecules within myofibrillar protein networks and modulates ice crystal formation during freezing to enhance WHC in muscle foods, such as pork or poultry. Fresh muscle samples will be sectioned into uniform strips and divided into three groups: EF-treated, conventionally frozen (untreated, frozen at −20°C), and non-frozen controls. MD will model myofibrillar proteins (myosin, actin) in explicit water using the force field, with an external EF applied to analyze HB lifetimes, water diffusion coefficients, and protein conformational changes. Experimentally, EF-treated and control samples will undergo freezing, and ice crystal morphology will be characterized using cryogenic scanning electron microscopy (Cryo-SEM) to quantify crystal size, distribution, and orientation. Simulations are expected to reveal prolonged hydrogen bonding between water and myofibrillar proteins under EF, aligning water dipoles along the field direction to stabilize hydration layers and delay ice nucleation. The research will establish a mechanistic link between EF-induced water stabilization and enhanced frozen meat quality, highlighting the potential for optimizing EF parameters to mitigate freeze-thaw damage in industrial applications.

7.2 The influence on freezing point and supercooling point

Theoretically, an EF can influence water molecules, which are permanent dipoles, by promoting a more ordered orientation. This alignment is hypothesized to disrupt the spontaneous nucleation process required for ice crystal formation. Consequently, one of the most significant potential impacts of EF is the depression of the supercooling point, allowing meat to remain in a liquid state at temperatures further below its theoretical freezing point without ice nucleation. This extended supercooled state is critically important, as it prevents the irreversible cellular damage and drip loss caused by the growth of large intracellular and extracellular ice crystals that form during conventional freezing. Furthermore, the freezing point itself might be subtly affected. By stabilizing the hydration shells around myofibrillar proteins and influencing the state of water, EF could alter the energy required for the phase transition, potentially leading to a insignificant shift in the recorded freezing point.

In the research, advanced techniques like differential scanning calorimetry (DSC) should be employed to meticulously track the latent heat of fusion and nucleation temperatures in real-time. Furthermore, research must correlate these thermal changes with ultra-structural observations (e.g., using Cryo-SEM) to definitively link the modified ice crystal morphology directly to the EF-induced suppression of nucleation.

If EF can reliably and significantly extend the supercooling state, it would pave the way for high-quality superchilled storage. This strategy effectively keeps meat

unfrozen but at sub-zero temperatures, drastically slowing microbial and enzymatic spoilage without the detrimental effects of freezing.

7.3 The influence on minor polar constituents

While the primary mechanisms of EF preservation are attributed to its effects on water molecules and proteins in this article, its influence on minor polar constituents, such as vitamins and minerals, presents a compelling yet underexplored frontier. The polar nature of many vitamins (B vitamins, vitamin C) and the ionic character of minerals make them theoretically susceptible to an EF. Potential impacts could include the modulation of oxidative degradation pathways for sensitive vitamins like riboflavin and vitamin C, potentially enhancing their retention. For dissolved minerals, EF-induced ion migration might subtly alter their local distribution or bioavailability. Future research should prioritize quantifying these effects using chromatographic and spectroscopic techniques to profile the stability of a broad micronutrient panel under varying EF parameters. Establishing a positive impact would significantly advance the technology's value proposition. Demonstrating that EF not only preserves textural and microbial quality but also safeguards, or even enhances, the nutritional profile of fresh meat would represent a major breakthrough, strengthening consumer acceptance and providing a powerful marketing advantage for the meat industry, ultimately pushing the boundaries of non-thermal preservation.

7.4 Optimization of EF parameters

Identifying the optimal EF parameters for various meat types and storage condition requires careful evaluation of voltage, frequency, and duration of EF. These factors play a crucial role in enhancing preservation efficiency and maintaining meat quality. For instance, ensuring uniform EF distribution in industrial-scale setups is critical. Computational modeling and sensor monitoring could promote the upgrade of electrode configurations to prevent localized overexposure or inefficacy.

7.5 Industrial scalability and economic viability

It would be desirable to develop low power EF systems compatible with the existing cold chain infrastructure. Comparing EF with conventional methods (vacuum packaging, chemical preservatives) will clarify environmental and economic benefits.

New EF devices designed for industrial meat processors must prioritize durability, safety, and compatibility with automated production lines. Modular designs could allow flexible deployment in varying facility layouts, supporting varied storage methods and both long- and short-distance transportation.

7.6 Technological innovations and digital integration

To improve real-time meat quality monitoring, IoT-enabled sensors can be integrated with EF devices, allowing for continuous assessment of key parameters such as pH and microbial load. These sensors can dynamically adjust EF parameters, while machine learning algorithms could predict optimal treatment protocols based on data.

The performance of EF should be evaluated across varying climatic conditions, particularly in regions where cold chain infrastructure is inconsistent and temperature

fluctuations may impact effectiveness. The appropriate refrigerant and compressor in combination with EF can reduce energy consumption. Portable EF units could support small scale producers in resource limited settings.

8. General conclusion

The three chapters collectively explore the application of EFs in meat preservation, focusing on microbial inhibition, WHC enhancement, and structural-functional maintenance of proteins. Each chapter employs distinct experimental designs to demonstrated the mechanisms by which EFs improve meat quality during CFPS.

Chapter 3 investigated the impact of different EF modes (single, interval, and continuous HVEF) on chilled fresh pork during CFPS. Results demonstrate that CHVEF effectively extends shelf life to 16 days by suppressing bacterial proliferation (Pseudomonas, Latilactobacillus) and stabilizing water molecules. Key freshness indicators, including pH, TVC, and TVB-N, were significantly improved in EF-treated groups. NMR imaging revealed reduced migration of immobilized to free water, corroborating enhanced WHC. This chapter highlights the role of EF in disrupting bacterial cell membranes via transmembrane potential changes and oxidative byproducts, which collectively delay spoilage.

Chapter 4 evaluated EF intensities (low and high voltage) during the early postmortem period, emphasizing WHC and myofibrillar integrity. HVEF reduced cooking loss and maintained immobilized water content, as evidenced by T2 relaxation and H-proton imaging. SEM confirmed that HVEF preserved muscle fiber integrity by mitigating actomyosin dissociation and sarcomere contraction. Particle size analysis and FTIR further revealed that EF stabilized protein-water interactions through charge redistribution, delaying rigor mortis-induced moisture loss. These findings suggest the potential of EF to modulate postmortem biochemical processes, thereby improving meat quality.

Chapter 5 conducted the molecular mechanisms of EF by examining its effects on myosin structure and gelation at varying pH levels. EF-treated myosin exhibited lower surface hydrophobicity, higher sulfhydryl group retention, and reduced aggregation, particularly under extreme pH conditions (pH 3.0 and 9.0). FTIR showed EF preserved α-helix content, while SDS-PAGE and SEM confirmed reduced protein degradation and denser gel networks. Enhanced WHC in EF-treated gels was attributed to optimized HB and electrostatic interactions, which immobilized water within the protein matrix. This chapter underscores the role of EF in maintaining protein functionality under pH stress, offering insights into its broader applicability in meat preservation.

The findings of this PhD research collectively establish electrostatic field (EF) technology as a multifaceted and powerful solution for fresh meat preservation. By effectively inhibiting microbial growth, stabilizing water dynamics, and preserving protein integrity, EF directly addresses the core challenges of spoilage and quality deterioration that have long plagued the industry. The synergistic effects of EF on key physicochemical and microbiological factors underscore its remarkable versatility, proving effective across the entire storage continuum, from the critical postmortem phase to extended chilled storage. This comprehensive action translates into tangible

real-world benefits: significantly extended shelf life, reduced product loss, and the consistent delivery of high-quality, fresh-looking meat to consumers. Consequently, EF technology emerges not merely as a laboratory finding, but as a viable, sustainable innovation with the profound potential to enhance food security, minimize economic waste, and elevate quality standards in the global meat supply chain.

Reference

Abbasi, M. S., Song, R., Kim, H., & Lee, J. (2019). Multimodal breakup of a double emulsion droplet under an electric field. In Soft Matter (Vol. 15, Issue 10, pp. 2292–2300). https://doi.org/10.1039/c8sm02230e

Ajide, M. T., & English, N. J. (2023). Effect of temperature on the dipole response, structural and dynamical properties of water under external electric fields. Journal of Molecular Liquids, 389, 122675. https://doi.org/10.1016/j.molliq.2023.122675

An, G., Yan, Y., Tao, Y., Sun, Q., Wang, Y., Zhang, Y., Chen, H., & Li, T. (2024). A molecular dynamics-based approach to the crystallization of bulk water in the presence of an electric field. Physica B: Condensed Matter, 674, 415555. https://doi.org/10.1016/j.physb.2023.415555

Batista Napotnik, T., Polajžer, T., & Miklavčič, D. (2021). Cell death due to electroporation – A review. Bioelectrochemistry, 141, 107871. https://doi.org/10.1016/j.bioelechem.2021.107871

Bi, X., Gu, Y., Wang, K., Jiang, M., Xiao, P., Luo, J., Fang, W., & Liu, B. (2024). Demulsification of W/O emulsions induced by terahertz pulse electric fields-driven hydrogen bond disruption of water molecules. Separation and Purification Technology, 349, 127819. https://doi.org/10.1016/j.seppur.2024.127819

Bover-Cid, S., Belletti, N., Aymerich, T., & Garriga, M. (2015). Modeling the protective effect of aw and fat content on the high pressure resistance of Listeria monocytogenes in dry-cured ham. Food Research International, 75, 194–199. https://doi.org/10.1016/j.foodres.2015.05.052

Bover-Cid, S., Belletti, N., Aymerich, T., & Garriga, M. (2017). Modelling the impact of water activity and fat content of dry-cured ham on the reduction of Salmonella enterica by high pressure processing. Meat Science, 123, 120–125. https://doi.org/10.1016/j.meatsci.2016.09.014

Braslavsky, I., Eickhoff, L., Dreischmeier, K., Zipori, A., Reicher, N., Sirotinskaya, V., Adar, C., Benbassat, S., Bissoyi, A., Chasnitsky, M., Rudich, Y., & Koop, T. (2019). Ice Nucleation By Antifreeze Proteins. Cryobiology, 91, 174. https://doi.org/10.1016/j.cryobiol.2019.10.114

Chavez-Manini, C. A., Reza-López, S. A., Arzate-Quintana, C., Quiñonez-Flores, C. M., Favila-Pérez, M. A., Camarillo-Cisneros, J., & Castillo-González, A. R. (2024). Effect of electric current in viability, biofilm formation and antibiotic resistance of Pseudomonas aeruginosa: A systematic review. Indian Journal of Medical Microbiology, 52, 100735. https://doi.org/10.1016/j.ijmmb.2024.100735

Chowdhury, M. S., Zheng, W., Kumari, S., Heyman, J., Zhang, X., Dey, P., Weitz, D. A., & Haag, R. (2019). Dendronized fluorosurfactant for highly stable water-in-fluorinated oil emulsions with minimal inter-droplet transfer of small molecules.

Nature Communications, 10(1), 4546. https://doi.org/10.1038/s41467-019-12462-5

Deng, Q., Wang, H., Zhu, X., Ding, Y., Chen, R., & Liao, Q. (2024). Molecular dynamics insights into electric Field-Induced heterogeneous ice nucleation. Journal of Molecular Liquids, 414, 126294. https://doi.org/10.1016/j.molliq.2024.126294

Fan, F., & Yin, Y. (2024). Study on enhancement of the interfacial water absorption process by an electrostatic field. In X. Wang (Ed.), Future Directions in Energy Engineering: Challenges, Opportunities, and Sustainability (pp. 107–115). Springer Nature Switzerland. https://doi.org/10.1007/978-3-031-62042-3_12

Fan, Y., Zhang, K., Liu, Q., Chen, Q., Xia, X., Sun, F., & Kong, B. (2025). Mechanism, application, and prospect of bioprotective cultures in meat and meat products. Food Chemistry, 476, 143474. https://doi.org/10.1016/j.foodchem.2025.143474

Fan, Z., Ren, X., Li, C., Chen, B., & Dong, S. (2025). Effects of different modes of high-voltage alternating electric field action on the freshness and metabolites of Litopenaeus vannamei during partial freezing storage. Food Control, 175, 111313. https://doi.org/10.1016/j.foodcont.2025.111313

Fernando A. G., da S. Jr., Jose Jarib, A.-E., Mateus M., da C., & Helinando P., de O. (2019). Low intensity electric field inactivation of gram-positive and gram-negative bacteria via metal-free polymeric composite. Materials Science and Engineering: C, 99, 827–837. https://doi.org/10.1016/j.msec.2019.02.027

Gabyshev, D. N. (2025). Condensational growth of spherical water droplets altered under external electric fields. Journal of Aerosol Science, 186, 106554. https://doi.org/10.1016/j.jaerosci.2025.106554

Guo, Z., Chen, Y., Wu, Y., Zhan, S., Wang, L., Li, L., Zhang, H., Xu, Z., Qiu, S., Cao, J., Guo, J., Niu, L., & Zhong, T. (2024). Changes in meat quality, metabolites and microorganisms of mutton during cold chain storage. Food Research International, 189, 114551. https://doi.org/10.1016/j.foodres.2024.114551

Hajjari, M. M., & Sharif, N. (2021). In-silico behavior of dissolved prolamins under electric field effect applied by electrospinning process using molecular dynamics simulation. Journal of Molecular Liquids, 344, 117778. https://doi.org/10.1016/j.molliq.2021.117778

He, X., Liu, R., Nirasawa, S., Zheng, D., & Liu, H. (2013). Effect of high voltage electrostatic field treatment on thawing characteristics and post-thawing quality of frozen pork tenderloin meat. Journal of Food Engineering, 115(2), 245–250. https://doi.org/10.1016/j.jfoodeng.2012.10.023

He, X., Wang, S.-L., Yang, Y.-R., Wang, X.-D., & Chen, J.-Q. (2020). Electro-coalescence of two charged droplets under pulsed direct current electric fields with various waveforms: A molecular dynamics study. In Journal of Molecular Liquids (Vol. 312). https://doi.org/10.1016/j.molliq.2020.113429

Heidarinejad, G., & Babaei, R. (2015). Numerical investigation of electro hydrodynamics (EHD) enhanced water evaporation using Large Eddy Simulation turbulent model. Journal of Electrostatics, 77, 76–87. https://doi.org/10.1016/j.elstat.2015.07.007

Holman, B. W. B., Coombs, C. E. O., & Hopkins, D. L. (2025). The quality of aged beef and aged-then-frozen lamb meat after up to 2 years of frozen storage at −12 or −18 ° C. Meat Science, 224, 109790.

https://doi.org/10.1016/j.meatsci.2025.109790

Huang, H., Sun, W., Xiong, G., Shi, L., Jiao, C., Wu, W., Li, X., Qiao, Y., Liao, L., Ding, A., & Wang, L. (2020). Effects of HVEF treatment on microbial communities and physicochemical properties of catfish fillets during chilled storage. LWT, 131, 109667. https://doi.org/10.1016/j.lwt.2020.109667

Hülsheger, H., Potel, J., & Niemann, E.-G. (1983). Electric field effects on bacteria and yeast cells. Radiation and Environmental Biophysics, 22(2), 149–162. https://doi: 10.1007/BF01338893

Im, C., Song, S., Cheng, H., Park, J., & Kim, G.-D. (2024). Changes in meat quality and muscle fiber characteristics of beef striploin (M. longissimus lumborum) with different intramuscular fat contents following freeze-thawing. LWT, 198, 116081. https://doi.org/10.1016/j.lwt.2024.116081

Jia, G., Liu, H., Nirasawa, S., & Liu, H. (2017). Effects of high-voltage electrostatic field treatment on the thawing rate and post-thawing quality of frozen rabbit meat. Innovative Food Science & Emerging Technologies, 41, 348–356. https://doi.org/10.1016/j.ifset.2017.04.011

Khursandov, J., Mashalov, R., Makhkamov, M., Turgunboev, F., Sharipov, A., & Razzokov, J. (2024). Exploring α-synuclein stability under the external electrostatic field: Effect of repeat unit. Journal of Structural Biology, 216(3), 108109. https://doi.org/10.1016/j.jsb.2024.108109

Kirov, M. V. (2025). Stability of drop-like water cluster. Chemical Physics Letters, 861, 141849. https://doi.org/10.1016/j.cplett.2024.141849

Li, D., Jia, S., Zhang, L., Li, Q., Pan, J., Zhu, B., Prinyawiwatkul, W., & Luo, Y. (2017). Post-thawing quality changes of common carp (Cyprinus carpio) cubes treated by high voltage electrostatic field (HVEF) during chilled storage. Innovative Food Science & Emerging Technologies, 42, 25–32. https://doi.org/10.1016/j.ifset.2017.06.005

Li, N., Sun, Z., Liu, W., Wei, L., Li, B., Qi, Z., & Wang, Z. (2021). Effect of electric field strength on deformation and breakup behaviors of droplet in oil phase: A molecular dynamics study. In Journal of Molecular Liquids (Vol. 333). https://doi.org/10.1016/j.molliq.2021.115995

Li, N., Sun, Z., Sun, J., Liu, W., Wei, L., Li, T., Li, B., & Wang, Z. (2022). Deformation and breakup mechanism of water droplet in acidic crude oil emulsion under uniform electric field: A molecular dynamics study. Colloids and Surfaces A: Physicochemical and Engineering Aspects, 632, 127746. https://doi.org/10.1016/j.colsurfa.2021.127746

Li, Q., Ning, Z., Li, J., & Jia, Z. (2024). Laboratory study on the transformation of oil-water interface properties under direct current electric field. Geoenergy Science and Engineering, 239, 212953. https://doi.org/10.1016/j.geoen.2024.212953

Li, Y., Yuan, Z., Gao, Y., Bao, Z., Sun, N., & Lin, S. (2022). Mechanism of trypsin activation by pulsed electric field treatment revealed based on chemical experiments and molecular dynamics simulations. Food Chemistry, 394, 133477. https://doi.org/10.1016/j.foodchem.2022.133477

Li, Y.-Q., Tian, W.-L., Mo, H.-Z., Zhang, Y.-L., & Zhao, X.-Z. (2013). Effects of pulsed electric field processing on quality characteristics and microbial inactivation of soymilk. Food and Bioprocess Technology, 6(8), 1907–1916.

https://doi.org/10.1007/s11947-012-0868-8
Lin, C.-J., Wang, J.-J., Jiang, Y., Chen, S.-L., Li, H.-F., Zhao, W.-H., Huang, Q.-R., Rong, C.-R., & Duan, X.-Z. (2024). Structural properties of Ions and polyelectrolytes in aqueous solutions under external electric fields: The Sign Effect. Chinese Journal of Polymer Science, 42(9), 1341–1352. https://doi.org/10.1007/s10118-024-3105-9
Liu, J., Zhu, F., Yang, J., Wang, Y., Ma, X., Lou, Y., & Li, Y. (2023). Effects of high-voltage electrostatic field (HVEF) on frozen shrimp (Solenocera melantho) based on UPLC-MS untargeted metabolism. Food Chemistry, 411, 135499. https://doi.org/10.1016/j.foodchem.2023.135499
Liu, T., Sarsenbekuly, B., & Kang, W. (2025). Breakdown mechanism and application of high frequency pulsed electric field-demulsifier combination on water-in-oil emulsion. Colloids and Surfaces A: Physicochemical and Engineering Aspects, 707, 135846. https://doi.org/10.1016/j.colsurfa.2024.135846
Ma, C., Zhang, J., Zhang, R., Zhou, L., Ni, L., & Zhang, W. (2024). Study on the effects of pre-slaughter transport stress on water holding capacity of pork: Insights from oxidation, structure, function, and degradation properties of protein. Food Chemistry: X, 24, 101913. https://doi.org/10.1016/j.fochx.2024.101913
Muhammedkutty, F. N. K., MacAinsh, M., & Zhou, H.-X. (2025). Atomistic molecular dynamics simulations of intrinsically disordered proteins. Current Opinion in Structural Biology, 92, 103029. https://doi.org/10.1016/j.sbi.2025.103029
Müller, W. A., Sarkis, J. R., Marczak, L. D. F., & Muniz, A. R. (2022). Molecular dynamics study of the effects of static and oscillating electric fields in ovalbumin. Innovative Food Science & Emerging Technologies, 75, 102911. https://doi.org/10.1016/j.ifset.2021.102911
Pan, D., Chu, P., Fu, X., Wen, D., Song, H., Bai, S., & Guo, X. (2025). Elucidating the underlying mechanism of the bactericidal effect facilitated by a crucial flagellar protein under high-voltage electrostatic conditions. Journal of Hazardous Materials, 491, 137963. https://doi.org/10.1016/j.jhazmat.2025.137963
Pandey, V. K. (2025). Exploring the significance of emerging blue food processing technologies for sustainable development. Food Research International, 200, 115429. https://doi.org/10.1016/j.foodres.2024.115429
Passot, S., Cenard, S., Douania, I., Tréléa, I. C., & Fonseca, F. (2012). Critical water activity and amorphous state for optimal preservation of lyophilised lactic acid bacteria. Food Chemistry, 132(4), 1699–1705. https://doi.org/10.1016/j.foodchem.2011.06.012
Phan, H. A., Nguyen, K., Pham, P. T., Do Quang, L., Thu, H. B., Lam, D. B., Jen, C.-P., Thanh, T. B., & Duc, T. C. (2025). On-demand electrostatic droplet sorting and splitting. Sensors and Actuators A: Physical, 385, 116311. https://doi.org/10.1016/j.sna.2025.116311
Puolanne, E. (2022). Chapter 10—Developments in our understanding of water holding in meat. In P. Purslow (Ed.), New Aspects of Meat Quality (Second Edition) (pp. 237–263). Woodhead Publishing. https://doi.org/10.1016/B978-0-323-85879-3.00018-0
Qi, M., Liu, Q., Liu, Y., Yan, H., Zhang, Y., & Yuan, Y. (2022). Staphylococcus aureus biofilm inhibition by high voltage prick electrostatic field (HVPEF) and the

mechanism investigation. International Journal of Food Microbiology, 362, 109499. https://doi.org/10.1016/j.ijfoodmicro.2021.109499

Qi, M., Liu, Y., Shi, S., Xian, Y., Liu, Q., Yan, H., Zhang, Y., & Yuan, Y. (2022). Inhibition mechanism of high voltage prick electrostatic field (HVPEF) on Staphylococcus aureus through ROS-mediated oxidative stress. LWT - Food Science and Technology, 155, 112990.

Qi, M., Yan, H., Zhang, Y., & Yuan, Y. (2022). Impact of high voltage prick electrostatic field (HVPEF) processing on the quality of ready-to-eat fresh salmon (Salmo salar) fillets during storage. Food Control, 137, 108918. https://doi.org/10.1016/j.foodcont.2022.108918

Ross, C. L. (2017). The use of electric, magnetic, and electromagnetic field for directed cell migration and adhesion in regenerative medicine. Biotechnology Progress, 33(1), 5–16. https://doi.org/10.1002/btpr.2371

Ruan, W. (2008). Structur e and electronic spectrum for water molecule under the external electr ic field. Journal of Jinggangshan University, 03, 5–8.

Sogabe, T., Nakagawa, H., Yamada, T., Koseki, S., & Kawai, K. (2022). Effect of water activity on the mechanical glass transition and dynamical transition of bacteria. Biophysical Journal, 121(20), 3874–3882. https://doi.org/10.1016/j.bpj.2022.09.001

Vanga, S. K., Wang, J., Jayaram, S., & Raghavan, V. (2021). Effects of pulsed electric fields and ultrasound processing on proteins and enzymes: A review. Processes, 9(4), Article 4. https://doi.org/10.3390/pr9040722

Wang, Q., Li, Y., Sun, D.-W., & Zhu, Z. (2018). Enhancing food processing by pulsed and high voltage electric fields: Principles and applications. Critical Reviews in Food Science and Nutrition, 58(13), 2285–2298. https://doi.org/10.1080/10408398.2018.1434609

Wang, R., Guo, P.-F., Yang, J.-P., Huang, Y.-Y., Wang, L.-H., Li, J., Lin, S.-Y., Sheng, Q.-L., Zeng, X.-A., & Teng, Y.-X. (2025). Exploration of the regulatory mechanism of pulsed electric field on the aggregation behavior of soybean protein isolates. Food Hydrocolloids, 160, 110761. https://doi.org/10.1016/j.foodhyd.2024.110761

Wang, W., Wang, X., Zhang, H., Wang, H., Wang, L., Zhang, N., & Yu, D. (2023). Effects of electric field intensity regulation on protein aggregation behaviour and foaming property of soybean 7S globulin. International Journal of Biological Macromolecules, 248, 125784. https://doi.org/10.1016/j.ijbiomac.2023.125784

Wu, G., Yang, C., Bruce, H. L., Roy, B. C., Li, X., & Zhang, C. (2023). Effects of alternating electric field assisted freezing-thawing-aging sequence on longissimus dorsi muscle microstructure and protein characteristics. Food Chemistry, 409, 135266. https://doi.org/10.1016/j.foodchem.2022.135266

Xie, Y., Chen, B., Guo, J., Nie, W., Zhou, H., Li, P., Zhou, K., & Xu, B. (2021). Effects of low voltage electrostatic field on the microstructural damage and protein structural changes in prepared beef steak during the freezing process. Meat Science, 179, 108527. https://doi.org/10.1016/j.meatsci.2021.108527

Xie, Y., Sun, Z., Chen, Y., Liu, T., Li, W., & Li, N. (2025). Mechanism analysis of oil-in-water-in-oil droplet deformation and breaking under pulsed alternating current field: A molecular dynamics study. Separation and Purification Technology, 360,

130864. https://doi.org/10.1016/j.seppur.2024.130864

Xie, Y., Zhou, K., Chen, B., Ma, Y., Tang, C., Li, P., Wang, Z., Xu, F., Li, C., Zhou, H., & Xu, B. (2023). Mechanism of low-voltage electrostatic fields on the water-holding capacity in frozen beef steak: Insights from myofilament lattice arrays. Food Chemistry, 428, 136786. https://doi.org/10.1016/j.foodchem.2023.136786

Xie, Y., Zhou, K., Chen, B., Wang, Y., Nie, W., Wu, S., Wang, W., Li, P., & Xu, B. (2021). Applying low voltage electrostatic field in the freezing process of beef steak reduced the loss of juiciness and textural properties. Innovative Food Science & Emerging Technologies, 68, 102600. https://doi.org/10.1016/j.ifset.2021.102600

Yang, C., Wu, G., Liu, Y., Li, Y., Zhang, C., Liu, C., & Li, X. (2024). Low-voltage electrostatic field enhances the frozen force of −12 ℃ to suppress oxidative denaturation of the lamb protein during the subsequent frozen storage process after finishing initial freezing. Food Chemistry, 438, 138055. https://doi.org/10.1016/j.foodchem.2023.138055

Yang, N., Yao, H., Zhang, A., Jin, Y., Zhang, X., & Xu, X. (2024). Effect of constant-current pulsed electric field thawing on proteins and water-holding capacity of frozen porcine longissimus muscle. Food Chemistry, 454, 139784. https://doi.org/10.1016/j.foodchem.2024.139784

Yusupov, M., Van der Paal, J., Neyts, E. C., & Bogaerts, A. (2017). Synergistic effect of electric field and lipid oxidation on the permeability of cell membranes. Biochimica et Biophysica Acta (BBA) - General Subjects, 1861(4), 839–847. https://doi.org/10.1016/j.bbagen.2017.01.030

Zheligovskaya, E. A., & Lyakhov, G. A. (2024). Structural Mechanisms of Transitions between Ices with Different Densities—Features of Water Phase Diagrams. Physics of Wave Phenomena, 32(3), 209–219. https://doi.org/10.3103/S1541308X24700183

Zheng, T. (2016). Treatment of oilfield produced water with electrocoagulation: Improving the process performance by using pulse current. Journal of Water Reuse and Desalination, 7(3), 378–386. https://doi.org/10.2166/wrd.2016.113

Zhou, X., Wang, H., Zhu, X., Chen, R., & Liao, Q. (2024). Numerical study of supercooled water droplet impacting on cold superhydrophobic surface under electric field. International Journal of Heat and Mass Transfer, 218, 124781. https://doi.org/10.1016/j.ijheatmasstransfer.2023.124781

Zuo, H., Han, L., Yu, Q., Niu, K., Zhao, S., & Shi, H. (2016). Proteome changes on water-holding capacity of yak longissimus lumborum during postmortem aging. Meat Science, 121, 409–419. https://doi.org/10.1016/j.meatsci.2016.07.010

Appendix A-Publications.

1. **Xu, Y.**, Wen, X., Zhang, D. et al. Changes in the freshness and bacterial community of fresh pork in controlled freezing point storage assisted by different electrostatic field usage frequencies. *Food Bioprocess and Technology* 17, 939–954 (2024). https://doi.org/10.1007/s11947-023-03180-4
2. **Xu, Y.**, Zhang, D., Xie, F. et al. Changes in water holding capacity of chilled fresh pork in controlled freezing-point storage assisted by different modes of electrostatic field action. *Meat Science* 204, 109269 (2024). https://doi.org/10.1016/j.meatsci.2023.109269
3. **Xu, Y.**, Leng, D., Li, X. et al. Effects of different electrostatic field intensities assisted controlled freezing point storage on water holding capacity of fresh meat during the early postmortem period. *Food Chemistry* 439, 138096 (2024). https://doi.org/10.1016/j.foodchem.2023.138096
4. **Xu, Y.**, Leng, D., Martine, S. et al. Structure and functional properties of myosin induced by electrostatic fields at different pH values. *Innovative Food Science & Emerging Technologies* 102, 104004 (2025). https://doi.org/10.1016/j.ifset.2025.104004
5. **Xu, Y.**, Yang Q., Zheng X., et al. Identification of volatile flavor substances in four key muscle portions of five Tibetan sheep breeds. *Journal of science of food and agriculture* 105, 11, 5950-5961. https://doi.org/10.1002/jsfa.14319
6. **Xu, Y.**, Leng, D., Xiao Z., et al. Effect of electrostatic field assisted controlled freezing point storage on early postmortem period glycolysis process of muscle. *Journal of Integrative Agriculture* (Under review)
7. Hou, C., **Xu, Y.**, Zhang D. Enhanced electrostatic field discharge device. ZL 2024 1 1110674.7. China Patent. Authorization.